DESIGN AND OPTIMIZATION OF WAVELET FOR DETECTING LIFE MENACING EVENTS FROM ELECTROCARDIOGRAM

A Thesis

Submitted by

BABY PAUL

for the award of the degree

of

DOCTOR OF PHILOSOPHY

(Faculty of Engineering)

Under the Guidance of

Dr. P. MYTHILI

DIVISION OF ELECTRONICS ENGINEERING
SCHOOL OF ENGINEERING
COCHIN UNIVERSITY OF SCIENCE AND TECHNOLOGY
KOCHI – 682 022

OCTOBER 2015

Design and Optimization of Wavelet for Detecting Life Menacing Events from Electrocardiogram

Ph. D. Thesis under the Faculty of Engineering

Author:

Baby Paul
Research scholar
Division of Electronics Engineering
School of Engineering
Cochin University of Science and Technology
Kochi - 682 022, Kerala, India
E-mail: babypaul321@yahoo.co.in

Research Advisor:

Dr. P. Mythili
Associate Professor
Division of Electronics Engineering
School of Engineering
Cochin University of Science and Technology
Kochi - 682 022, Kerala, India
E-mail: mythili@cusat.ac.in

October 2015

DIVISION OF ELECTRONICS ENGINEERING
SCHOOL OF ENGINEERING
COCHIN UNIVERSITY OF SCIENCE AND TECHNOLOGY
Kochi - 682 022, Kerala, India

Dr. P. Mythili
Associate Professor
E-mail: mythili@cusat.ac.in

Certificate

This is to certify that the thesis entitled "**Design and Optimization of Wavelet for Detecting Life Menacing Events from Electrocardiogram**" is a bonafide record of research work carried out by Mr. Baby Paul under my supervision and guidance in the Division of Electronics Engineering, School of Engineering, Cochin University of Science and Technology, Kochi, Kerala, India. No part of this thesis has been presented for the award of any other degree from any other university.

Kochi
03rd October 2015

Dr. P. Mythili, Ph.D.
(Supervising Guide)

Declaration

I hereby declare that the work presented in the thesis entitled "**Design and Optimization of Wavelet for Detecting Life Menacing Events from Electrocardiogram**" is based on the original work done by me under the supervision of Dr. P. Mythili, Associate Professor, Division of Electronics Engineering, School of Engineering, Cochin University of Science and Technology, Kochi, Kerala, India as Research guide. No part of this thesis has been presented for the award of any other degree from any other institution.

Kochi
03rd October 2015

Baby Paul

Dedicated to my Parents

Acknowledgement

First and foremost, I would like to thank God Almighty for his blessings showered on me for the successful completion of the thesis work.

I would like to thank the Principal, School of Engineering, Cochin University of Science & Technology, Kerala, India for providing me the resources and facilities to carry out this thesis work.

I wish to put on record my deep sense of gratitude and thanks to my guide Dr. P. Mythili, Associate Professor, Division of Electronics Engineering, School of Engineering, Cochin University of Science and Technology, who has been the key source of motivation and providing me with an excellent atmosphere for doing research. Her valuable guidance and inspiration throughout this research work has been of the greatest help in carrying out this work in its present form. I was able to successfully finish the work and deliver this thesis only because of her able guidance and immense patience.

I am very much grateful to Dr. R. Gopikakumari, Professor, Division of Electronics Engineering, School of Engineering, Cochin University of Science and Technology, for the encouragement, support and suggestions offered to me during the research work.

I am very much indebted to Dr. Binu Paul, Head of Department, Division of Electronics Engineering, School of Engineering, Cochin University of Science and Technology, for her support in pursuing the Ph.D. programme in the department.

I would like to extend my sincere gratitude to Dr. S. Mridula, Associate Professor, Division of Electronics Engineering, School of Engineering, Cochin University of Science and Technology, for her suggestions and support given to me during the research work.

This research work is supported by University Grants Commission, Bangalore, India under the scheme "Faculty Improvement Programme". I extend my heartfelt thanks to the Commission in helping me to complete this work successfully.

My sincere thanks are due to Mr. Shanavaz K.T., Mr. Philip Cherian, Mr. Anjith T. A. and Mrs. Rema N.R. Research Scholars, Division of Electronics Engineering, School of Engineering, Cochin University of Science and Technology, for giving me inspiration for the timely completion of the work.

I acknowledge Dr. Benjamin Varghese P., Head of the Department of Electronics, Baselios Poulose II Catholicos College, Piravom, for helping and inspiring me in doing the research work.

I would like to express my sincere thanks to all Faculty and Staff members of Division of Electronics Engineering, School of Engineering, Cochin University of Science and Technology for their support and cooperation during the entire research work.

My special thanks goes to my wife Asha, my children Paul and Joseph, for their love, care, understanding, patience and sacrifice to achieve this target.

Finally I would like to dedicate this thesis to my mother Smt. Annamma and the memories of my beloved father Sri. K.K. Paul, who have worked hard to provide me education right from my childhood.

Baby Paul

Abstract

Electrocardiogram gives the information regarding the health of the patients by monitoring the bioelectric potentials generated by the sinoatrial node in the heart. These signals can be collected by using electrodes suitably placed on the body of a patient. The normal human ECG lie in the frequency range of 0.05-100 Hz and the most useful information is contained in the range of 0.5-45 Hz. Even though a large amount of work has already been done in the field of ECG classification, no classification system has made an attempt in identifying the isolated abnormalities which pose a silent threat to patients.

An adaptive filtering technique for denoising the ECG which is based on Genetic Algorithm (GA) tuned Sign-Data Least Mean Square (SD-LMS) algorithm is proposed. This algorithm gave an average signal to noise ratio improvement of 10.75 dB for baseline wander and 24.26 dB for power line interference. It is seen that the step size 'μ' optimized with GA helps in obtaining better SNR value without causing any damage to the information content in the ECG.

A new wavelet for automatic classification of arrhythmias from electrocardiogram is proposed. This new wavelet is formed as a sum of shifted Gaussians so that it resembles a normal ECG. This shape has been chosen with the aim of extracting maximum information from the ECG under analysis. The classification performance was studied using the most commonly used database, the MIT-BIH Arrhythmia database. The shifted and summed Gaussian wavelet was then optimized using GA. The optimum wavelet for classification was obtained after several runs of the GA algorithm. The ECG class labeling was done according to the Association for the Advancement of Medical Instrumentation (AAMI). The wavelet scales corresponding to

the different frequency levels giving maximum classification performance were identified by selecting finer scales. Probabilistic Neural Network classifier was used for classification purpose. The proposed classification system offered better results than that reported in literature by giving an overall sensitivity of 97.01% for Normal beats, 75.20% for Supraventricular beats and 93.06% for Ventricular beats. As mentioned above this technique could exclusively identify some of the isolated abnormalities present in the patient records.

The major contribution of this research includes the

- Development of a new wavelet for ECG classification purposes.
- Identification of isolated abnormalities which pose a threat to patients.
- Design of a less complex adaptive filter that could be implemented on hardware targets such as portable ECG monitors.

Contents

List of Tables

List of Figures

List of Abbreviations

AAMI	Association for the Advancement of Medical Instrumentation
*a*AP	Aberrated Atrial Premature Beat
ADC	Analog-to-Digital Converter
AE	Atrial Escape Beats
AF	Adaptive Filters
AP	Atrial Premature Beat
AR	Autoregressive
ASICs	Application-Specific Integrated Circuits
AV	atrioventricular
BLW	Baseline Wander
CWT	Continuous Wavelet Transform
DCT	Discrete Cosine Transform
DSP	Digital Signal Processing
DWT	Discrete Wavelet Transform
ECG	Electrocardiogram
ELM	Extreme Learning Machine
F	Fusion Beat
FIR	Finite Impulse Response
fPCG	Fetal Phonocardiography
*f*PN	Fusion of Paced and Normal Beats
*f*VN	Fusion of Ventricular and Normal Beats
GA	Genetic Algorithm
GLM	Generalized Linear Model
ICA	Independent Component Analysis
IIR	Infinite Impulse Response
LA	Left Arm
LBBB	Left Bundle Branch Block

LDA	Linear Discriminant Analysis
LL	Left Leg
LMS	Least Mean Square
LS-SVM	Least Square-Support Vector Machine
MIT-BIH	Massachusetts Institute of Technology-Beth Israel Hospital
MLL	Modified Limb Lead
MLLII	Modified Limb Lead II
MMF	Modified Morphological Filtering
N	Normal
NE	Nodal Escape Beats
NN	Neural Network
NP	Nodal Premature Beat
P	Paced
P^+	Positive Predictivity
PCA	Principal Component Analysis
PLI	Power Line Interference
PNN	Probabilistic Neural Network
PPV	Positive Predictive Value
PSO	Particle Swarm Optimization
PVC	Premature Ventricular Contraction
Q	Unknown Beat Class
RA	Right Arm
RBBB	Right Bundle Branch Block
RBF	Radial Basis Function
RLS	Recursive Least-Squares
S	Sensitivity
SA	sinoatrial
SD-LMS	Sign Data-Least Mean Square Algorithm
SP	Supraventricular Premature Beat

SSG-Wavelet	Shifted and Summed Gaussian Wavelet
S_v, SVEB	Supraventricular Ectopic Beat
SVM	Support Vector Machine
V	Ventricular Ectopic Beat
VE	Ventricular Escape Beat
WTC	Wavelet Transformed Coefficients

Chapter 1

INTRODUCTION

Contents

This chapter introduces the background of Electrocardiogram (ECG). The working of the heart can be analyzed by monitoring the ECG of a patient. The commonly used methods for recording the ECG waveform are explained briefly. The different types of ECG waveforms usually encountered are presented. Further the different types of noises such as baseline wander, power line interference and muscle noise, which are encountered while recording ECG are described. Finally the basic idea of a general ECG classification system is discussed.

1.1 Electrocardiogram

Since its intervention in 1903 by Willem Einthoven, ECG has become an important tool in diagnosing the condition of a person. Various techniques for the analysis have been introduced till date which includes techniques from understanding the heart rate of the patient to complex systems that maps the exact conditions of the heart and the associated organs.

For continuous monitoring as well as Holter monitoring, several techniques have been designed and implemented by different people. These techniques were further developed into specific instruments that provide clinical monitoring for both the patient and doctor, that support the diagnosis in real time. It also helps in improving mortality rates for people especially who live in rural areas.

Since enormous data has been generated and recorded in the process of continuous ECG monitoring, much care should be given to the analysis, particularly when we are looking for diseases that do not manifest often. Such isolated abnormalities in ECG do pose a threat to a patient. The isolated abnormalities if detected at an earlier stage could be helpful for the patient.

1.1.1 Physiological background of ECG

The fundamental concepts of Electrocardiographic signal and its origin are presented in this section. The different types of cardiac arrhythmias such as auricular and ventricular ectopic heart beats, branch blocks, fusion beats etc., based on the Association for the

Advancement of Medical Instrumentation (AAMI) standard are discussed.

1.1.2 Electrocardiographic signals

Electrocardiography is a discipline of medicine that is concerned with the electrical activity of the heart. An electrocardiographic signal originating from the sinoatrial node (SA) can completely describe the functioning of the heart. These signals are usually captured by means of surface electrodes placed on the body of the patient.

The heart is divided into four main chambers as shown in Figure 1.1. The two upper chambers are called the left and right atria and the two lower chambers are called the left and right ventricles. The atria and ventricles work together, alternately contracting and relaxing to pump blood through the heart. The electrical system of the heart is the power source that makes this possible. Figure 1.2 depicts the conduction system of the heart. The heartbeat is triggered by electrical impulses that travel down a special pathway through the heart. The impulse starts in a small bundle of specialized cells located in the right atrium, called the SA node. It is also known as the heart's natural pacemaker. The electrical activity spreads through the walls of the atria and causes them to contract. This forces blood into the ventricles. The SA node sets the rate and rhythm of the heartbeat. The atrioventricular (AV) node is a cluster of cells in the center of the heart between the atria and ventricles, and it slows the electrical signal before it enters the ventricles. This delay gives the atria time to contract before the ventricles do. His-Purkinje network is a pathway

of fibers that sends the impulse to the muscular walls of the ventricles and causes them to contract. This forces blood out of the heart to the lungs and body. The electrical triggering cycle repeats that make the heart to beat again and again (Catalano, 2002).

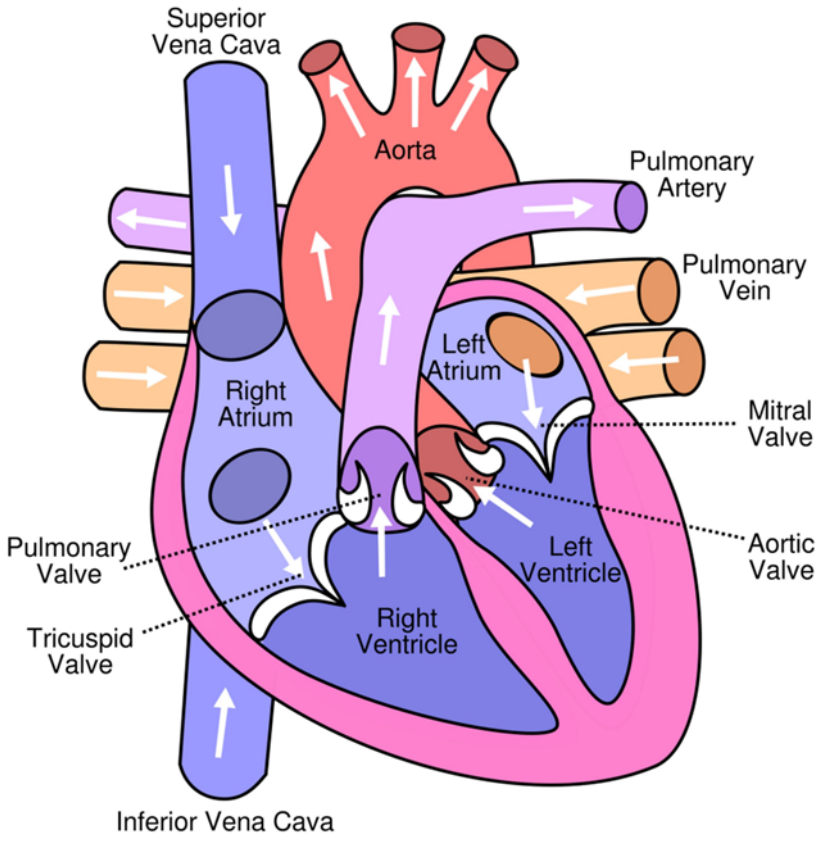

Figure 1.1: Structure of the heart

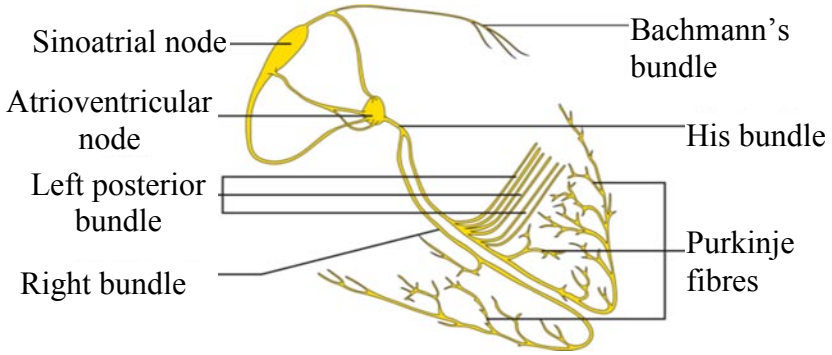

Figure 1.2: Conduction system of the heart

A normal ECG is illustrated in the Figure 1.3. The main part of the ECG contains a P wave, QRS complex, and T wave. The P wave indicates atrial depolarization. The QRS complex consists of a Q wave,

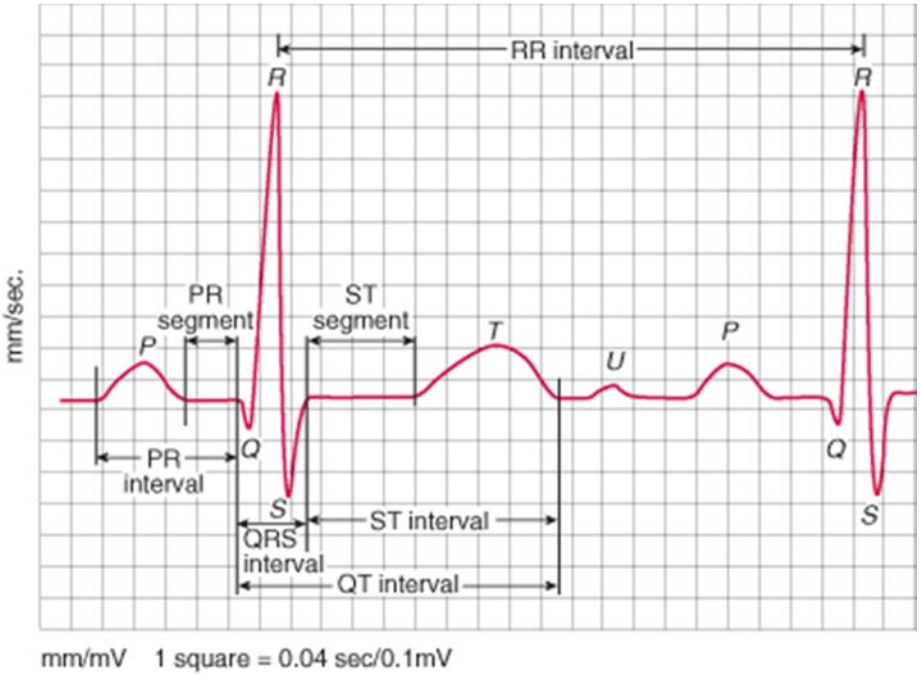

Figure 1.3: A normal ECG Signal

R wave and S wave. The QRS complex represents the combined activity of ventricular depolarization and atrial repolarization. The T wave comes after the QRS complex and indicates ventricular repolarization (Catalano, 2002). Amplitude of P wave is usually less than 3 mV with duration between 0.06 to 0.1 seconds. The PR interval is from 0.12 to 0.2 seconds. The QRS complex which follows the P wave has duration between 0.08 to 0.12 seconds. The duration of the Q wave is less than 0.03 seconds. QT interval is less than 50% of the preceding RR interval. From the end of the QRS complex to the start of the T wave is the ST segment with a slight curve at proximal T wave. The T wave is asymmetric and slightly rounded.

1.2 ECG lead system

The standard 12 lead ECG system utilizes at least five electrodes: one for each limb, plus a floating electrode on the chest wall. The system is divided into three lead systems: standard limb leads, augmented leads, and precordial leads.

1.2.1 Standard limb leads

The limb leads are formed by keeping electrodes on the right and left wrists, arms and ankles. The direction of flow of electrical current in the limb leads lies in the frontal plane; a flat plane parallel to the chest. The direct path between two electrodes or between two electrodes or between an electrode and a reference point is called the axis of that lead (Lewis K., 2010).

The recording positions of bipolar leads I, II & III are shown in Figure 1.4 (J. Malmivuo, 1995).

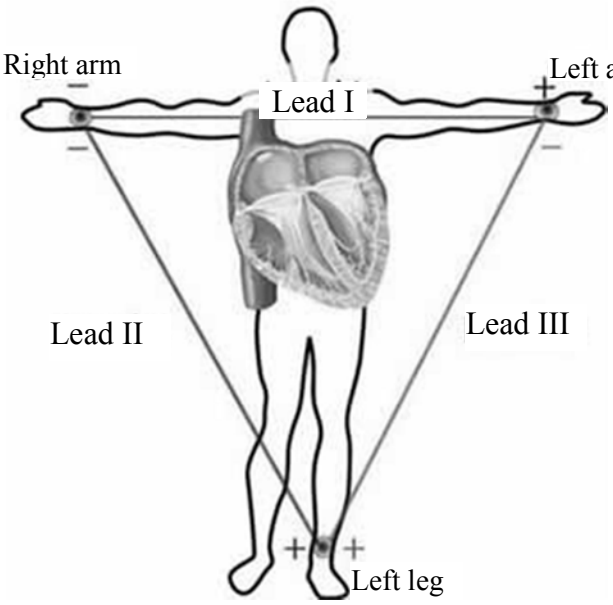

Figure 1.4: Standard limb leads

In lead I, the recording is done with Left Arm (LA) as the positive electrode and the Right Arm (RA) as the negative electrode. Lead I records electrical activity from left to right across the chest, giving a view of left lateral wall of the heart. In lead II the negative electrode is on the RA, and the positive electrode is on the Left Leg (LL). Lead II provides the view of the inferior surface of the heart. The waveform in lead II will be either diphasic or predominantly negative. In lead III the positive electrode is on the LL and the negative electrode is on the LA. This lead provides a view of right inferior surface of the heart. Lead III is usually positive deflection.

1.2.2 Other ECG lead systems

The augmented limb leads (Unipolar)-aVL, aVR, aVF

The signals from the limb electrodes can be combined to give further views of the heart called the augmented leads. One of the limb electrodes serve as positive electrode. The negative electrode is virtual, being the average of the signals from the remaining two limb electrodes. The augmented leads are known as unipolar leads (Acharya UR, 2007).

The precordial leads (Unipolar) Leads V_1-V_6

There are six electrodes V_1 to V_6 giving rise to six views of the heart signals across the front of the chest. The views fall across the transverse plane. The positive electrode is the chest electrode. The negative electrode is a virtual electrode commonly called the Wilson central terminal. This virtual electrode is realized by electrically averaging the signal from the three electrodes LA, RA and LL. These six leads known as precordial leads are unipolar.

All the six unipolar chest leads view the heart from different angles. Together with the limb leads a total of 12 views are usually used for diagnosis resulting in the 12 lead ECG standard. These leads usually monitor the left side of the heart. If monitoring to the right side of the heart is needed, leads are place on the right side of the heart on the chest designated from $V_{1R} – V_{2R}$ (Acharya UR, 2007).

In addition, to these leads there are other leads which can be used for monitoring the ECG of patients. One of them is the ‘modified chest

leads'. These leads give a view of the heart similar to the chest leads, but uses bipolar leads. Here the positive electrode is placed on the chest and the negative electrode at a location that approximates the electrical axis of the heart.

Another lead system used for recording is the 'Modified Limb Lead' (MLL). ECG can be recorded with the RA electrode placed in the 3rd right intercostal space slightly to the left of the mid-clavicular line, the LA electrode placed in the 5th right intercostal space slightly to the right of the mid-clavicular line and the LL electrode placed in the 5th right intercostal space on the mid-clavicular line. Modified limb lead II recording from MIT-BIH Arrhythmia database is used for the analysis in this work.

1.3 Cardiac Arrhythmias

Arrhythmia is a disturbance of the heart's usual rhythm. It is also known as cardiac dysrhythmia. Arrhythmias happen when the electrical signals that the heart uses to beat do not start in the right place or move across the heart properly. In general, the arrhythmias can be divided into two groups. The first one is the ventricular arrhythmia which is life threatening and can sometimes be fatal. The second group includes supraventricular or atrial arrhythmias. The proposed work relates to the arrhythmias in the second group. In accordance with the AAMI standard, the heart beats are classified as Normal labeled heartbeats (termed as N), Supraventricular ectopic beat (S_v), Ventricular ectopic beat (V), Fusion beat (F) and unknown beat class (Q). The MIT-BIH

arrhythmia is the most commonly used database to evaluate the performance of algorithms by most of the researchers (Mariano Llamedo, march 2011). The records in this database are sampled at a rate of 360 samples/sec. The different types of arrhythmias in this database are grouped into the AAMI type as given in Table 1.1.

Table 1.1: Arrhythmias analyzed according to AAMI standard

AAMI heartbeat type	Description of arrhythmia	Type of MIT-BIH heartbeat	Class
V	Ventricular ectopic beat	Premature Ventricular contraction (PVC), Ventricular Escape beat (VE)	III
F	Fusion beat	Fusion of ventricular and normal beats, Fusion of paced and normal beats	
Q	Unknown beat	Paced, Not classified beats	-
Sv	Supraventricular ectopic beat	Atrial Premature beat (AP), Aberrated Atrial Premature beat (aAP), Nodal Premature beat(NP), Supraventricular Premature beat (SP)	II
N	Any beat not in the S_v, V, F, Q	Normal, Left Bundle Branch Block beats, Right Bundle Branch Block beats, Atrial Escape beats, Nodal Escape beats	I

It is seen that AP, *a*AP, NP and SP beats are grouped under Supraventricular (S_v) type (Class II). Similarly PVC, VE comes in Ventricular (V) type. Since the fusion beats (F) are marginally represented in the database, a modification to the AAMI recommendation suggested by Mariano Llamedo (2011) was adopted for classification purpose. It

consists of merging the ventricular and fusion types. The V and F types were together named as Class III. All other beats which were not in S_v, V and F type are grouped under N type, except Q type which was discarded since its number is very less and it represents only the paced and unclassified beats. The types of Arrhythmia in each group are described below.

1.3.1 Normal labeled heart beats (N)

As per the recommendations of AAMI this group contains the normal, bundle branch block, atrial escape and nodal escape beats.

Normal ECG: The normal ECG shown in Figure 1.5 is a scalar representation that shows deflections resulting from cardiac activity as changes in the magnitude of voltage and polarity over time. It comprises the P wave, QRS complex and T and U waves.

Left Bundle Branch Block (LBBB): Blockage of conduction in the left bundle branch prior to its bifurcation, results primarily in delayed depolarization of the left ventricle. In LBBB, the septum depolarizes from right to left, since its depolarization now is initiated by the right bundle branch. In this condition, activation of the left ventricle is delayed, which causes the left ventricle to contract later than the right ventricle. Though LBBB is prominently characterized by using chest leads with a QRS interval slightly greater than 0.12 seconds, other leads also show significant variation. Unlike Right bundle branch block, LBBB always gives a sign of organic heart disease, e.g. ischemia, cardiomyopathy, conduction tissue disease, hyper tension heart disease,

infiltration (Saul G. Myerson, 2009). A sample of the LBBB taken from lead II is shown in Figure 1.6.

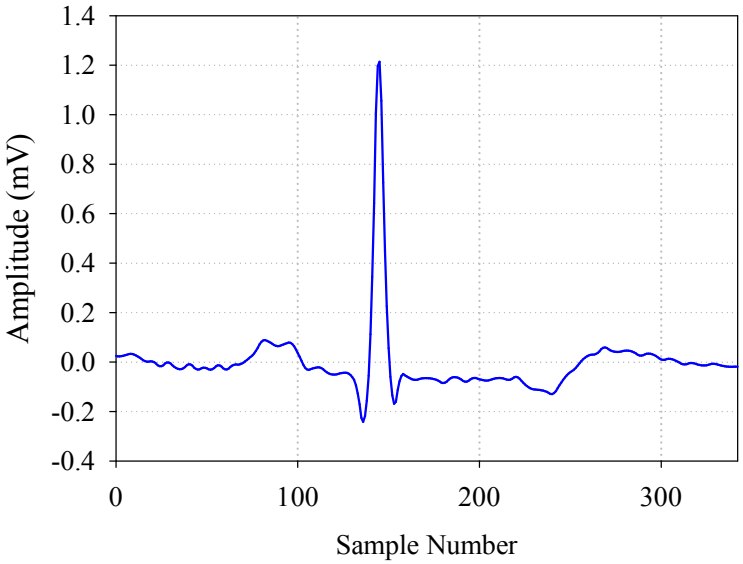

Figure 1.5: Normal ECG signal

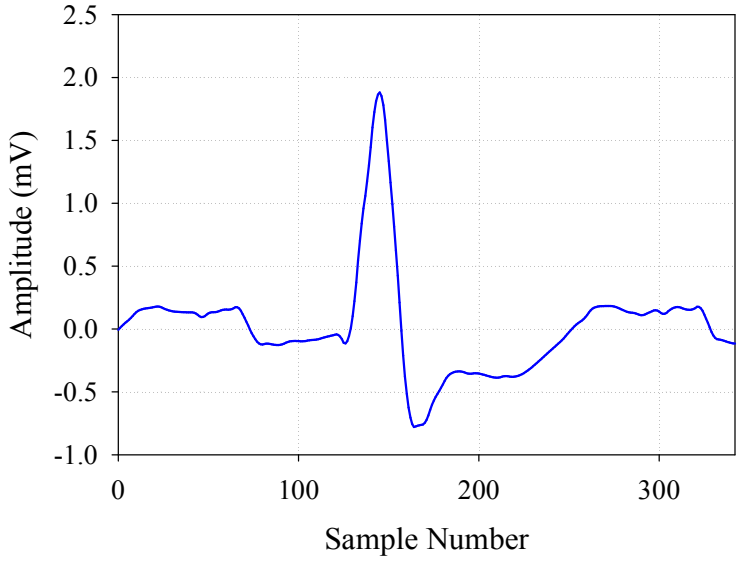

Figure 1.6: ECG signal with LBBB

*Right Bundle Branch Block (RBBB)**:*** Septal depolarization results in a small R wave in chest lead V_1. Left ventricular depolarization results in S wave. Right ventricular depolarization produces a second R wave. The delayed depolarization of the right ventricle causes an increased width of the QRS complex to at least 0.12 seconds. Hence, RBBB is characterized in chest leads with a QRS complex slightly greater than 0.12 seconds. A corresponding change does occur in lead II which is plotted in Figure 1.7.

Atrial escape beat (AE): As shown in Figure 1.8, AE is a cardiac dysrhythmia occurring when sustained suppression of sinus impulse formation causes other SA node to act as cardiac pacemakers (Sandra Atwood, 2011).

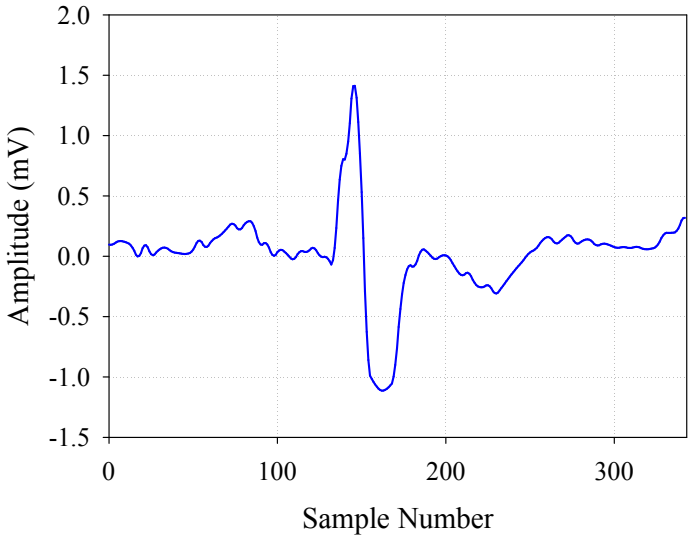

Figure 1.7: ECG signal with RBBB

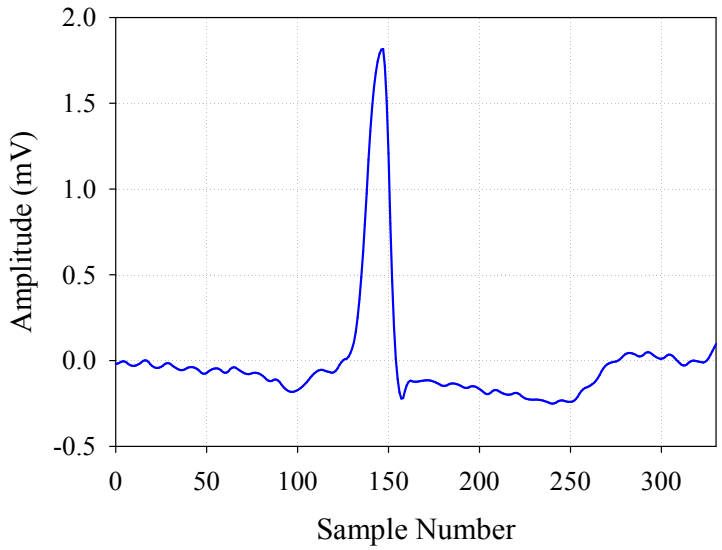

Figure 1.8: ECG signal with AE

Nodal escape beat: These ECG cycles are produced when the normal pattern of atrial depolarization does not occur. Failure of the SA node to initiate an impulse or blockage of SA node impulse in the atrial conduction system produces a pulse in the cardiac cycle. The first backup pacemaker in the cardiac conduction system is the AV junction. All escape beats come late in the cardiac cycle. When the normal pacemaker of the heart doesn't produce an impulse, the escape or backup pacemaker protects the heart from stopping completely. This may occur after normal beats or premature beats or even after an isolated beat. They are recognizable by the location and shape of the P-wave and is given in Figure 1.9 (Catalano, 2002).

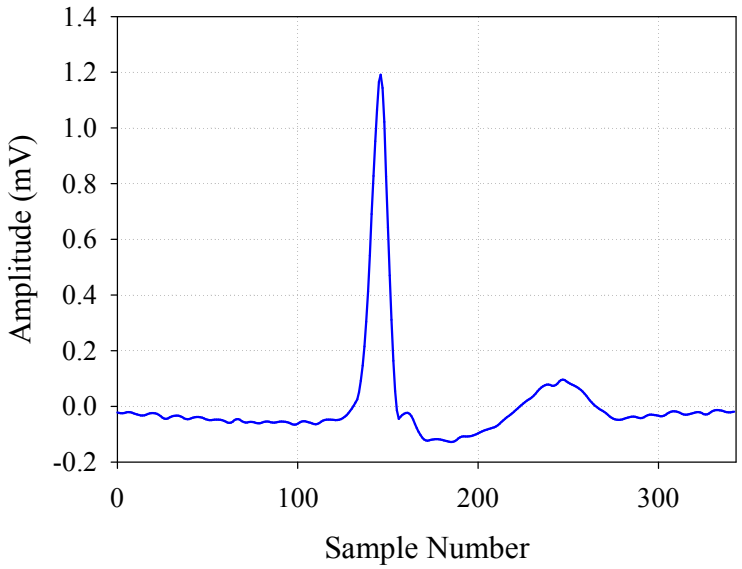

Figure 1.9: ECG signal with nodal escape beat

1.3.2 Supraventricular ectopic beats (S_V)

As per the recommendations of AAMI this group consists of atrial premature beat, aberrated atrial premature beat, nodal premature beat and supraventricular premature beat.

Atrial premature beat (APB): Atrial premature contractions are produced when a single irritable area of the atria discharges an impulse before the next regular SA node is able to discharge. This early discharge interrupts the regularity of the underlying rhythm with premature ectopic beats. Since these impulses arise from the atria, the ectopic beat has an abnormally shaped P-wave before the QRS complex. Figure 1.10 shows a typical APB (Catalano, 2002).

Aberrated atrial premature beat: Aberration is conduction of the supraventricular impulse to the ventricles in a markedly different manner from the usual conduction. Any type of supraventricular rhythm may show aberrancy. The ECG shown in Figure 1.11 is conducted aberrantly and is due to an APB. One of the reasons for an aberrated atrial premature beat is that cardiac cycle before the beat preceding the APB is a long cycle. Aberration occurs when heart rate increases (Ziad Issa, 2012).

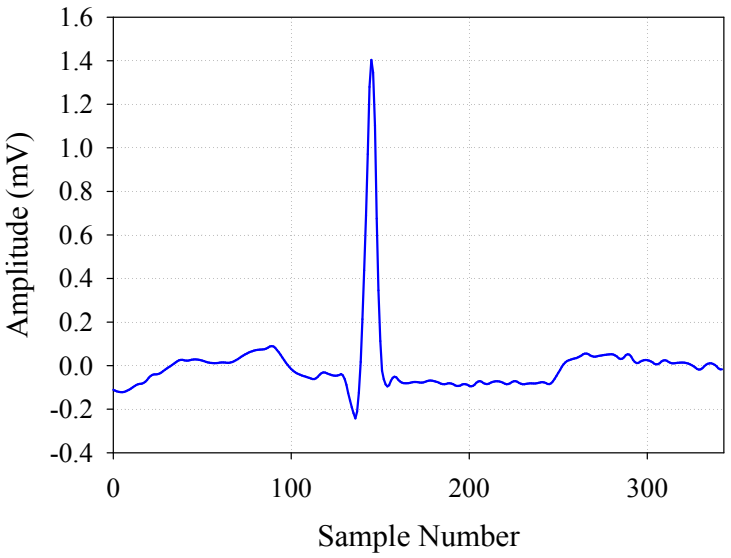

Figure 1.10: ECG signal with APB

Nodal premature beat: A premature nodal contraction shown in Figure 1.12 occurs when a single irritable area in the AV junction discharges an impulse before the next regular SA node impulse is due to be delivered.

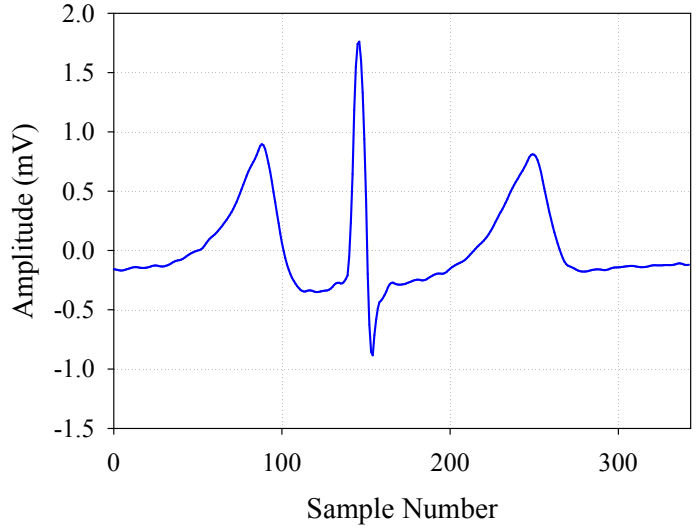

Figure 1.11: ECG signal with aberrated atrial premature beat

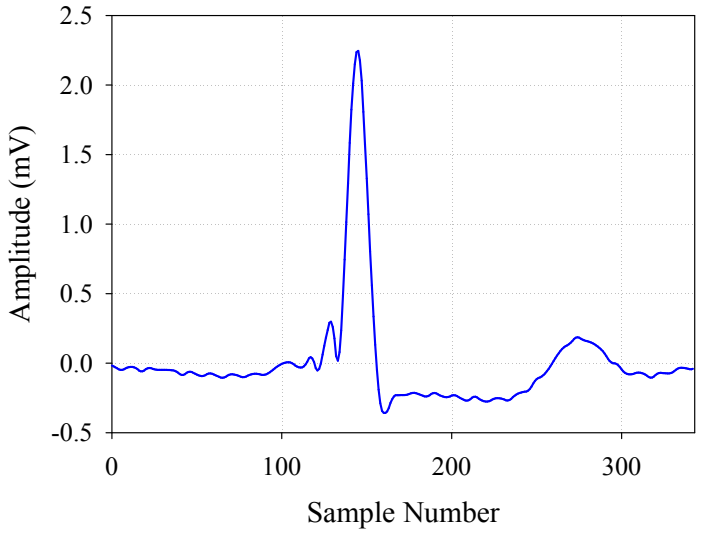

Figure 1.12: ECG signal with nodal premature beat

Supraventricular premature beats: Supraventricular premature beats represent premature activation of the atria from a location other than the sinus node and can originate from the atria or AV node. As shown in Figure 1.13 they have narrow QRS complex.

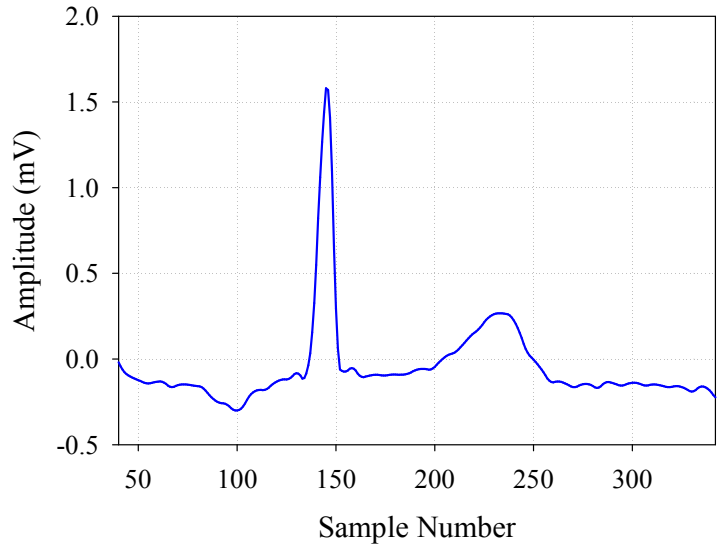

Figure 1.13: ECG signal with supraventricular premature beat

1.3.3 Ventricular ectopic beat (V)

As per the recommendations of AAMI, this group includes Premature Ventricular Contraction and ventricular escape beat.

Premature Ventricular Contraction (PVC): This type of ECG occurs as a result of increased automatism of the ventricular muscles, i.e. An ectopic focus somewhere in the ventricles discharge and causes early or premature contraction of the ventricles. Since the premature discharge of the focus originates in the ventricles and the impulse is

not usually conducted back to the atria, the QRS complex of the PVC is not preceded by the P wave as given in Figure 1.14 (Viljoen, 1989).

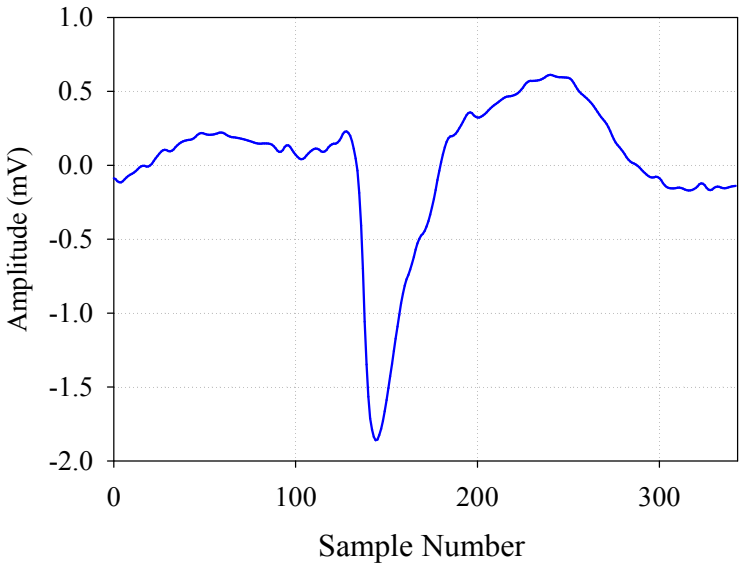

Figure 1.14: ECG signal with PVC

Ventricular escape beat: Ventricular escape beat occur when there is a failure of the higher pacemaker sites to initiate impulses. As a result, some area in the ventricular conduction system becomes the pacemaker site by default. Complete AV blocks and SA node blocks may also cause ventricular escape beats to occur. The same condition can also produce ventricular escape rhythm as shown in Figure 1.15 (Catalano, 2002).

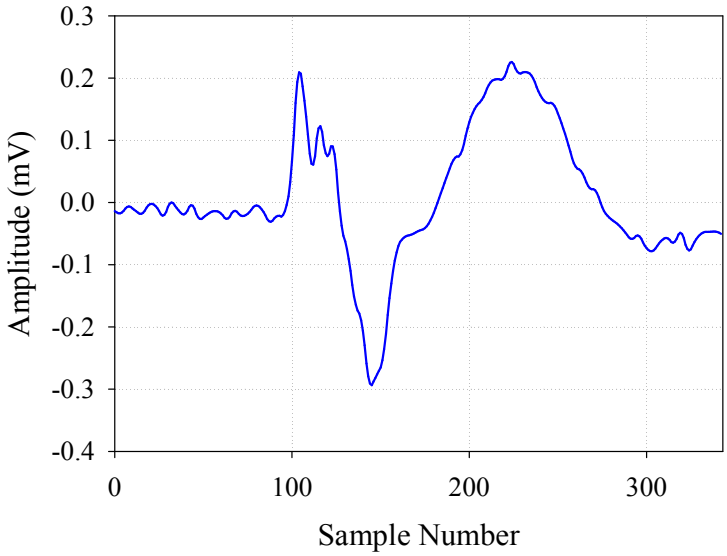

Figure 1.15: ECG signal with ventricular escape beat

1.3.4 Fusion beats (F)

As per the recommendations of AAMI, the fusion of ventricular and normal beats and fusion of paced and normal beats comes under this group. Fusion heartbeats occur when either the atria or the ventricles are activated by simultaneously invading impulses and can be measured in the P wave or the QRS complex of the ECG (Henry Marriott, 2000). Ventricular fusion beats occur when a normal impulse from the sinus node has depolarized the atria and is beginning to depolarize the ventricles, at the same time an irritable ventricular focus also initiates an impulse. The two impulses collide in their travel to depolarize the ventricles. The result is a beat that usually has a sinus P wave in front of it but looks neither like the normal beat nor the PVC as given in Figure 1.16.

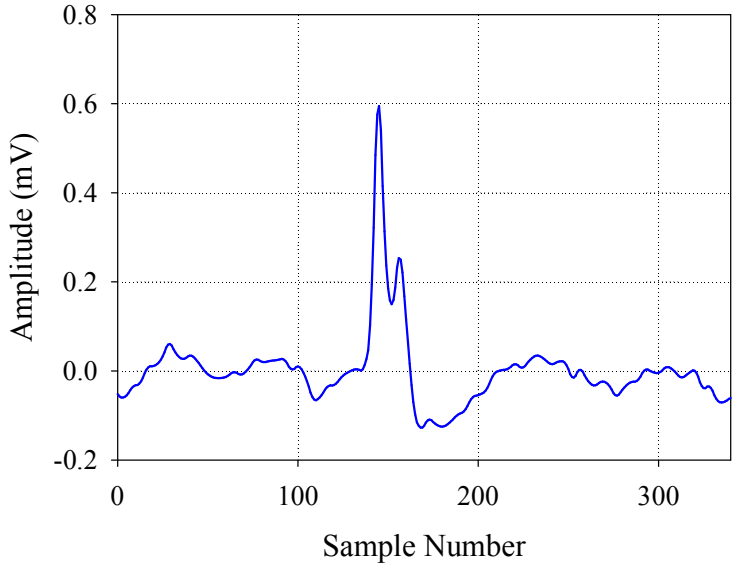

Figure 1.16: ECG signal with fusion of ventricular and normal beats

1.3.5 Unknown heart beats (Q)

Unknown or unclassified heartbeats (Type Q) corresponds to heartbeats that do not contain any significant information, mainly due to some external conditions such as electrode disconnection, saturation of acquisition system, artifacts, or heartbeats originated by pacemakers fixed in the body of a patient.

It is necessary to isolate these kinds of heartbeats from the training space in order to obtain a satisfactory diagnosis. The number of beats of these types are relatively low in the database. A sample of this type of ECG is shown in Figure 1.17.

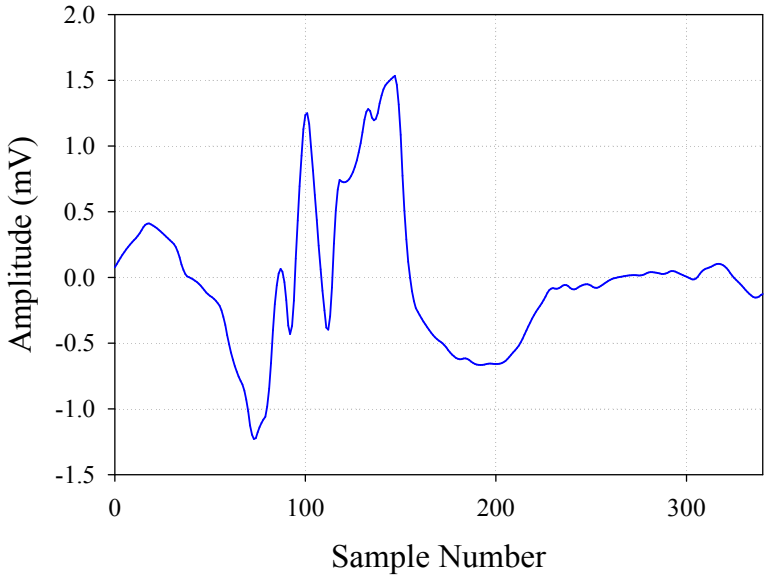

Figure 1.17: Unknown ECG signal

1.4 Noise in ECG Signal

ECG signals are always more likely to be affected by noise (Adam Gacek, 2011). The different types of noise that affect ECG are Power line Interference (PLI), Baseline Wander (BLW), electrode motion artifacts and electrical potential due to muscular contraction. Noise reduction methods focus mainly on the signal, after having been filtered. The ECG should not lose its characteristics such as morphology and duration. This is a complex task since some bands of noise frequencies falls in the frequency range of ECG.

1.4.1 Power line interferences

PLI contains 50/60 Hz pickup because of improper grounding of the recording system. It is indicated as an impulse or spike at 50/60 Hz,

and will appear as additional spikes at integral multiples of the fundamental frequency. The amplitude of the noise is usually 50% of peak-to-peak ECG signal amplitude. A 50 Hz notch filter is generally used to remove the PLI. Figure 1.18 shows an ECG waveform corrupted with 50 Hz PLI.

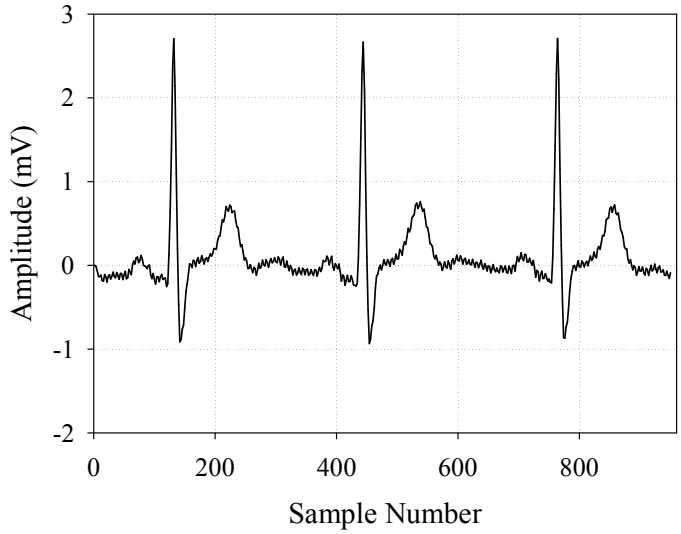

Figure 1.18: ECG signal corrupted with PLI

1.4.2 Baseline wander

BW may be caused in chest-lead ECG signals with large movement of the chest due to cough or breathing, or when an arm or leg is moved in the case of limb-lead ECG acquisition. Baseline drift can sometimes cause variations in temperature and bias in the amplifiers. Its frequency range generally falls below 0.5 Hz. To remove baseline drift a high pass filter with cut-off frequency 0.5 Hz is usually used. A sample wave is given in Figure 1.19.

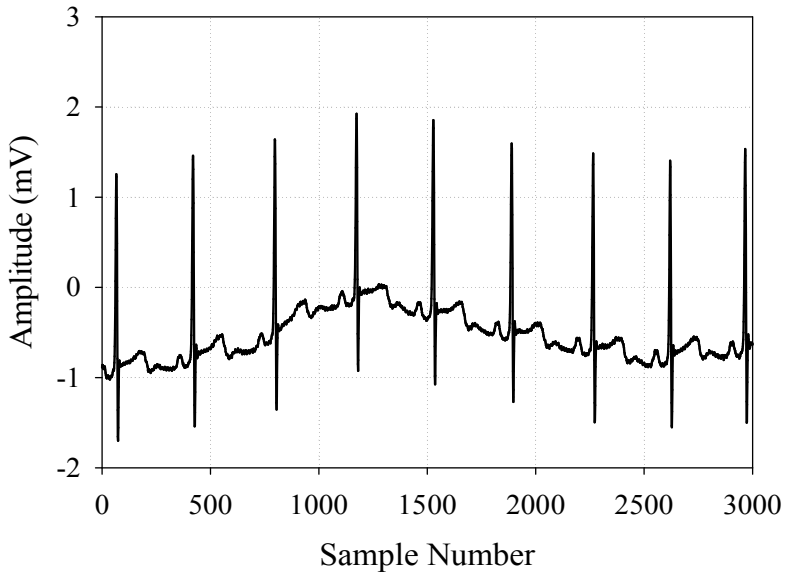

Figure 1.19: ECG signal with baseline wander

1.4.3 Electrode motion artifacts

Motion artifact is the noise introduced to the ECG that results from motion of the ECG electrode. Specifically, electrode movement causes deformations of the skin around the electrode site, which in turn cause changes in the electrical characteristics of the skin around the electrode.

Motion artifact can produce large amplitude signals in the ECG and can resemble the P, QRS, and T waveforms of the ECG. Motion artifact is prevalent during ambulatory monitoring and treadmill stress testing. As shown in Figure 1.20, it can generate larger amplitude signal in ECG waveform. An adaptive filter can be used to remove the interference of motion artifacts.

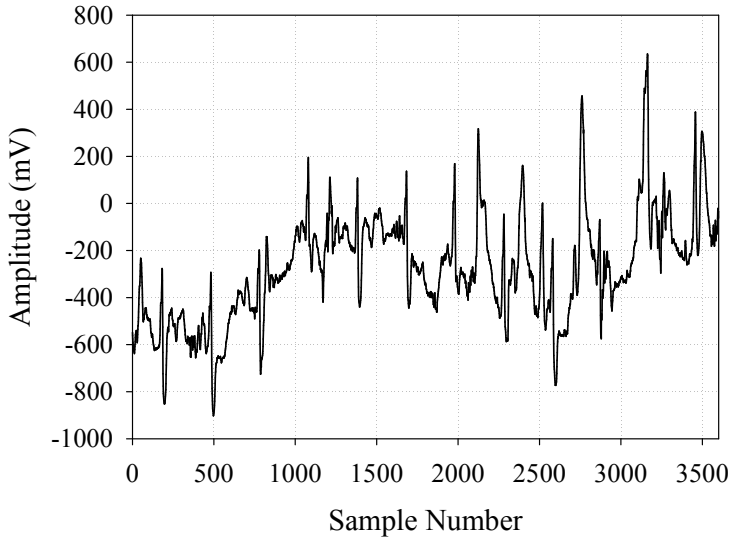

Figure 1.20: Electrode motion artifact

1.4.4 Muscle contraction

Generally muscle contraction is produced due to muscle electrical activity. The signals resulting from muscle contraction is assumed to be transient bursts of zero-mean band-limited Gaussian noise. Electromyogram (EMG) interferences generate rapid fluctuation which is faster than ECG wave. As shown in Figure 1.21 The frequency spectrum of the EMG signal collected with commonly used sensors ranges from 0 to 400 Hz (Carlo J. De Luca, 2010).

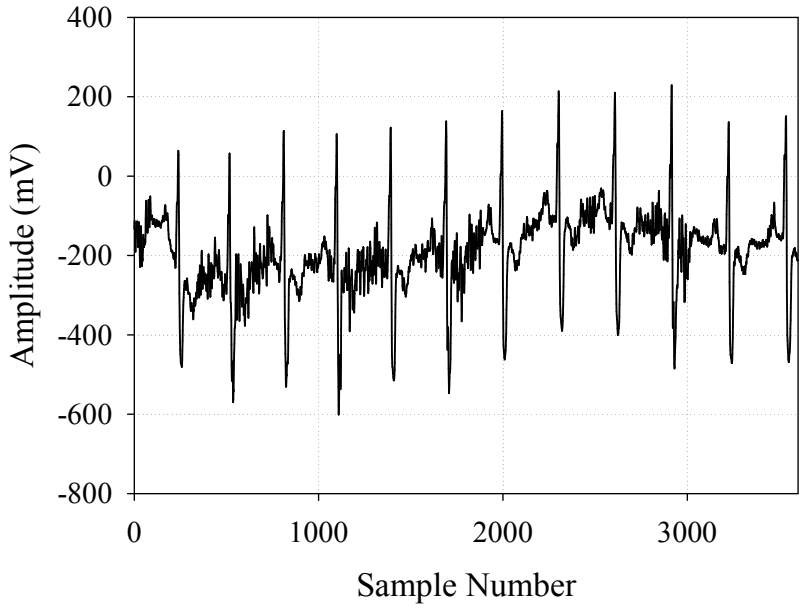

Figure 1.21: Muscle artifact

1.5 General ECG classification system

The ECG signal can be used as a reliable indicator of heart diseases. Usually in Holter monitors when the recording of ECG signal is complete usually after 24 or 48 hours, the physician need to perform the signal analysis. Since it would be extremely time consuming to go through a long ECG signal, an automatic analysis process may be required which determines different types of heart beats, rhythms etc.

A general ECG classification system shown in Figure 1.22 may include three stages, viz data acquisition and signal processing, feature extraction, and an ECG classifier. The goal of data acquisition is to capture the ECG signal and encode in a form suitable for computer processing. At this stage, care should be given to make sure that no information

is lost. The aim of signal conditioning is to eliminate or reduce unnecessary components such as noise from the ECG. Often, this is done by using suitable filters.

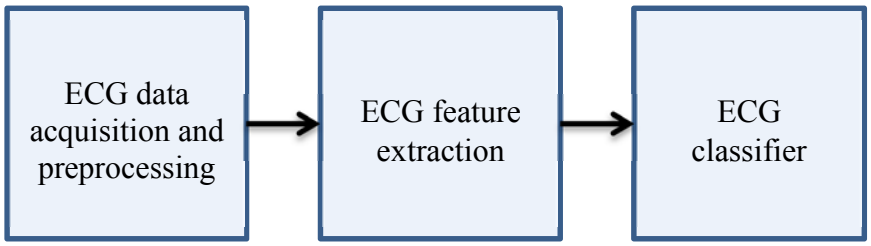

Figure 1.22: Block diagram of ECG classification system

The next stage of the classification system is the feature extraction stage which includes identifying and measuring a small number of parameters or features that best characterize the information of interest in an ECG signal. The features generated can be used as input to a suitable classifier which can effectively identify the different types of ECG signals. Logical processing and pattern recognition, using rule-based expert systems, fuzzy logic algorithms, probabilistic fuzzy logic algorithms or Bayesian analysis, cluster analysis, artificial neural networks, and others techniques may be used to derive conclusions, interpretation and diagnosis.

1.6 Chapter summary

ECG signals are pseudo periodic, non-stationary in nature and whose behaviour may change with time. The proper processing of ECG signal and its correct detection is very important since it determines the condition of the heart. Noises present in ECG signal may lead to

improper diagnosis. To avoid this, a good filtering mechanism is needed for proper ECG diagnosis. As seen from Figure 1.22, the ECG classification system could be implemented by acquiring the data, filtering it for noise, extracting the features and performing the classification using a suitable classifier which is explained in the following chapters.

In chapter 2, a comprehensive up to date literature review was performed on the available noise removal and ECG classification techniques. ECG filtering as well as classification methods used by different authors are examined. It was observed that for better classification accuracy an ECG with high signal-to-noise ratio and low distortion is needed. Further it was observed that adequate importance was not given for the isolated abnormalities present in the ECG. These findings are consolidated in this chapter.

In chapter 3, an introduction to the database selected for the ECG classification (MIT-BIH arrhythmia from Physionet) is described. The filtering method employed for the removal of Baseline Wander (BLW) and PLI is explained. An adaptive filtering technique for the removal of BLW and PLI which is based on GA is proposed. The proposed GA tuned Sign-Data Least Mean Square (SD-LMS) algorithm is implemented. The algorithm was applied to the records from the selected database for removing the BLW and 60Hz PLI. The proposed algorithm gave better signal to noise ratio.

Chapter 4 details the design and development of a new wavelet proposed for ECG classification. The new wavelet is checked for the admissibility conditions. The scales corresponding to the different classes were identified. The designed unoptimized wavelet was evaluated for ECG classification. Results obtained was observed to be better than the existing results reported in literature.

In chapter 5, the proposed wavelet is fine-tuned by GA to further improve classification performance. The optimum wavelet for classification was obtained after several runs of the GA algorithm. Sensitivity and positive predictivity were used to evaluate the performance of the classifier. Results indicate that the classification accuracy increased substantially.

In chapter 6, an attempt to still improve the classification accuracy by exploring it at finer scales was made. The scales corresponding to maximum classification accuracy for each class was identified. It was observed that the optimized wavelet selected at finer scales could effectively differentiate the frequencies in each class. Good time-frequency resolution of the new wavelet transform has helped to successfully differentiate the different types of ECG efficiently.

Chapter 7 gives the conclusion and contribution of this research work. It also suggests the scope for further work.

Chapter 2

LITERATURE SURVEY

Contents

This chapter explores the earlier works done for noise removal and ECG classification. Based on the exhaustive literature survey the limitation of the existing methods and the general objective of this thesis are presented.

2.1 Review of filtering methods

Several methods have been proposed to work out for the removal of BLW. Filtering techniques reported includes linear filters like Finite Impulse Response (FIR) filter and Infinite Impulse Response (IIR) filters, nonlinear filters, polynomial interpolation and wavelet filters. Nitish V. Thakor (1991) used a simple adaptive filtering technique for the removal of BLW, but it lacks a suitable reference signal. Y. Sun (2002), used a Modified Morphological Filtering (MMF) technique for signal conditioning in order to accomplish baseline correction and noise suppression with minimum signal distortion. MMF performs well in terms of the filtering characteristics, but its application may result in waveform distortion. By applying Kalman filters (MA Mneimneh, 2006) BLW noise can be effectively removed, but the Signal-to-Noise Ratio (SNR) is relatively low.

Mohammad Zia Ur Rahman (2010) used a normalized Sign-Sign Least Mean Square (SS-LMS) algorithm for the removal of BLW. Even though the method is less computationally complex, the SNR improvement and the waveform shape are inadequate. He has compared the performance of several signed Least Mean Square (LMS) based adaptive filters with the conventional adaptive LMS algorithm for the elimination of PLI, BLW, muscle and motion artifacts. Linear filters designed by Johnson (2010) and Seema Rani (2011) are used to remove BLW but their fixed cut off frequency may result in a loss of information from the ECG signal. Weituo Hao (2011) introduced a nonlinear mean-median filter that preserves the outline of the BLW. It

avoids distortion caused by the median filter. The reported values are comparatively lower.

Inaki Romero (2011) proposed a system approach to motion artifact reduction in ambulatory recordings, including: selection of electrode configuration, algorithms for motion artifact filtering, custom analog front-ends and integration in wearable electrode patches. Two algorithm methods were tested. The first method applies Independent Component Analysis (ICA) for de-noising multi-lead ECG recordings. The second method was an adaptive filter that uses skin/electrode impedance as the measurement of noise. Also, a wireless patch was presented, which records 3-lead ECG, 1-lead electrode tissue impedance and 3D-acceleration, thus providing the necessary data to test and implement motion artifact algorithms. Results obtained showed that ICA achieves some amount of noise reduction.

P. Mithun (2011) proposed a denoising technique for suppressing EMG noise and motion artifact in ambulatory ECG. EMG noise was reduced by thresholding the wavelet coefficients using an improved thresholding function combining the features of hard and soft thresholding. Motion artifact is reduced by limiting the wavelet coefficients. Thresholds for both the denoising steps are estimated using the statistics of the noisy signal. Denoising of simulated noisy ECG signals resulted in an average SNR improvement of 11.4 dB. It significantly improved R-peak detection, but lacks a common database for comparison. The reconstructed signal quality measured in terms of R peak detection alone.

Fakroul Ridzuan Hashim (2012) reported a new wavelet based Motion Artifact noise removal system . It comprises of two stages. In the first stage wavelet denoising techniques with several threshold methods were employed. In the second stage a combination of a high and low frequency filters is used in order to reduce motion artifact noise. Even though good results have been obtained in terms of SNR, no parameter to measure the quality of the reconstructed signal have been discussed.

Hassan (2014) has described a type of multiple sub-adaptive filters that can remove Power Line Interference from Electrocardiogram. A three sub-adaptive filter of order 30 gave an MSE value of 1.12×10^{-6} and SNR of 20.4 db while removing PLI from ECG.

2.2 Review of ECG classification methods

Automatic classification of ECG have been reported by many investigators. The classification system used inputs like ECG wave interval features (Yeap T.H., 1990 and Hu Y.H., 1993), ECG morphology features, frequency based features (Senhadji L., 1995) and Karhunen-Loeve expansion of ECG morphology (Hu Y.H., 1997).

AI-Fahoum (1999) developed a classifier using wavelet transforms for extracting features and then used a radial basis function neural network to classify the arrhythmia. Six energy descriptors are derived from the wavelet coefficients over a single-beat interval from the ECG signal. Nine different continuous and discrete wavelet transforms are considered for obtaining the feature vector. By utilizing

the Daubechies wavelet transform, an overall classification of 97.5% was obtained. The dataset used for classification consisted of only 159 ECG cycles.

Dingfei Ge (2002) developed a simpler autoregressive(AR) modeling technique to classify normal sinus rhythm and various cardiac arrhythmias including atrial premature contraction, premature ventricular contraction, supraventricular tachycardia, ventricular tachycardia and ventricular fibrillation. The AR coefficients were computed using Burg's algorithm and were classified using a generalized linear model (GLM) based algorithm in various stages. The technique achieved an average sensitivity of 96.78% for the six classes of ECG beats but the classification was performed on a selective database that contained only 856 ECG cycles.

Mohamed I. Owis (2002) presented a study of the nonlinear dynamics of ECG signals for arrhythmia characterization. The correlation dimension and largest Lyapunov exponent were used to model the chaotic nature of five different classes of ECG signals. The model parameters were evaluated for a large number of real ECG signals within each class and the results were reported. The algorithm presented allows automatic calculation of the features. It is seen that it is useful in ECG arrhythmia detection, but discrimination between different arrhythmia types was difficult using such features. The techniques were implemented and applied to ECG signals from the MIT-BIH Arrhythmia Database. The data used was composed of five different types of ECG records but each type was represented by only

64 independent signals for the design set and another 32 signals for the test with each signal 3 sec. long.

Philip de Chazal (2004) described a method for automatic processing of ECG for the classification of the heart beat into five classes based on the recommendations of AAMI EC57:1998 standard. The classifier used feature sets based on ECG morphology, heart beat intervals and RR intervals. They obtained a sensitivity of 75.9% for the supraventricular ectopic beat and 77.7% for ventricular ectopic beat.

Omer T. Inan (2006) proposed a neural network based classifier and achieved good classification accuracy for larger data sets. They had combined wavelet-transformed ECG waves with timing information for the feature set used for classification. In order to demonstrate robustness, the author has chosen 40 files for the first experiment in which 22 were completely foreign to the classifier. The ECG cycles used for training the neural network were selected from the remaining 18 files. The classification accuracy obtained after using 93281 ECG cycles also included ECG cycles that were used to train the neural network.

Abdelhamid Daamouchea (2011) has proposed a Discrete Wavelet Transform (DWT) optimization approach for ECG classification. Particle Swarm Optimization technique and Support Vector Machine were used for classification. Apart from the wavelet features, a few temporal features were also included in the feature set which means the classifier is not fully dependent on the optimized wavelet features. The overall accuracy obtained was 88.84%.

Mariano Llamedo (2011) described a simple classifier based on ECG feature models selected to improve generalization capability. They used both interval and morphological features in their model. For classification purpose interval based features from RR sequence and wavelet based features were used and they have reported a sensitivity of 95% for normal beats, 61% for Supraventricular beats and 75% for ventricular beats.

Roshan Joy Martis (2012 June, 2012 October, 2013 March) have automatically classified normal, RBBB, LBBB, atrial premature contraction and PVC. They used the features from the principal components of segmented ECG beats, DWT coefficients, DCT coefficients and bispectrum of the ECG for classification purpose. These approaches were independently classified using feed forward Neural Network and Least Square-Support Vector Machine. Using 34,989 ECG beats from MIT-BIH database they obtained an average accuracy of 93.48%, average sensitivity and specificity of 99.27% and 98.31% respectively with Least Square-Support Vector Machine (LS-SVM) having Radial Basis Function (RBF) as kernel.

Roshan Joy Martis (2013 August, 2013 September) proposed two methods for ECG characterization of which the first work included the time based methods like linear prediction, Principal Component Analysis (PCA), Linear Discriminant Analysis (LDA), Independent Component Analysis (ICA) and Discrete Wavelet Transform(DWT) for dimensionality reduction. These dimensionality reduced features were fed to the support vector machine, neural network and PNN classifiers

for automated diagnosis. They attained an average sensitivity, specificity, PPV and accuracy of 99.97%, 99.83%, 99.21% and 99.28% respectively. In the other work two approaches, one using cumulant features of segmented ECG and other using cumulants of DWT coefficients were used for the classifier. Classification was done using a three layered neural network and obtained an average accuracy of 94.52%, sensitivity of 98.61% and specificity of 98.41%. TE author has used a 10-fold cross validation technique for training and testing of classifier, ie., the entire data set is sub-sampled into 10 sets each having same distribution of samples for each class, which gives higher percentage of classification.

Karpagachelvi (2014) used an Extreme Learning Machine (ELM) classifier which works by searching for the best value of the parameters that tune its discriminant function, and upstream by looking for the best subset of features that feed the classifier. The ECG data from the Physionet arrhythmia database is used to classify five kinds of abnormal waveforms and normal beats. In particular, the sensitivity of the ELM classifier was tested and that was compared with SVM combined with two classifiers, namely the KNN classifier and the Radical Bias Function (RBF) neural network classifier, with respect to the dimensionality and the number of available training beats. A total of the morphology and temporal features used for the classifier equals 303 for each beat. With 40416 test beats the overall and average accuracies obtained were only 89.74% and 89.78% respectively.

Morita (2015) has done a study to analyze the discrepancy of interpretation by physicians from different specialties and a computer-generated ECG reading in regard to a T Wave Inversion (TWI) in lead aVL. In this multidisciplinary prospective study, a single ECG with isolated TWI in lead aVL that was interpreted by the computer as normal, was given to all participants to interpret in writing. The readings by all physicians were compared by level of education and by specialty to one another and to the computer interpretation. A total of 191 physicians participated in the study. Of the 191 physicians 48 (25.1%) identified and 143 (74.9%) did not identify the isolated TWI in lead aVL.

Eskola MJ (2007) described a case of isolated temporary occlusion of the major side branches of the Right Coronary Artery (RCA) during percutaneous coronary intervention, recognized by angiography findings and typical ECG changes. Isolated right ventricular infarction (RVI) is a rare event. The electrocardiographic (ECG) pattern of RVI, ST-elevation in lead V_{4R} and in anterior chest leads V_{1-3} is similar to that of a proximal occlusion of a small, non-dominant RCA. The ECG changes may be misinterpreted as signs of infarction of the anterior wall. This paper demonstrates how one might avoid wrong decisions even in the catheterization laboratory by putting attention to the anatomical interpretation of the ECG.

2.3 Present issues and remedies

Based on the detailed study of the published works, it is seen that ECG detection and classification is given much importance in the field of biomedical signal processing. The first stage of ECG classification is acquiring the signal and pre-processing it for the removal of noise. The commonly seen noises in ECG are baseline wander, power line interference and muscle noise.

Filtering techniques reported includes linear filters like FIR filter and IIR filters, nonlinear filters, polynomial interpolation and wavelet filters. A modified morphological technique used for signal conditioning performs well in terms of the filtering characteristics, but its application may result in waveform distortion. BLW noise could be removed effectively by applying Kalman filters, but it was seen that the Signal-to-Noise Ratio was relatively low. A less computationally complex method using signed LMS for the removal of the different noises was reported. The method used signed LMS methods that gave good results but SNR improvement and the waveform shape were inadequate.

ECG classification is one of the important areas where a vast amount of work is still going on. The different classification techniques implemented uses interval features, morphological features as well as frequency based features. Some of the features include heart beat & RR intervals, wavelet based features, principal components of segmented ECG beats, DCT coefficients, bispectrum of the ECG, cumulant

features of segmented ECG & DWT coefficients. The different classification methods employed includes NN, SVM, RBF, ELM classifiers etc. Even though different classification methods were used it is seen that even though the results obtained are acceptable, it needs an improvement.

It is seen that in some of the works the authors have obtained high percentage of sensitivity, specificity and positive predictive value. They have used reconstructed databases for classification and the classification was performed by using a ten-fold cross validation scheme. In this scheme the dataset for testing and training was built by dividing the entire ECG cycles in the selected database into ten sets each having similar proportion of samples. Nine sets were used for training and the remaining one set used for testing. The training and testing process was repeated for all the ten sets. The average of the ten performance measures was taken as the final value which gave high levels of accuracy.

The main requirement of ECG classification is a reliable database that could provide enough ECG records and valid descriptions on the different cycles for proper validation. Even though many databases are available including the Physionet, it is seen that many of the researchers do not use such standard databases.

On observing a few case studies on isolated ECG abnormalities, it is seen that there is a discrepancy of interpretation of these cycles by physicians in many situations. It is observed that none of the works

related to ECG classification have given importance in this area. Hence there is a need for sucessfully identifying the isolated abnormalities.

The following are some of the drawbacks found based on the literature survey.

(i) A few techniques for ECG noise removal that could be used for ambulatory monitoring does exist, still a simple and efficient method that could be implemented on a portable ECG monitor need to be introduced.

(ii) Even though the classification results obtained were acceptable, an improvement in classification accuracy is desired.

(iii) No attempt has been reported in the literature for identifying the isolated abnormalities, which pose a silent threat to patients.

(iv) Not all of the methods have chosen a standard classification scheme of arrhythmia such as AAMI EC57:1998 standard.

2.4 Objective of the thesis

The objective of this work includes;

(i) Design of a less complex adaptive filter that could be implemented on hardware targets such as portable ECG monitors.

(ii) Design and optimization of a new wavelet for ECG classification with better classification accuracy.

(iii) Identification of isolated abnormalities which pose a threat to patients.

Chapter 3

DATA ACQUISITION AND ECG NOISE REMOVAL

Contents

In this chapter the reasons for selecting a particular ECG database and the need for noise removal are discussed. Further a method for effectively reducing noise has been proposed. The proposed method has been verified, tested and the results are analysed.

3.1 ECG Database

3.1.1 PhysioNet

PhysioNet is a website that offers free web access to large collections of recorded physiologic signals and related open-source software. PhysioNet is intended to develop interaction among investigators from many different disciplines. The worldwide community of PhysioNet users includes basic scientists, mathematicians, clinicians, educators, engineers and students working in biomedical sciences and related areas. One of the main components of the PhysioNet is the PhysioBank which is a large and growing archive of well-characterized digital recordings of physiologic signals and related data for use by the biomedical research community. PhysioBank currently includes databases of multi-parameter cardiopulmonary, neural, and other biomedical signals from healthy subjects and patients with a variety of conditions with major public health implications, including sudden cardiac death, congestive heart failure, epilepsy, gait disorders, sleep apnea, and aging (PhysioNet, 2015).

Nearly 27 ECG databases are present in the server out of which some of the prominent ones are

- ANSI/AAMI EC13 Test Waveforms
- European ST-T Database
- Long-Term ST Database
- MIT-BIH Arrhythmia Database
- MIT-BIH Noise Stress Test Database

- BIDMC Congestive Heart Failure Database
- ECG-ID Database
- Post-Ictal Heart Rate Oscillations in Partial Epilepsy
- QT Database
- Smart Health for Assessing the Risk of Events via ECG
- Abdominal and Direct Fetal ECG Database.
- AF Termination Challenge Database
- Creighton University Ventricular Tachyarrhythmia Database
- Electrocardiographic Imaging of Myocardial Infarction
- Intracardiac Atrial Fibrillation Database
- Long-Term AF Database.
- MIT-BIH Atrial Fibrillation Database
- MIT-BIH ECG Compression Test Database
- MIT-BIH Long-Term Database
- MIT-BIH Malignant Ventricular Arrhythmia Database
- MIT-BIH ST Change Database.
- MIT-BIH Supraventricular Arrhythmia Database
- Non-Invasive Fetal Electrocardiogram Database
- PAF Prediction Challenge Database
- St. Petersburg Institute of Cardiological Technics 12-lead Arrhythmia Database
- Sudden Cardiac Death Holter Database
- T-Wave Alternans Challenge Database

As shown in Figure 1.22, the first stage of ECG classification system is acquiring ECG data and preprocessing it for noise removal. ECG databases selected for analysis were the MIT-BIH Noise Stress Test database and MIT-BIH Arrhythmia database.

3.1.2 MIT-BIH Noise Stress Test database

The MIT-BIH Noise Stress Test database includes different ECG waveforms and artifact that an arrhythmia detector might encounter in routine clinical use. It includes twelve, ½ hour ECG recordings and three, ½ hour recordings of noise typically encountered in ambulatory ECG recordings (A.L. Goldberger, 2000). The BLW used for the validation of the proposed SD-LMS filter was taken from this database.

3.1.3 MIT-BIH Arrhythmia Database Directory

The source of the ECGs included in the MIT-BIH Arrhythmia Database is a set of over 4000 long-term Holter recordings that were obtained by the Beth Israel Hospital Arrhythmia Laboratory between 1975 and 1979 (Moody R. M., 1997). Approximately 60% of these recordings were obtained from inpatients. The database contains 48 records labelled from 100 to 124 and 200 to 234 which includes a variety of rare but clinically important phenomena that would not be well-represented by a small random sample of Holter recordings. The phenomena included were complex ventricular, junctional, and supraventricular arrhythmias and conduction abnormalities. The records in the database belonged to 25 men aged between 32 and 89 years, and 22 women aged between 23 and 89 years. The wavelet optimization and

ECG classification were performed using this database. Each of these record is almost 30 minutes long.

3.1.3.1 *Digitization*

The analog outputs of the ECG recorder were filtered to limit analog-to-digital converter saturation and for anti-aliasing, using a pass band from 0.1 to 100 Hz relative to real time, well beyond the lowest and highest frequencies recoverable from the recordings. The band pass-filtered signals were digitized at 360 Hz per signal relative to real time. The ADCs were unipolar, with 11-bit resolution over a ±5 mV range. The digitized file is stored in the WFDB signal file formats (Moody G. B., 2014). For each database record, a header file specifies the names of the associated signal files and their attributes like record name, number of signals, sampling frequency etc.

3.1.3.2 *Annotations*

The PhysioBank databases include validated annotations for each recording that point to specific locations within a recording and describe events at those locations. The standard set of annotation codes was originally defined for ECGs, and includes both beat annotations and non-beat annotations. These annotations were validated by qualified cardiologists. In addition to these annotations, ECG rhythms, signal quality labels and comments are also made available. The symbols used in the annotations are given in Table 3.1. The ECG records used for training and testing and the number of cycles corresponding to various diseases are shown in Table 3.2 and 3.3 (Moody R. M., 1997).

In this work the implementation of the filtering and classification algorithms was done in MATLAB R2009a. Corresponding to each patient record there is an ECG data file, an annotation file and a header file giving details of the patient. These files are not readable by MATLAB. It could be converted to the required format by using functions available in WFDB directory which operates in Cygwin environment.

Table 3.1: Symbols used in the annotations

Normal labelled beats	N	Normal Beat
	L	Left Bundle Branch Block beat
	R	Right Bundle branch block beat
	e	Atrial escape beat
	J	Nodal (junctional) escape beat
Supraventricular ectopic beats	A	Atrial Premature beat
	a	Aberrated atrial premature beat
	j	Nodal (junctional) premature beat
	S	Supraventricular premature beat
Ventricular ectopic beats	V	Premature ventricular contraction
	E	Ventricular escape beat
Fusion beats	F	Fusion of ventricular and normal beat
	f	Fusion of paced and normal beat
Unknown beats	P	Paced rhythm
	Q	Unclassified beat
Ignored	!	Ventricular flutter wave
	p	Recording tape pause interval

Table 3.2: Types of beat in the training set

Record	Type of beat															
	N	**L**	**R**	**A**	**a**	**J**	**S**	**V**	**F**	**!**	**e**	**j**	**E**	**P**	**f**	**p**	**Q**
101	1860			3													2
106	1507							520									
108	1739			4				17	2			1					11
109		2492						38	2								
112	2537			2													
114	1820			10		2		43	4								
115	1953																
116	2302			1				109									
118			2166	96				16									10
119	1543							444									
122	2476																
124			1531	2		29		47	5			5					
201	1625			30	97	1		198	2			10					37
203	2529				2			444	1								4
205	2571			3				71	11								
207		1457	86	107				105		472			105				
208	1586						2	992	373								2
209	2621			383				1									
215	3195			3				164	1								
220	1954			94													
223	2029			72	1			473	14		16						
230	2255							1									

Table 3.3: Types of beat in the testing set

Record	Type of beat															
	N	L	R	A	a	J	S	V	F	!	e	j	E	P	f	p	Q
100	2239			33				1									
103	2082			2													
105	2526							41									5
111		2123						1									
113	1789				6												
117	1534			1													
121	1861			1				1									
123	1515							3									
200	1743			30				826	2								
202	2061			36	19			19	1								
210	2423				22			194	10				1				
212	923		1825														
213	2641	-		25	3			220	362								
214	-	2003						256	1								2
219	2082			7				64	1							133	
221	2031							396									
222	2062			208		1						212					
228	1688			3				362									
231	314		1254	1				2								2	
232	-		397	1382								1					
233	2230			7				831	11								
234	2700					50		3									

3.1.4 WFDB library

Wave Form Data Base (WFDB) library is a portable set of functions for reading and writing files in the formats used in PhysioBank (Moody G. B., 2014). This software package was originally developed by Massachusetts Institute of Technology (MIT) for viewing, analyzing, and creating recordings of physiologic signals. It uses package header files to specify the format and attributes of signal files. The ECG patient records from MIT-BIH arrhythmia database were converted to *'.mat'* and its annotations into *'.txt'* format using the subroutines in this library.

3.1.5 Cygwin

Cygwin is a collection of tools that provide a Linux look and feel environment for Windows. Building the WFDB Software Package using Cygwin assures that WFDB applications will behave on MS-Windows as much as possible like they do on other platforms. (Moody G. B.). It is possible to launch Windows applications from the Cygwin environment, as well as to use Cygwin tools and applications within the Windows operating context. The subroutines in WFDB library were run in the Cygwin environment.

3.2 ECG noise removal

ECG signal processing is a huge challenge since the actual signal is measured in a noisy environment. As explained in section 1.4 the main sources of noise are PLI, BLW, electrode motion artifacts and electrical potential due to muscular contraction. BLW is a low

frequency component present in the ECG. This may be due to various reasons like offset voltages in the electrodes, respiration activity, patient movement and loose electrodes during recording. Baseline noises occur in the frequency range of 0.05 to 0.5 Hz. while the 50/60Hz PLI may be due to improper grounding of the ECG recording device. The different types of filters commonly used for ECG noise removal include linear filters like finite impulse response filter and infinite impulse response filters, nonlinear filters, wavelet filters and adaptive filtering techniques.

3.3 Adaptive filtering algorithms

Adaptive Filters (AF) work on the principle of minimizing an error function, generally the mean squared difference, between the filter output signal and a target signal. These filters are advantageous because they do not require a prior knowledge of signal as in the case of fixed filters. An AF learns statistics of the input source and tracks them if they vary slowly. AF can thus be used efficiently for estimation and identification of non-stationary signals like ECG. LMS algorithm and Recursive Least Squares algorithm (RLS) and their variants can be used to solve this problem (Rangayyan, 2004). Compared to RLS algorithms, the LMS algorithms do not involve any matrix operations and hence require fewer computational resources and memory. The implementation of the LMS algorithms is easier than the RLS algorithms. To further reduce the amount of computation, signed LMS can be used, especially when the input data rate is high. These filters perform well when it is meant to be implemented on an embedded system.

3.3.1 LMS algorithm

Figure 3.1 shows a block diagram of the system identification model. The unknown system is modeled by an FIR filter with adjustable coefficients. Both the unknown time-variant system and FIR filter model were excited by an input sequence $u(n)$. The adaptive FIR filter output $y(n)$ was compared with the unknown system output $d(n)$ to produce an estimation error $e(n)$. The estimation error represents the difference between the unknown system output and the model (estimated) output. The estimation error $e(n)$ was then used as the input to an adaptive control algorithm which corrected the individual tap weights of the filter. This process was repeated through several iterations until the estimation error $e(n)$ becomes sufficiently small in some statistical sense. The resultant FIR filter response now represents that of the previously unknown system.

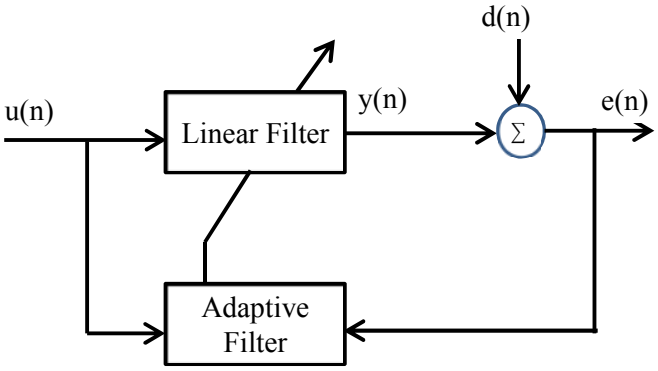

Figure 3.1: Adaptive filter

3.3.2 Sign LMS

Some adaptive filter applications require implementation of adaptive filter algorithms on hardware targets, such as digital signal

processing devices, FPGA targets, and application-specific integrated circuits. These targets require a simplified version of the standard LMS algorithm. The signum function, as defined by the following equation, can simplify the standard LMS algorithm.

$$sgn(x) = \begin{cases} 1; & x > 0 \\ 0; & x = 0 \\ -1; & x < 0 \end{cases} \quad \text{..... (3.1)}$$

Applying the signum function to the standard LMS algorithm leads to three types of sign LMS algorithms (Haykin, 2009).

3.3.2.1 *Sign-error LMS algorithm*

The signum function is applied to the error signal $e(n)$. This algorithm updates the coefficients of an adaptive filter using the following equation

$$\overline{w}(n+1) = \overline{w}(n) + \mu . sgn\big(e(n)\big).\overline{u}(n) \quad \text{.....(3.2)}$$

Here when $e(n)$ is zero, this algorithm does not involve any multiplication operations. When $e(n)$ is not zero, this algorithm involves only one multiplication operation (Haykin, 2009).

3.3.2.2 *Sign-sign LMS algorithm*

The signum function is applied to both $e(n)$ and $\overline{u}(n)$. This algorithm updates the coefficients of an adaptive filter using the following equation

$$\overline{w}(n+1) = \overline{w}(n) + \mu . sgn(e(n)).sgn(\overline{u}(n)) \text{.....(3.3)}$$

When either $e(n)$ or $\overline{u}(n)$ is zero, this algorithm does not involve multiplication operations. When neither $e(n)$ or $\overline{u}(n)$ is zero, this algorithm involves only one multiplication operation.

3.3.2.3 ***Sign-data LMS algorithm***

In the Sign-data LMS algorithm (SD-LMS) the signum function is applied to the input signal vector $\overline{u}(n)$. This algorithm updates the coefficients of an adaptive filter using the following equation

$$\overline{w}(n+1) = \overline{w}(n) + \mu.e(n).sgn(\overline{u}(n)) \quad \text{.....(3.4)}$$

When $\overline{u}(n)$ is zero, this algorithm does not involve multiplication operations. When $\overline{u}(n)$ is not zero, this algorithm involves only one multiplication operation (Haykin, 2009).

In Equations 3.2 through 3.4 the vector w contains the weights applied to the filter coefficients and vector u containing the input data. $e(n)$ is the error at time n which has to be minimized. The constant μ is a step size, which controls the amount of gradient information used to update each filter coefficient (Simon Haykin, 2003). The step size directly affects how quickly the filter will converge towards the reference input. If μ is very small, then the coefficient will change only a small amount on each update, and the filter may converge very slowly. With a larger step size more gradient information may be included in each update and the filter may converge quickly, but if the step size is very large, the coefficients may change too quickly and the filter may diverge. So choosing a correct value of step size is important.

3.4 Proposed Adaptive Filter using GA tuned SD-LMS algorithm

This section explains an adaptive filtering technique for denoising the ECG which is based on GA tuned SD-LMS algorithm. This technique minimizes the mean-squared error between the primary input, which is a noisy ECG, and a reference input which can be either noise that is correlated in some way with the noise in the primary input or a signal that is correlated with ECG, in the primary input. Noise in ECG is used as the reference signal in this work. The block diagram of the proposed method used for noise removal is shown in Figure 3.2.

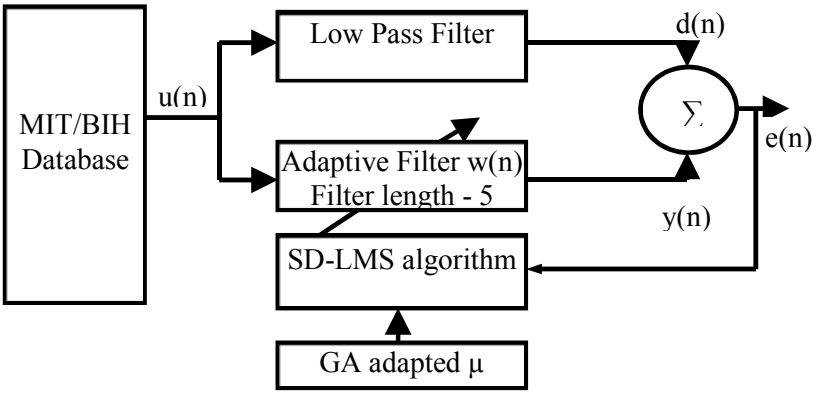

Figure 3.2: Block diagram of the proposed ECG noise removal Filter.

The SD-LMS algorithm used here requires two datasets, one the primary input $x(n)$ which is the ECG corrupted with BLW/PLI/any other noise. Here $x(n)$ was obtained by adding the noise with ECG record of MIT BIH Arrhythmia database. Four thousand samples from each record were selected. The BLW noise used to corrupt the ECG was taken from MIT-BIH NSTDB database (Goldberger AL, 2000) and

the PLI used to corrupt the ECG was an artificial sine wave generated with a frequency of 60 Hz, amplitude of 1mV and a sampling frequency of 360 Hz.

The reference input containing noise signal $d(n)$ was obtained by filtering the noisy ECG with a Kalman filter (Filtering & Processing Tools, 2000).

In the figure, $e(n)$ is the error signal and $w(n)$ the weights applied to the filter coefficients. The filter length was set to 5. The step size $'\mu'$ was optimized with GA. Since GA combines survival of the fittest among chromosomes with structured and randomized information (Mitchell, 1998), it has the ability to identify the optimum value of step size. Reproduction, Crossover and Mutation are the basic operators in GA which helps in the convergence of the solution. Improvement in SNR was taken as the fitness function. The number of generations was chosen as 500 and population size 50. The initial values of μ's were randomly set in the range of 0.0001 to 0.1. Roulette wheel selection technique was used. Elite count was set as 2 and cross over fraction 0.8. Scales and shrink are two important parameters for mutation function.

Scale controls the standard deviation of the mutation at the first generation and shrink controls the rate at which the average amount of mutation decreases. The scale and shrink parameters decide the standard deviation of the Gaussian distribution used in the mutation function. Record 105 was used for training. Theoretically to ensure a good convergence rate and stability, μ should be within the practical bounds as given by Equation 3.5.

$$0 < \mu < \frac{1}{N(Input\ Signal\ Power)} \quad \text{.....(3.5)}$$

where *N* is the number of samples in the signal. It is ensured that the optimized value of μ satisfies this condition.

In order to evaluate the performance of the filter few ECG records were selected from MIT/BIH Arrhythmia database (Moody R. M., 1997). This record was corrupted with real BLW noise from MIT-BIH NSTDB database (Goldberger AL, 2000) and an artificial PLI. It gave an average SNR improvement of 10.75 dB for BLW and 24.26 dB for PLI which is better than the reported results (Weituo Hao (2011), Mohammad Zia Ur Rahman (2009), Y. Sun (2002) and Hassan (2014)).

3.5 Results and Discussion

The proposed filter was implemented in Matlab. The first five records from the MIT-BIH Arrhythmia database were added with BLW noise and PLI noise. These ECG records with noise were given as input to the proposed filter.

3.5.1 ECG with BLW

The optimum value of μ obtained for the SD-LMS algorithm was 0.00563 in the case of BLW noise. The SNR was calculated using equation (3.5).

$$SNR = 10log_{10}\left(\frac{S_p}{N_p}\right) \quad \text{.....(3.5)}$$

where S_p and N_p denotes the power of the signal and noise respectively.

Figure 3.3 shows the plot of a few cycles from record 100 & 105. BLW noise taken from MIT-BIH NSTDB database is shown in Figure 3.4. These signals were added to give the corrupted ECG as shown in Figure 3.5.

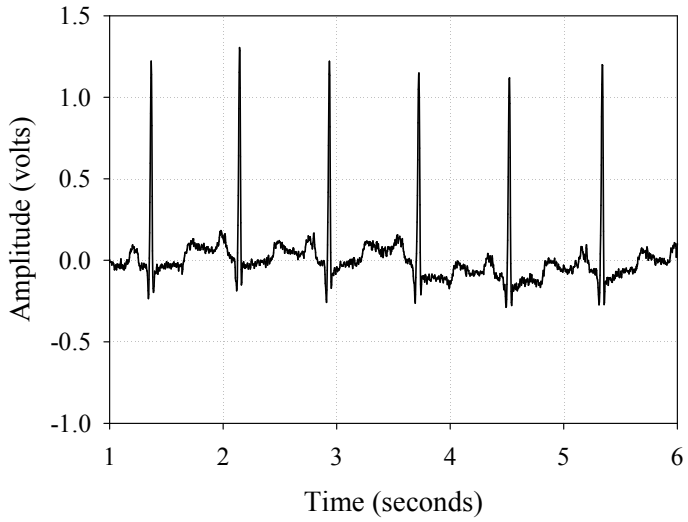

Figure 3.3a: ECG Record 100 from MIT-BIH database

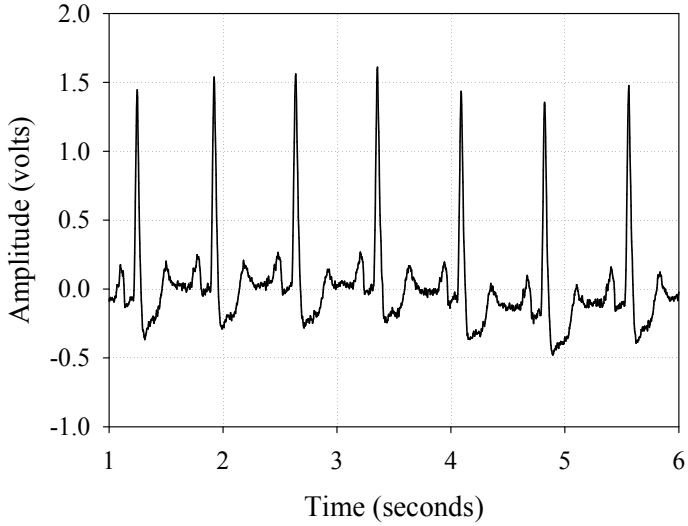

Figure 3.3b: ECG Record 105 from MIT-BIH database

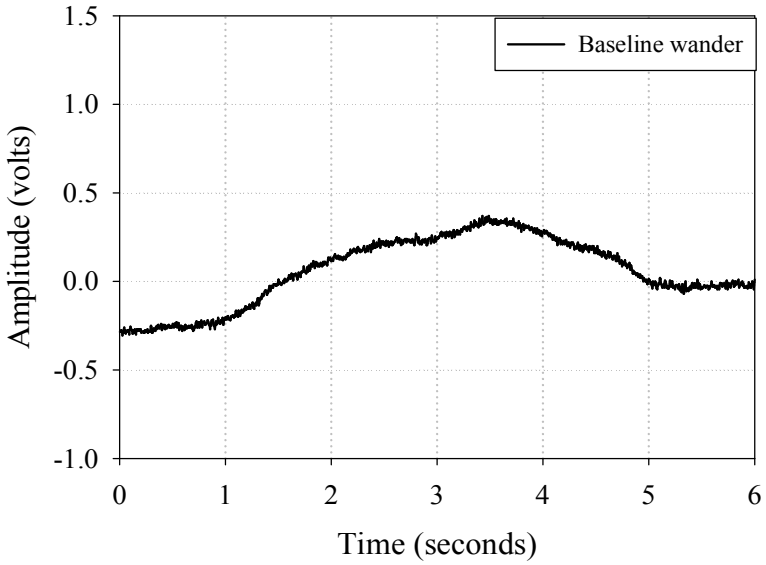

Figure 3.4: BLW from MIT-BIH-NSTDB

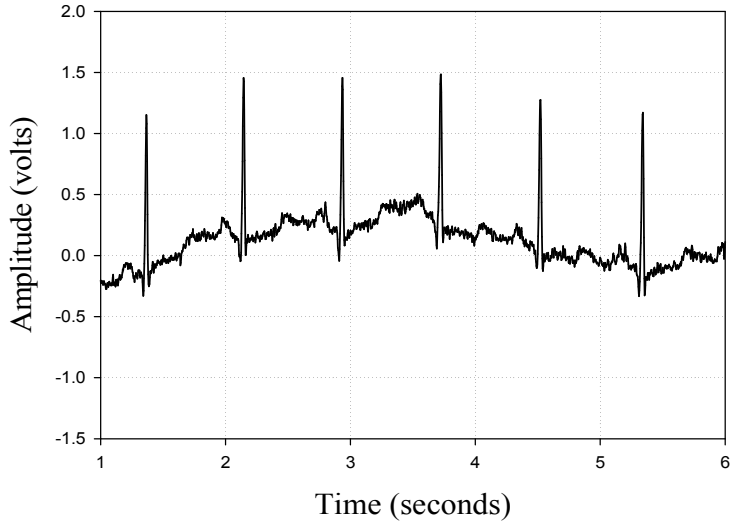

Figure 3.5a: ECG Record 100 corrupted with BLW

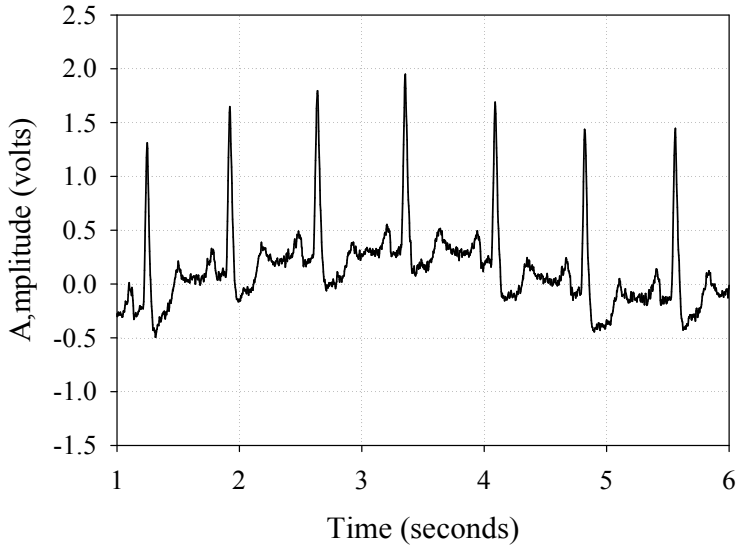

Figure 3.5b: ECG Record 105 corrupted with BLW

Table 3.4 shows the SNR improvement and the correlation coefficient obtained for BLW removal on five records from MIT-BIH Arrhythmia database. The average SNR improvement obtained is 10.75 dB. The SD-LMS filtered ECG is shown in Figure 3.6.

Table 3.4: SNR improvement and correlation coefficient for BLW

Record	SNR before filtering (dB)	SNR after filtering (dB)	SNR improvement (dB)	Correlation coefficient
100	0.8218	11.2061	10.3843	0.9626
105	2.5370	15.4090	12.8719	0.9863
108	1.1365	11.2618	10.1253	0.9651
203	2.3729	13.5545	11.1816	0.9791
228	3.6689	12.8811	9.2122	0.9768
Average	2.10742	12.8625	10.7551	0.9739

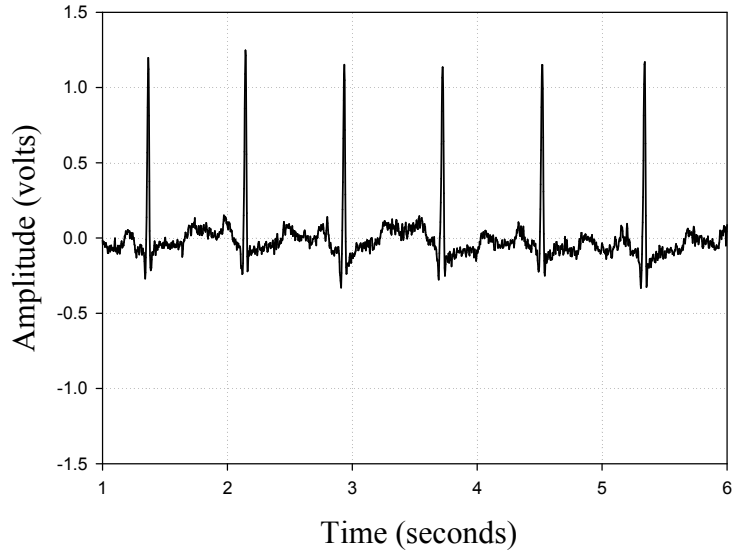

Figure 3.6a: New SD-LMS filtered ECG (Record 100)

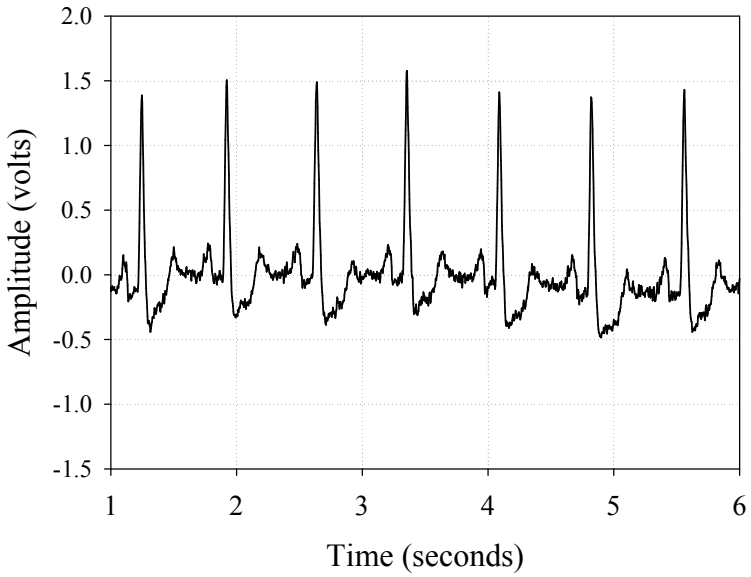

Figure 3.6b: New SD-LMS filtered ECG (Record 105)

Comparing the results with that obtained by Mohammad Zia Ur Rahman (2009) the results are better. Figure 3.7 shows a comparison between ECG noise removal using the proposed algorithm and Kalman filtering algorithm. From the Table 3.4 and Figure 3.3 through 3.7, it can be seen that the proposed algorithm removes BLW more efficiently. The disturbances arising in the output of Kalman filter is reduced in SD-LMS filtered output. Correlation coefficient gives a measure of the closeness of the filtered output to the original ECG. From Table 3.4 it is seen that the values close to 1 suggest that there is a positive linear relationship between the original and filtered ECG signals.

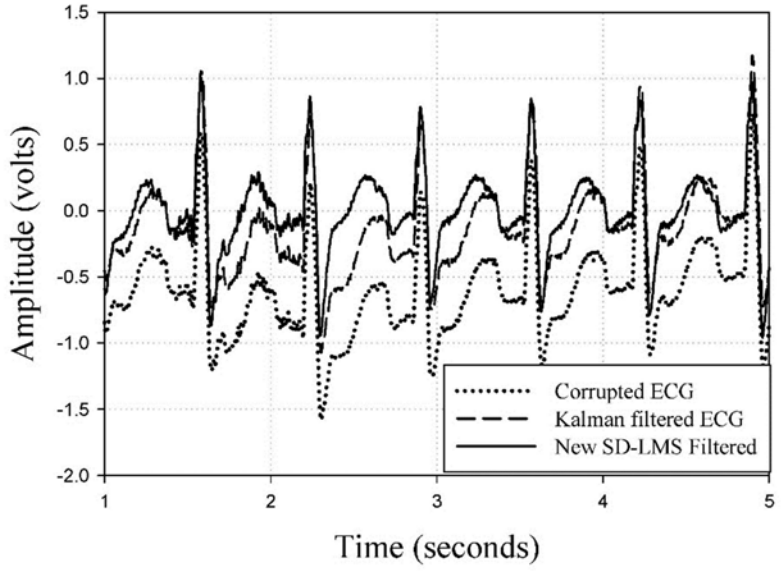

Figure 3.7: Comparison of results obtained for the removal of BLW using Kalman filter and the new SD-LMS algorithm

3.5.2 ECG with PLI

For the removal of PLI the value of μ in the SD-LMS algorithm set was 0.008564. This value was obtained after optimization. An artificially generated sine wave was used as the reference input. This was added with ECG to get the corrupted signal. SNR and correlation coefficients were computed for the first five records of the database and is shown in Table 3.5. An average SNR improvement of 24.26 dB is achieved which is better than the previously reported results (Mohammad Zia Ur Rahman 2010, Hassan 2014). Figure 3.8 shows the first few cycles from record 105 added with PLI and Figure 3.9 gives the filtered output. ECG with PLI and Figure 3.9 gives the filtered output. The peridogram power spectral density estimate with and without PLI is shown in Figure 3.10 and 3.11. It can be seen from Figure 3.11 that the peak corresponding to the 60 Hz has been removed. From these plots it is evident that PLI can also be eliminated successfully.

Table 3.5: SNR improvement and correlation coefficient for PLI

Record	SNR before filtering (dB)	SNR after filtering (dB)	SNR improvement (dB)	Correlation coefficient
100	15.4858	40.4888	25.0030	1.0000
105	8.1129	31.8853	23.7724	0.9997
108	14.9415	38.6769	23.7354	0.9999
203	8.6042	31.9102	23.3060	0.9997
228	13.0096	38.4940	25.4844	0.9999
Average	12.0308	36.2910	24.2602	0.9998

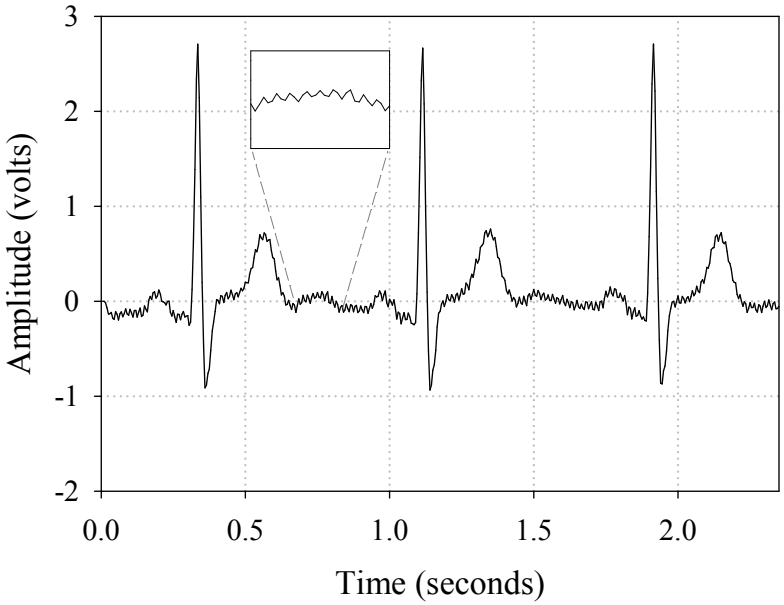

Figure 3.8: ECG corrupted with 60 Hz PLI

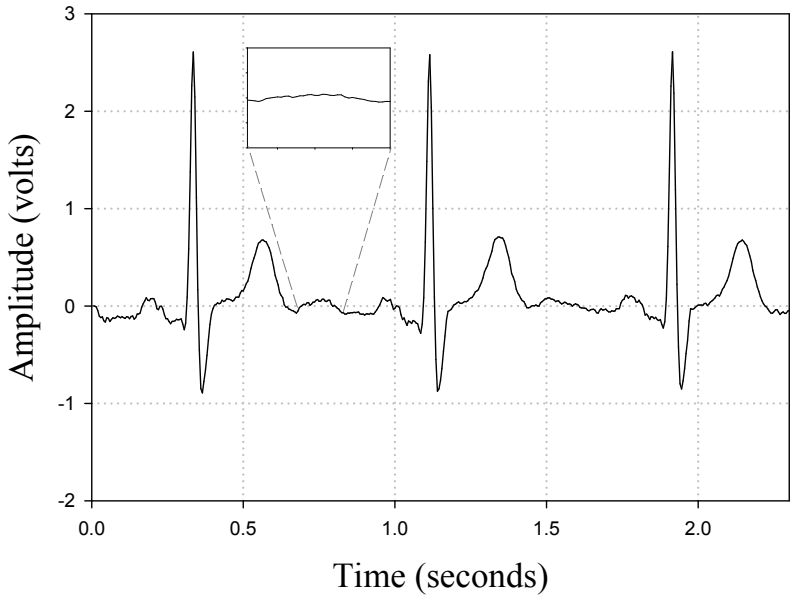

Figure 3.9: ECG filtered for PLI with the proposed SD-LMS filter

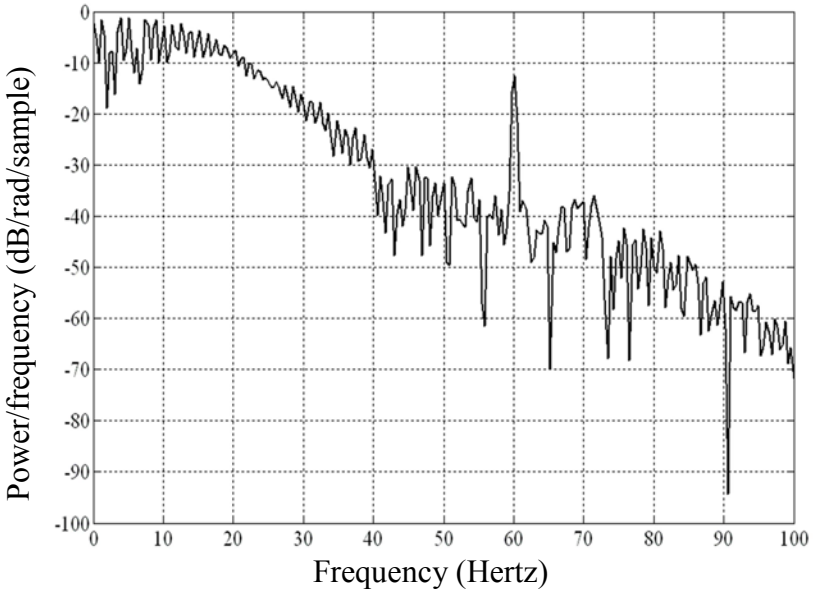

Figure 3.10: Peridogram PSD of ECG with 60 Hz interference

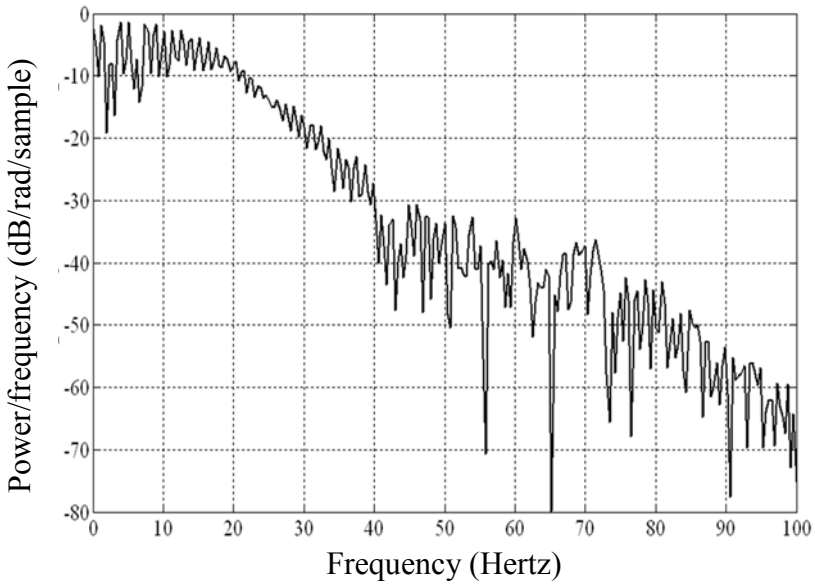

Figure 3.11: Peridogram PSD of PLI filtered ECG

3.6 Chapter summary

In this chapter, an adaptive filter that use the GA tuned SD-LMS algorithm for the removal of BLW and PLI from ECG signals is proposed. The adaptive filter requires a reference input that is uncorrelated with the signal of interest, but closely correlated with the interference or noise in some manner. The reference signal generated by Kalman filter, was highly correlated with the noise in the ECG and hence yielded a good result. It is seen that the step size 'μ' optimized with GA helps in obtaining a better SNR value.

In order to access the impact of introducing the filtering technique the following measures were taken: (i) The value of correlation coefficient was calculated and it was found to be near to '1' which indicates a close resemblance of the filtered ECG signal with the original ECG signal. (ii) The classification of the complete database was done using original as well as filtered ECG records and it was noted that percentage accuracy was better with filtered ECG signal. These results showed that the useful information in the ECG were preserved even after the application of the algorithm.

Chapter 4

DEVELOPMENT OF A NEW WAVELET FOR ECG CLASSIFICATION

Contents

This chapter explains the construction of the proposed mother wavelet which is achieved by shifting and summing up five different Gaussians functions corresponding to the different peaks of the ECG. Before proceeding into the design, an introduction to wavelet transforms, neural networks, basic components used for wavelet design, selection of training & testing dataset and feature extraction is given. The performance of the wavelet was evaluated by classifying the ECG records using features generated with the new wavelet. The results obtained are presented.

4.1 Introduction

Wavelet transforms have become a renowned tool for ECG characterization and many of the works in ECG signal processing have adopted this technique to perform ECG analysis. In this chapter a new Continuous Wavelet Transform (CWT) is designed for ECG classification. The classification was performed with features generated with the new wavelet by a Probabilistic Neural Network (PNN). The recommendations of the AAMI for class labeling and results presentation was followed. The use of the new CWT provides better overall classification sensitivity and positive predictivity for normal beats (Class I), supraventricular beats (Class II) and ventricular beats (Class III) including isolated abnormalities.

4.2 Wavelet Transforms

Wavelets are purposefully crafted to have specific properties that make them useful for signal processing. They are a mathematical function that splits up data into temporal and frequency components simultaneously, hence giving a time-frequency representation of the signal with a resolution matched to its scale. They perform well in analyzing physical situations where the signal contains discontinuities and sharp sudden changes. Wavelets can be used as an exciting new method for solving problems in engineering including wave propagation, data compression, signal processing, image processing, pattern recognition and computer graphics. Wavelets can be combined, using a "shift, multiply and sum" technique called convolution, with portions of an unknown signal to extract information from the unknown

signal. As the wavelet decompose data without gaps or overlap, the decomposition process is mathematically reversible. Thus, sets of complementary wavelets are useful in wavelet based compression/ decompression algorithms where it is desirable to recover the original information with minimal loss.

Continuous wavelet transform

The CWT is computed separately for different segments of the time-domain signal. In CWT, the analyzing function is a wavelet usually denoted by 'ψ'. It compares the signal to shifted and compressed or stretched versions of a wavelet. Stretching or compressing a function is usually referred to as *dilation* or *scaling.* By comparing the signal to the wavelet at various scales and positions, we obtain a function of two variables (K.P. Soman, 2005).

Starting from the mother wavelet , ψ a family of $\psi_{\tau,s}$ of daughter wavelets can be simply obtained by scaling and translating ψ.

$$\psi_{\tau,s} = \frac{1}{\sqrt{|s|}}\psi\left(\frac{t-\tau}{s}\right), s, \tau \in \mathbb{R}, s \neq 0, \quad \text{.....(4.1)}$$

where *s* is a scaling or dilation factor that controls the width of the wavelet and τ is the translation parameter controlling the location of the wavelet. Scaling a wavelet simply means stretching it $(|s| > 1)$ or compressing it $(|s| < 1)$, while translation is simply shifting its position in time. Given a time series $x(t) \in L^2(\mathbb{R})$, its CWT with respect to wavelet ψ is a function of two variables, is given as

$$W_{x;\psi}(\tau, s) = \int_{-\infty}^{+\infty} x(t)\frac{1}{\sqrt{|s|}}\psi^*\left(\frac{t-\tau}{s}\right)dt \quad \text{.....(4.2)}$$

The position of the wavelet in time domain is given by τ, while its position in frequency domain is given by s. The translation and dilation operations applied to the mother wavelet are performed to calculate the wavelet transformed coefficients, which represent the correlation between the wavelet and a localized section of the signal. The wavelet transformed coefficients are calculated for each wavelet segment, which gives time-scale function relating the wavelets correlation to the signal. The absolute values of Wavelet Transformed Coefficients (WTC) are used to form the feature vector for the classifier.

Admissibility Criterion

While using a transform to get a better understanding into the properties of a signal, it should be ensured that the signal can be perfectly reconstructed from its form of representation. For the wavelet transform the condition that must be met in order to ensure perfect reconstruction is

$$C_\psi = \int_0^\infty \frac{|\Psi(\omega)^2|}{|\omega|}\, d\omega < \infty \quad \text{.....(4.3)}$$

This condition is known as the admissibility condition for the wavelet $\psi(t)$, where $\Psi(\omega)$ is the Fourier transform of the mother wavelet $\psi(t)$ (Mertins, 1999). The inverse wavelet transform can exist only if the admissibility condition is met. This condition ensures that $\Psi(\omega)$goes to zero quickly as $\omega \to 0$. To guarantee that $C_\psi < \infty$, we must see that $\Psi(0) = 0$, which is equivalent to

$$\int_{-\infty}^{+\infty} \psi(t)dt = 0. \quad \text{.....(4.4)}$$

A secondary condition imposed on wavelet function is unit energy (K.P. Soman, 2005).

$$\int_{-\infty}^{+\infty}|\psi(t)|^2 dt = 1. \quad \text{.....(4.5)}$$

Inverse CWT

If the condition $C_\psi < +\infty$, called wavelet admissibility condition is satisfied and the wavelet ψ is real, it is possible to reconstruct $x(t)$ using the formula

$$x(t) = \frac{2}{\psi}\int_0^{\infty}\left[\int_{-\infty}^{+\infty} W_x(\tau, s)\psi_{\tau,s}(t)d\tau\right]\frac{ds}{s^2} \text{.....(4.6)}$$

It can be seen that no information is lost if we restrict the computation of the transform only to positive values of scaling parameter '*s*'.

4.2.1 Scale

Like the concept of frequency, scale '*s*' is another useful property of signals. A term 'scale factor' can be defined in order to see how much stretching or shrinking of the wavelet has taken place. The scale factor is inherently positive quantity, *s>0*. The smaller the scale factor, the more "compressed" the wavelet. Conversely, the larger the scale, the more "stretched" the wavelet.

It is seen that there is a relationship between scale and frequency. Higher scales correspond to the most "stretched" wavelets. The more stretched the wavelet, the longer the portion of the signal with which it is being compared, and therefore the coarser the signal features

measured by the wavelet coefficients. Wavelet analysis allows the use of long time intervals where you want more precise low-frequency information, and shorter regions where you want high-frequency information. Few wavelets that have been used for ECG classification are Daubechies, Biorthogonal and Mexican hat wavelet.

4.3 Neural networks

Artificial Neural Networks (ANNs) are relatively crude electronic models based on the neural structure of the brain. The brain learns from practice. Artificial neural networks try to replicate the functioning of human brain. The brain stores information as patterns. Some of these patterns are very complicated. ANN also stores information as patterns, utilizes these patterns, and then solves the problem, which do not utilize traditional programming but involves the creation and training of massively parallel networks to solve specific problems.

4.3.1 Structure of ANN

An artificial neural network (ANN) is a computational model based on the structure and functions of biological neural networks. As the information flows through the network the structure of the neural network changes or learns. Figure 4.1 shows a simple structure of an ANN having three stages input, summation and transfer function. The first stage is to multiply each of the inputs that enter into the network by their respective weighting factor $W(n)$. These modified inputs are then fed into the summing function, which usually sums these products, which are propagated forward.

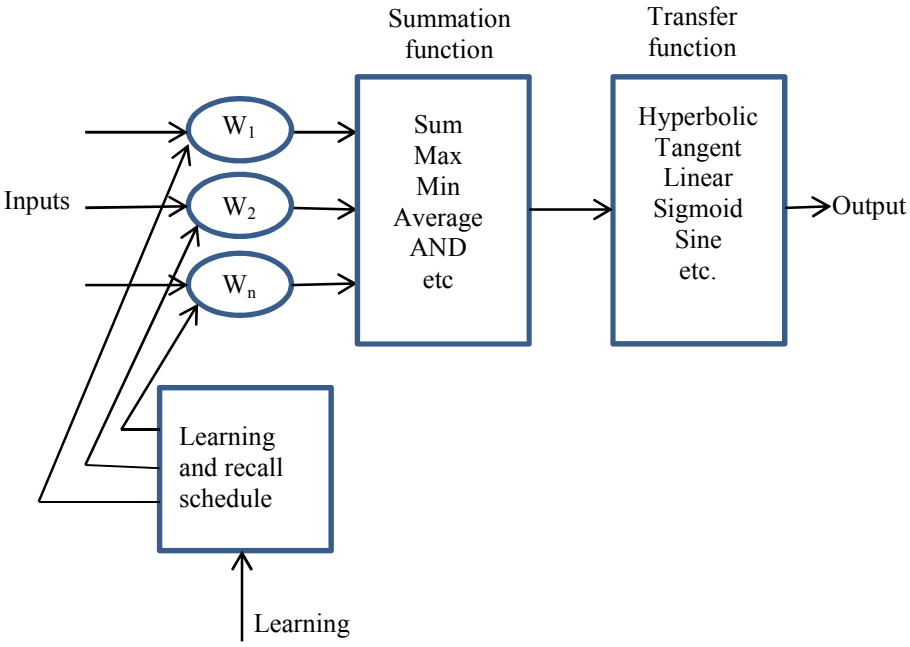

Figure 4.1: Structure of ANN

The output of the summing function is then sent into a transfer function, which turns this number into a real output (0 or 1, -1 or +1 etc.). The transfer function for neural networks must be differential and therefore continuous to enable correcting error. Derivative of the transfer function is required for computation of local gradient.

One such example of a suitable transfer function is the sigmoid function given in Equation 4.7 which is the most common forms of transfer function.

$$g(x) = \frac{1}{1+e^{-ax}} \quad \text{.....(4.7)}$$

Because of the easy relationship of the function with its derivative at a point, it reduces the computational load for training and is defined as a strictly increasing function. Mathematically its derivative is always positive. It exhibits a graceful balance between linear and nonlinear behavior.

4.3.2 Neural Network as ECG classifier

Studies have shown that the neural network systems perform well for detection and recognition of abnormal ECG (Silipo R., 1998), (Roshan Joy Martis, 2013 September). The use of neural systems in ECG signal analysis offers several advantages over conventional techniques. The neural network can perform the necessary transformations and the clustering operations automatically and simultaneously. They are able to recognize complex and nonlinear groups of data. Three commonly used techniques of neural network are Back Propagation (BP), Self Organising Maps (SOM) and Radial Basis Function (RBF). RBF function produce more specific, accurate and sensitive results for classification of cardiac health state as compared to BP and SOM (N. Kannathal, 2007). There are two variants of radial basis networks, Generalized Regression Neural Networks (GRNN) and Probabilistic Neural Networks (PNN) (Wasserman, 1993). PNN is used for ECG classification in this work.

4.3.3 Probabilistic Neural Network

PNN is chosen since ECG classification is difficult to be solved using ordinary rule based programming and are much faster and more accurate than multilayer perceptron networks. For the network used shown in Figure 4.2, the first layer input weights are set to the transpose

of the matrix formed from the training pairs whose size is $Q \times R$. When an input is presented the first layer computes euclidean distances from the input vector to the training input vectors and produces a vector whose elements indicate how close the input is to a training input. These elements are multiplied, element by element, by the bias and sent to the RBF (S.N. Sivanandam, 2006). The second layer weights are set to the matrix of target vectors (size:$K \times Q$). Each vector has a 'one' only in the row associated with that particular class of input, and 'zeros' elsewhere. The second layer after multiplication of the target vector by the output of the first layer, sums these contributions for each class of inputs to produce its net output, a vector of probabilities. Finally, a competitive transfer function on the output of the second layer picks the maximum of these probabilities and produces a '1' for correct class and a '0' for the other classes (S.N. Sivanandam 2006), (Wasserman 1993).

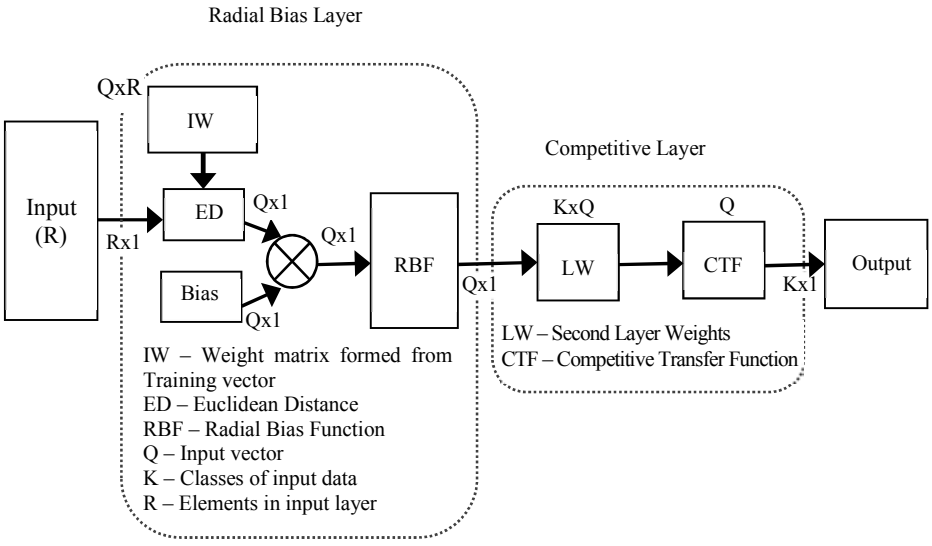

Figure 4.2: Schematic of the PNN

Thus, the network has classified the input vector into a specific 'one of *K* classes' because that class had the maximum probability of being correct.

The PNN needs a single spread value for probabilistic density function estimation. If the value of spread is near to zero, the network acts as a nearest neighbor classifier. As spread becomes larger, the designed network takes into account several nearby design vectors. Jackknifing technique was used to test and find the best performing value of spread (Wolter, 2007). In this test each sample from training set was removed and checked whether PNN classifies that sample correctly. This was repeated for every sample in the training set. The number of correct classifications over the entire process is a measure of the performance for that value of spread. The optimum value for spread is 0.5. This was checked by using a simple GA program that gave the same value of spread for this classifier.

4.4 Basic component of the new wavelet

The Gaussian function has been used as the basic unit to construct the raw wavelet. As shown in Figure 4.3 it has a characteristic symmetric "bell curve" shape. In one dimension, the Gaussian function is the probability density function of the normal distribution (Lifshits, 1995) given by

$$f(x) = \frac{1}{\sigma\sqrt{2\pi}} e^{-(x-\mu)^2/(2\sigma^2)} \quad \text{.....(4.8)}$$

which are sometimes called the frequency curve.

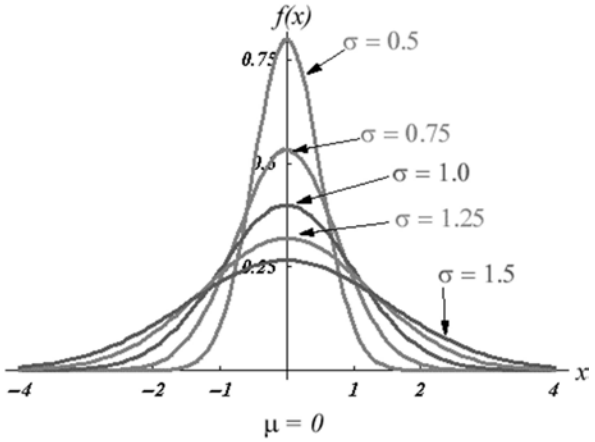

Figure 4.3: Gaussian function

The parameter μ is the position of the centre of the peak and σ the standard deviation sometimes called the Gaussian RMS width which controls the width of the bell. Gaussian functions are widely used in statistics where they describe the normal distributions and its tails drop toward zero very rapidly, much faster when compared with other common functions such as decaying exponentials or $\frac{1}{x}$. In signal processing they serve to define Gaussian filters and in image processing two-dimensional Gaussians are used for Gaussian blurs. They are also used in mathematics to solve heat equations and diffusion equations.

4.5 Design of the Wavelet

A new custom made mother wavelet was constructed using summing up Gaussian functions mentioned in the preceding section in such a way that its shape was almost similar to that of a normal ECG. A Gaussian is used for the construction of the wavelet because it is symmetric around its mean, gains its maximum value at the mean and

goes very fast to zero, similar to an ECG peak. The amplitude and duration of the PQRST complex (5 peaks) of the normal ECG were taken as reference for constructing the wavelet.

The custom made mother wavelet was constructed by shifting and summing up five different Gaussians corresponding to the five peaks of the ECG, which can be called as the 'Shifted and Summed Gaussian Wavelet' (SSG-Wavelet). The equation corresponding to this SSG-Wavelet is given by Equation 4.9.

$$\psi(t) = P + Q + R + S + T. \quad \text{.....(4.9)}$$

where $\psi(t) =$ SSG-Wavelet.

$$\left.\begin{aligned} P &= \frac{1}{\sigma_1\sqrt{2\pi}} e^{\frac{-(t+5)^2}{2{\sigma_1}^2}} \\ Q &= \frac{1}{\sigma_2\sqrt{2\pi}} e^{\frac{-(t+1)^2}{2{\sigma_2}^2}} \\ R &= \frac{1}{\sigma_3\sqrt{2\pi}} e^{\frac{-(t)^2}{2{\sigma_3}^2}} \\ S &= \frac{1}{\sigma_4\sqrt{2\pi}} e^{\frac{-(t-1)^2}{2{\sigma_4}^2}} \\ T &= \frac{1}{\sigma_5\sqrt{2\pi}} e^{\frac{-(t-5)^2}{2{\sigma_5}^2}} \end{aligned}\right\} \quad \text{..... (4.10)}$$

Here $\sigma_1, \sigma_2, \sigma_3, \sigma_4$ and σ_5 are the standard deviation of each Gaussian under consideration. Since σ and peak are inversely proportional, the lower peaks were approximated by higher values of σ and higher peaks were approximated by lower values of σ. The corresponding five values of σ chosen for each Gaussian wave P, Q, R, S and T where $\sigma_1 = 1,\ \sigma_2 = -0.4,\ \sigma_3 = 0.25,\ \sigma_4 = -0.2$ and $\sigma_5 = 1$ respectively. The value of mean(μ) value which are responsible for the position of Gaussian were chosen as -5,-1,0 1 & 5 for the P, Q, R, S, T waves. The negative sign for σ_2 and σ_4 indicates that the amplitude corresponding to Q & S are negative. The U wave was not taken into consideration, since this wave is small in amplitude and appears often only as a slight undulation. Each separately designed Gaussian functions are added to get an approximate version of the signal closer to ECG which has been considered as the raw mother wavelet. The effective support of the wavelet was set as [-8,+8] on a 1024-pint regular grid. The raw mother wavelet was then normalized by dividing it with the standard deviation of the third Gaussian component σ_3. An averaging operation is also performed to make sure that the wavelet satisfied the admissibility conditions. The initial values of mean and variance and their relative separations of the Gaussians were selected in such a way that the new wavelet mimics a normal ECG cycle. The plot of the normalised SSG-wavelet and typical ECG wave is shown in Figure 4.4 & 4.5 to indicate the similarity between them.

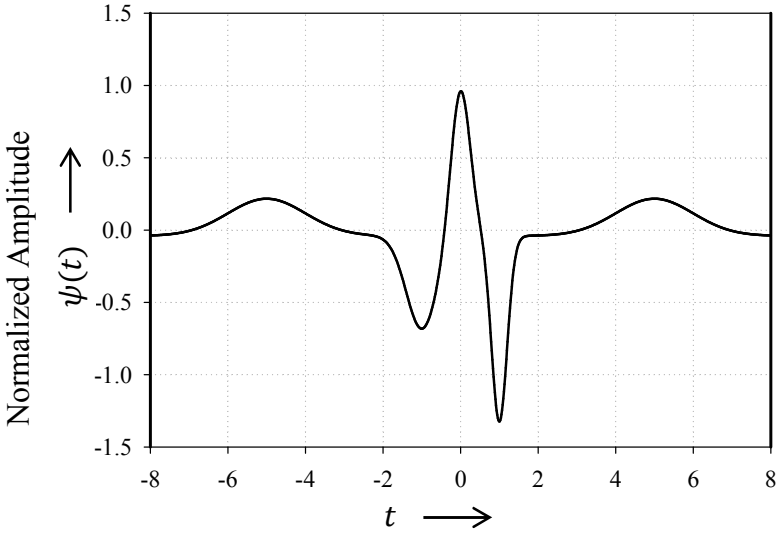

Figure 4.4: Normalized SSG-Wavelet

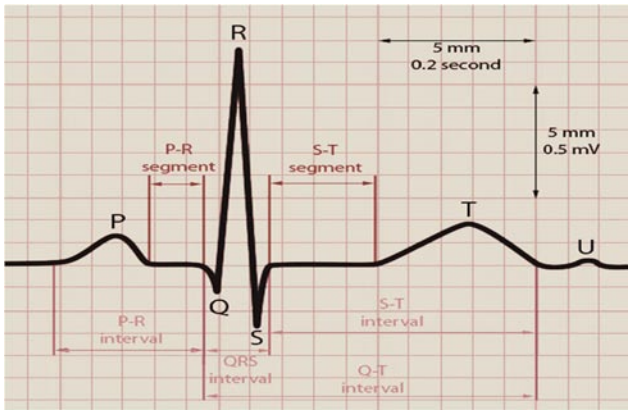

Figure 4.5: One cycle of normal ECG

This wavelet was tested for admissibility conditions. The Fourier spectrum $\Psi(\omega)$ for this wavelet is shown in Figure 4.6. From the figure it can be seen that it has no frequency component at $\omega = 0$ and it exhibits band pass characteristics.

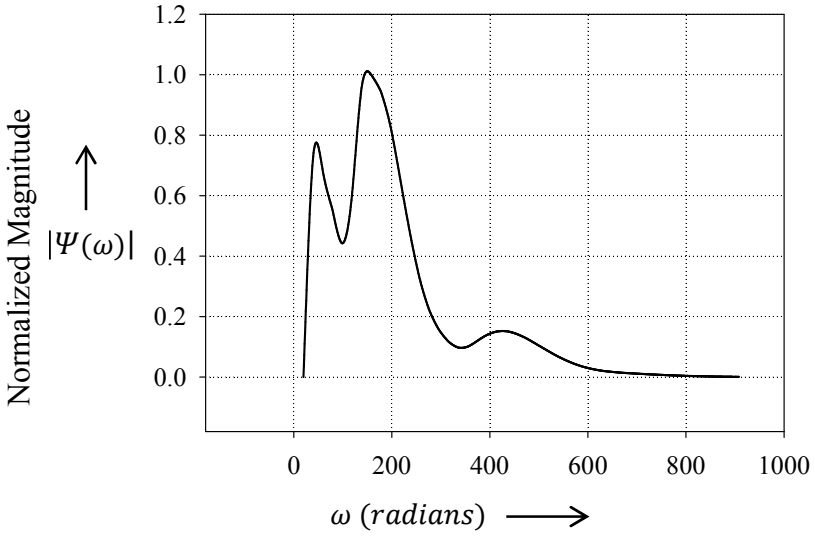

Figure 4.6: Fourier spectrum for the SSG-wavelet

4.6 Training and testing data set selection

MIT-BIH-AR database (Moody R. M., 1997) has been used for training and testing purposes. Entire database consisting of 97072 cycles is divided into two sets, one for training & optimization (Set 1) and other for testing (Set 2) purpose, each having 22 records as given in Table 4.1 (a-d). Training set was formed by selecting just 250 cycles randomly from the 22 records in Set 1. It was ensured that almost equal importance was given to the different abnormalities including the isolated ones. The remaining ECG beats in Set 1 were used to optimize the wavelet in chapter five. ECG cycles in Set 2 consisting of 22 records having 49629 cycles were used for validation purpose (testing).

Table 4.1: Training and Testing datasets

a. Beats from Class I

ECG type	N	LBBB	RBBB	AE	NE
PNN Training (Set 1)	30	22	22	22	22
Wavelet optimization (Set 1)	38051	3927	3761	16	10
Testing (Set 2)	36368	4126	3476	-	51

b. Beats from Class II

ECG type	AP	*a*AP	NP, S_v
PNN Training (Set 1)	22	22	22
Wavelet optimization (Set 1)	788	78	26
Testing (Set 2)	1736	50	213

c. Beats from Class III

ECG Type	PVC	VE	*f*VN, *f*PN
PNN Training (Set 1)	22	22	22
Wavelet optimization (Set 1)	3660	83	393
Testing (Set 2)	3220	1	388

d. Total beats for testing and training

	Class I	Class II	Class III	Total
PNN Training (Set 1)	118	66	66	250
Wavelet optimization (Set 1)	42165	892	4136	47193
Testing (Set 2)	44021	1999	3609	49629

4.7 Performance analysis indices

The performance in recognition and classification by the PNN was evaluated by means of the following performance indices. They are sensitivity and positive predictive value (N. Kannathal, 2007)

Sensitivity indicates the rate of true positive events for a diagnostic class and is given as

$$Sensitivity = \frac{Number\ of\ classified\ positive\ events}{Total\ number\ of\ true\ positive\ events} \quad \text{.....4.11}$$

Positive Predictive Value (PPV) is the rate of true positive events among all the classified events in a diagnostic class and is given by

$$PPV = \frac{Number\ of\ classified\ true\ positive\ events}{Total\ number\ of\ classified\ positive\ events} \quad \text{.....4.12}$$

4.8 Initialization of scale and features

4.8.1 Selection of scale

The frequencies present in ECG fall in the range of 0-100 Hz. The three classes of ECG cycles i.e. normal, supraventricular and ventricular, lie in different frequency bands. In order to get good classification, the frequency or its corresponding wavelet scale for each class needs to be identified.

The PNN classifier mentioned in section 4.3.3 was trained using wavelet transformed (features) coefficients of 250 ECG cycles from the training set 1 at an arbitrary scale (200 WTC for each cycle). The scale was assumed to be the same for all the classes.

Using the remaining records in set 1 classification was performed at various scales using the PNN classifier, into one of the three classes. The scale that gave the maximum sensitivity corresponding to each class were identified. PNN was then trained with features corresponding to these new scales. The classification was again performed using the 55821 cycles in Set 1. The training and classification is repeated until maximum classification for each class was identified and the corresponding scales were found to be 20 for class I, 6 for class II and 45 for class III.

4.8.2 Selection of optimum features

A study on the effect of the number of WTC coefficients used for classification of PNN was performed. It was observed that PNN can perform well when the selected feature vector used for training and testing purpose are optimum. This was done by fixing the scales for each class as described above. The number of WTC coefficients for PNN was varied and the sensitivity was observed in each case. Table 4.2 shows how the sensitivity of each class varied while changing number of wavelet coefficients as features. It was seen that the maximum average sensitivity was obtained with 86 features. The PNN was then trained using 250 ECG cycles from set 1 using these 86 features. This network was fixed for further classification in subsequent chapters.

Table 4.2: Selection of WTC as feature vectors

Pattern adopted in selecting the WTC	No. of WTC as feature vectors	% Sensitivity			
		Class I	Class II	Class III	Average sensitivity
All WTC	200	92.06	83.40	88.90	88.12
Every third WTC discarded	125	91.90	85.34	89.05	88.76
Alternate WTC selected	100	91.76	86.22	90.68	89.55
Alternate WTC after discarding seven WTC from either sides	**86**	**92.06**	**86.92**	**92.79**	**90.59**
Every third WTC selected	66	91.78	88.34	90.85	90.32
Every fourth WTC selected	50	91.45	88.12	89.80	89.79

4.9 Classification of ECG

ECG records in Set 2 consisting of 49629 cycles were used for testing purpose. Steps involved in the process for classification is given in the Figure 4.7. From each record, one complete cycle is taken out and it is preprocessed for the removal of noise (PLI & BLW). By performing the CWT operation using the new SSG-Wavelet, optimal WTC vectors were extracted for the identified scales from the different classes.

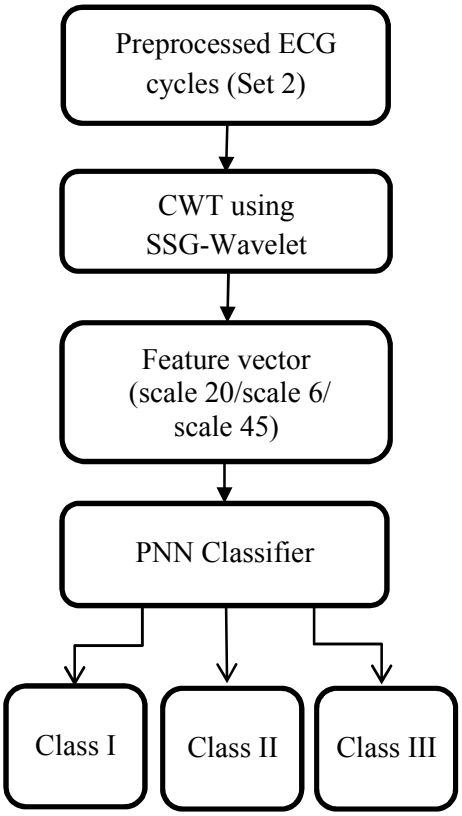

Figure 4.7: Steps involved in the classification process of the ECG records

Classification for each scale was performed using PNN Classifier. The results were validated by using the available annotations. Sensitivity and positive predictivity for each cycle as well for each class were calculated.

4.10 Results and discussion

The results of classification obtained using PNN classifier with optimal number of WTC features for selected scales are given in Table 4.3. The percentage of classification is obtained in terms of percentage sensitivity and percentage positive predictivity. The average sensitivity obtained for class I, class II & class III are found to be 96.13%, 73.25% & 90.13% and the positive predictivity are found to be 91.77%, 59.63% & 81.88% respectively. Comparing these results with that obtained by Mariano Llamedo (2011) it is seen that percentage sensitivity in all the classes are better while positive predictivity in class II and class III seems to be less. The average sensitivity obtained for all the three classes is 88.68% and positive predictivity is 79.83%. The overall improvement in sensitivity is 6.82%. Almost all the isolated abnormalities in the Set 2 records as mentioned in Table 3.3 were identified. From the above results, it can be seen that the new SSG-Wavelet can be used for classifying ECG cycles into normal beats (Class I), supraventricular beats (Class II) and ventricular beats (Class III) effectively.

Table 4.3: Classification using the SSG-wavelet

	Class I		Class II		Class III		Average	
Record	**% Sensitivity**	**% Positive Predictivity**	**% Sensitivity**	**% Positive Predictivity**	**% Sensitivity**	**% Positive Predictivity**	**% Sensitivity**	**% Positive Predictivity**
100	100	98	18	46	100	100	73	82
103	100	100	100	40	-	-	100	70
105	99	99	-	-	90	45	95	72
111	100	100	-	-	100	1	100	51
113	100	100	100	75	-	-	100	88
117	100	100	100	2	-	-	100	51
121	100	100	100	6	100	50	100	52
123	100	100	-	-	100	100	100	100
200	89	75	33	53	79	100	67	76
202	97	97	35	73	90	56	74	75
210	100	94	64	82	77	90	80	89
212	100	100	-	-	-	-	100	100
213	71	85	75	88	83	80	71	85
214	98	93	-	-	77	93	88	93
219	99	97	100	70	89	97	96	88
221	100	98	-	-	65	100	83	99
222	100	91	47	92	-	-	74	92
228	71	77	100	60	99	99	90	79
231	100	100	100	1	100	100	100	67
232	100	22	92	99	-	-	96	61
233	91	94	86	67	93	99	90	87
234	100	99	22	100	100	100	74	100
Average	**96.13**	**91.77**	**73.25**	**59.63**	**90.13**	**81.88**	**88.68**	**79.83**

* isolated abnormalities are highlighted.

4.11 Chapter summary

A novel SSG-Wavelet has been proposed in this chapter. On observing the results it is seen that percentage sensitivity obtained were better than that reported in the literature. This shows that the wavelet whose shape is similar to that of normal ECG is a promising non-invasive tool in identifying the time-frequency components in the signal. Performance of the SSG-wavelet can be enhanced by optimizing the σ values with a suitable technique while the admissibility condition is met, is explained in the next chapter.

Chapter 5

SSG-WAVELET OPTIMIZATION APPROACH FOR BETTER CLASSIFICATION

Contents

A technique for optimizing the SSG-Wavelet for better ECG classification using GA is proposed in this chapter. The optimum wavelet for classification was obtained after several runs of the GA algorithm. Sensitivity and positive predictivity were used to evaluate the performance of the classifier. This chapter is made up of two main sections. The first section discusses the basics of GA used for optimization. The second part deals with the methodology employed in achieving the optimized wavelet and the results obtained.

5.1 Introduction

Optimization is an important tool in making decisions and in analyzing physical systems. In mathematical terms, an optimization problem means finding the best solution from among the set of all feasible solutions. The first step in the optimization process is constructing an appropriate model by identifying and expressing the objectives, variables and constraints in mathematical terms. Objective is a quantitative measure of the performance of the system that we want to minimize or maximize, variables are the components of the system for which we want to find optimum values and constraints are the functions that describe the relationships among the variables and that define the tolerance values for the variables (Mitchell, 1998). In the following sections a method for optimizing the SSG-Wavelet is explained. GA is used as the optimization tool.

5.2 Genetic Algorithm

Genetic Algorithms are the heuristic search and optimization techniques that has its roots in the principles of genetics. GAs have been used widely as a tool in computer programming and artificial intelligence, optimization, neural network training and many other areas. GA can do better than conventional optimization techniques while dealing with complex real-world optimization problems. Conventional optimization techniques have a single point approach (Goldberg, 1989), whereas GA uses a multi-point approach with a population of solutions at a time. A population of individuals is maintained within search space for a GA, each representing a possible

answer to a given problem. Each individual is coded as a finite length vector of components, or variables, in terms of some alphabet, usually the binary alphabet. Each bit in this string can represent some characteristic of the solution. To continue the genetic analogy these individuals are equated to chromosomes and the variables are similar to genes. Thus a chromosome (our solution) is composed of several genes (variables). There are many other ways of encoding. This depends mainly on the problem to be solved (S. Rajashekaran, 2013).

Search Space

The space of all feasible solutions is called a search space. Each and every point in the search space represents one possible solution. So each possible solution can be obtained by its fitness value, depending on the problem definition. Using GA we look for the best solution, among a number of possible solutions in a search space. The best solution means either a minimum or maximum depending on the definition of that particular problem (S.N. Sivanandam, 2006).

Population

A population is a collection of individuals being tested, the phenotype parameters define the individuals and some information about the search space. The important aspects of population used in GA are initial population generation and population size. The population size depends on the complexity of the problem. The first population should have a gene pool as large as possible in order to be able to explore the full search space. Usually the population is finalized randomly.

Gene encoding

Before a GA can be put to work on any problem, a method is need to encode the potential solutions to that problem. In GA individual genes are represented as codes. Gene encoding can be done using bits, numbers, arrays, or any other object which usually depends on the problem. Table below shows an example of chromosomes in a population of five individuals (chromosomes), where a real number represents each chromosome. In this work the σ values' corresponding to each Gaussian function used in the design of the new wavelet forms a chromosome and is shown below.

Chromosome	$\sigma_1\sigma_2\sigma_3\sigma_4\sigma_5$

Operators in GA

GA begins by creating an initial set of random solutions called as initial population. An individual representing a solution to a particular problem is called a chromosome. A chromosome is formed by a string of symbols which is called as genes. The consecutive iterations of the GA are called generations. In each generations, the fitness of each individual is evaluated to find best individual or solution. The subsequent generations are formed by creating new individuals called off spring. Selection, crossover and mutation are three main operators used in GA.

Selection

During each successive generation, a proportion of the existing population is selected to raise a new generation. Individual solutions are selected through a fitness process, where the right solutions are typically more likely to be selected. Certain selection methods rate the fitness of each solution and select the best solutions. Other methods rate only a random sample of the population, as this process may be very time-consuming. Most functions are stochastic and designed so that a small proportion of less fit solutions are selected. This helps to keep the diversity of the population large, preventing premature convergence on poor solutions. Popular and well learnt selection methods include roulette wheel selection and tournament selection.

Roulette wheel selection used in this work. The fitness for each input is first calculated and then it is represented on the roulette wheel in terms of percentages. The size of an individual's slot in the wheel is proportional to its fitness. In a search space of 'N' number of chromosomes, we spin the roulette wheel. Chromosome with bigger fitness has the probability of being selected more times (D Andina, 2009).

Crossover

The crossover operator selects genes from parent chromosomes and generates a new offspring. This recombination operator permits individual solutions to exchange information like what is done while organisms reproduce. The simplest way to do this is to choose randomly some crossover point. A new solution is obtained by copying

everything before this point from a first parent and then everything after a crossover point from the second parent. This is called single point crossover and is the simplest crossover operation (S. Rajashekaran, 2013).

Mutation

After a crossover is performed, mutation takes place. This is to prevent falling all solutions in population into a local optimum of solved problem (S. Rajashekaran, 2013). Mutation changes randomly the new offspring. Mutation helps the GA to prevent premature convergence of the algorithm. It helps GA to explore new search areas.

Elitism

Search speed can be significantly enhanced by keeping the best (elite) individual among generations. Making sure the transmission of the elite individual from one generation to the next is termed as elitism. The elite member copied should not be altered by crossover or mutation

Initialization

Initially many individual solutions are randomly generated to form an initial population. The population size depends on the nature of the problem, but typically contains several hundreds or thousands of possible solutions. Traditionally, the population is generated randomly, covering the entire range of possible solutions or the so called search space.

Parameters of GA

For the effective working of GA certain parameters need to be chosen, since they have considerable effects on its performance. The

value of these parameters depends on the optimization problem. The parameters of simple GA include, population size, crossover rate, mutation rate and convergence criteria.

Population Size

Population size represents the number of individuals in a population and its size depends on the problem complexity. If the population size is small only narrow search regions will be explored, on the other hand a large population size has more computational complexity. So effectiveness of GA in finding the optimum solution greatly depends upon population size.

Crossover rate

It determines the number of pairs of chromosome to be crossed in each generation. It is defined as the ratio of the number of chromosome pairs to be crossed to the population size (S. Rajashekaran, 2013). With the higher value for the crossover rate a large area of search space can be explored, with the expense of large computational time. While low cross over rate causes reduction in the speed for convergence of solution.

Mutation rate

Mutation rate is defined as the percentage of the total number of bits mutated in the population. If the mutation rate goes above a particular value the offspring lose their similarities with the parents, which make them unable to learn from the previous search information. Too low mutation causes many useful changes in bit states of strings to be tried out.

Convergence

The computational time complexity of finding a global optimal solution is judged through analyzing a Genetic Algorithm's convergence rate. It can be presumed that GA met convergence when a particular percentage of individuals in the population turned out to become the same or when the average fitness of the population comes very near to the best individual's fitness. Then there will be little variation between the average and the best individual fitness (Goldberg, 1989).

5.2.1 Algorithm of the basic GA

Implementation of the genetic algorithm can be explained as follows

i) [Start] Generate random population of 'n' chromosomes (suitable solutions for the problem)

ii) [Fitness] Evaluate the fitness 'F(x)' of each chromosome 'x' in the population

iii) [New population] Create a new population by repeating following steps until it reaches population size.

   (a) [Selection] Select two parent chromosomes from a population according to their fitness. It is seen that the better is the fitness, the bigger is the chance to be selected.

   (b) [Crossover] After choosing a crossover probability, perform crossover operation on the parents to form an new offspring. If no crossover was performed, offspring is an exact copy of parents.

(c) [Mutation] After choosing a mutation probability, mutate new offspring at every position in chromosome.

(d) [Accepting] Place the new offspring in a new population.

iv) [Replace] Use new generated population to run the algorithm again.

v) [Test] If the number of populations or improvement of the best solution is not satisfied, Go to step ii

vi) [Solution] Return the best solution.

Parameters used in GA

As mentioned above there are certain parameters that need to be selected for effective working of GA. Proper selection of these parameters will have an effect on its performance. The following GA parameters were used.

1. Fitness function 'F' based on classification accuracy is formed to evaluate the wavelets as given in Equation (5.1).

$$F = \frac{1}{1-\text{average sensitivity}} \quad \text{.....(5.1)}$$

2. Population size represents the number of individual in a population. Typical population size (n) chosen was 100.

   The initial population was formed using the chromosome formed with the σ values used in the design of the new wavelet. A sample set of chromosomes is shown below.

Chromosomes	σ_1	σ_2	σ_3	σ_4	σ_5
Chromosome 1	1	-0.4	0.25	-0.2	1
Chromosome 2	0.45	0.5	-3	0.6	-4
Chromosome 3	0.33	4	3.5	-0.7	1
-					
Chromosome 100	-5	-42	0.87	0.43	-0.9

3. Crossover rate represents the number of chromosomes to be to be crossed in each generation. The crossover rate selected was 0.8
4. Elitism which is the keeping the best individual from one generation to next was set as 2.
5. The reproduction operator chosen was Roulette wheel.

5.3 Optimizing the proposed SSG-Wavelet

Mean and standard deviation of the SSG-wavelet could be considered for optimization. Since the pulse width of the different waves in ECG, changes with the different arrhythmia, standard deviation was considered for optimization. The optimal SSG-Wavelet was obtained from the raw wavelet by optimizing the standard deviation values 'σ' of each Gaussian under consideration. The optimization procedure is shown in Figure 5.1. As mentioned in the section 4.5 we initialize the chromosome values and perform the extraction of WTC coefficients for the identified scales. Using these features, ECG cycles are classified with the trained PNN network. Percentage sensitivity is used as a measure of fitness function and it is calculated considering the three classes of ECG signals. If this calculated value is less than desired fitness function, a new set of values for the σ is evolved to generate a new population by crossover, mutation

and selection process. If the desired classification accuracy is met, GA will stop the iteration process and return the optimum values for the given constraints.

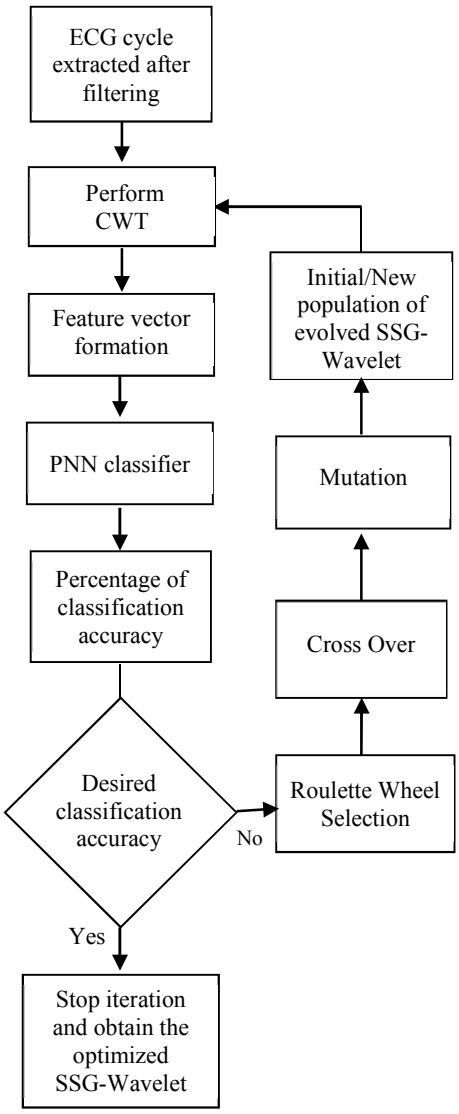

Figure 5.1: Method of generating the optimized wavelet for ECG classification using GA

The optimal SSG-wavelet is derived from the basic one using GA by repeated evolution until satisfactory classification is achieved.

ECG records in set-1 was selected for this purpose after filtering. Adaptive filtering technique for denoising the ECG based on GA tuned SD-LMS algorithm was used. Each cycle from the records is extracted after identifying the R-wave using the annotations available at the database. Absolute values of WTC were obtained with the identified scales for the different ECG cycles using the SSG-Wavelet. Classification based on three different scales was performed using PNN classifier that was obtained during the training process. The corresponding classification accuracies were obtained. Based on the classification accuracy a new generation of wavelets were obtained by cross over and mutation. This process continues until an optimized SSG wavelet is obtained. The optimized values of σ that gave the highest fitness values were found to be $\sigma_1 = 6.0414, \sigma_2 = 14.9955,\ \sigma_3 = 23.1669,\ \sigma_4 = 5.9103,\ \sigma_5 = 1.1767.$ These values when applied in Equations 4.9 and 4.10 yielded the optimized SSG-Wavelet given in Figure 5.2.

Optimized SSG-Wavelet was further checked for all the properties of a traditional continuous wavelet (Paul S, 2002) including the admissibility conditions Equation 4.4 and 4.5. These conditions ensures that $\Psi(f)$ goes to zero quickly as $\omega \to 0$ and wavelet function has unit energy. The corresponding frequency spectrum $|\Psi(\omega)|$ of this optimized wavelet is shown in Figure 5.3. It can be observed that it satisfies the necessary conditions.

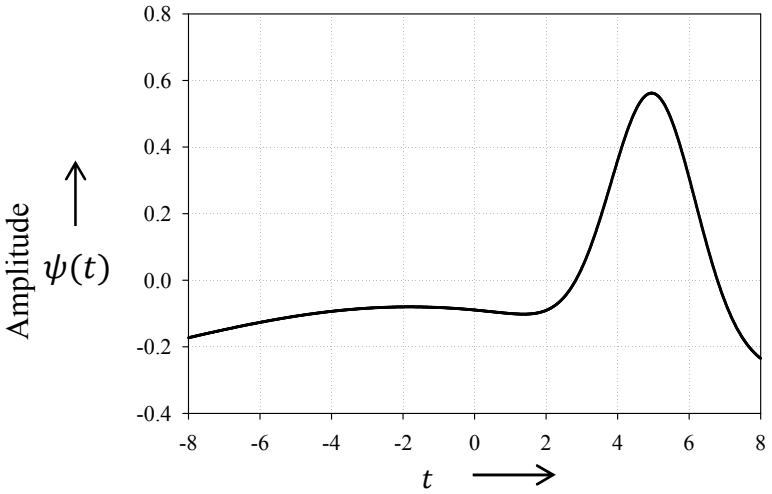

Figure 5.2: Optimized SSG-Wavelet

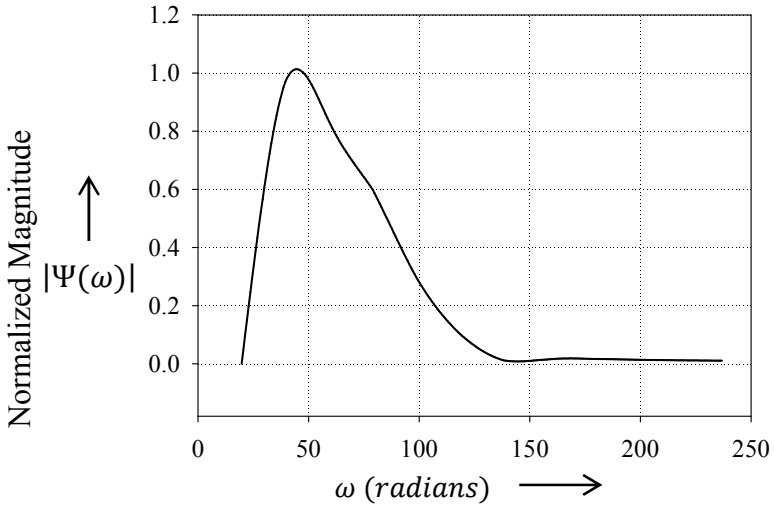

Figure 5.3: Fourier spectrum for the optimized SSG-wavelet

5.4 Results and discussion

Classification was performed for each cycle of the ECG records in set 2 using the classifier given in Figure 4.7. The percentage sensitivity and positive predictivity were evaluated using Equations 4.11 and 4.12 given in section 4.7.

The system performance is evaluated by means of two performance indices, classification sensitivity and positive predictivity. The results are given in Table 5.1. From the table, it is seen that the proposed system yields promising values. The average values of sensitivity obtained for class I is 96.88%, for class II it is 74.56% and for class III it is 92.92%. Similarly, the average value of positive predictivity obtained for class I, class II and class III are 91.96%, 73.08% and 83.05% respectively. The overall sensitivity is 90.37% and positive predictivity 83.39% and all the isolated abnormalities in the Set 2, except one cycle from record 233 are identified correctly.

Comparing the results with that obtained in chapter 4, it is seen that after optimizing the wavelet there is an improvement in percentage sensitivity by 0.75% for class I, 1.31% for class II and 2.79% for class III. The improvement in percentage positive predictive value by 0.19% for class I, 13.45% for class II and 1.17% for class III.

It may be noted that a fairly good result was obtained by performing classification using the SSG-wavelet that is similar to normal ECG. So, it cannot be completely ruled out that a typical QRS complex cannot act as a good model for classification. The optimized SSG-wavelet could identify the isolated abnormalities effectively. Although isolated abnormalities contribute only a small percentage of the total number of cycles, they are important since failure to diagnose these conditions with subsequent inappropriate management may have fatal consequences. Hence even though there is only a small percentage of increase in sensitivity and positive predictivity, it was also due to the isolated abnormalities. The

classification performance enhanced in terms of sensitivity and positive predictivity.

Table 5.1: Classification using the optimized wavelet

Record	Class I		Class II		Class III		Average	
	Percentage sensitivity							
	Before optimization	After optimization	Before optimization	After optimization	Before optimization	After optimization	Before optimization	After optimization
100	100	100	18	18	100	100	73	73
103	100	100	100	100	-	-	100	100
105	99	99	-	-	90	90	95	95
111	100	100	-	-	100	100	100	100
113	100	100	100	100	-	-	100	100
117	100	98	100	100	-	-	100	99
121	100	100	100	100	100	100	100	100
123	100	100	-	-	100	100	100	100
200	89	90	33	47	79	93	67	76
202	97	95	35	35	90	90	74	73
210	100	100	64	64	77	77	80	80
212	100	100	-	-	-		100	100
213	71	71	75	75	83	83	71	76
214	98	98	-	-	77	77	88	88
219	99	99	100	100	89	89	96	96
221	100	99	-	-	65	98	83	99
222	100	100	47	57	-	-	74	78
228	71	95	100	100	99	95	90	97
231	100	100	100	100	100	100	100	100
232	100	100	92	90	-	-	96	95
233	91	91	86	86	93	93	90	90
234	100	99	22	22	100	100	74	74
Average	**96.13**	**96.88**	**73.25**	**74.56**	**90.13**	**93.06**	**88.68**	**90.37**

While performing a comparative description between the some of the existing wavelets like Coiflets, Daubechies and Symlets it is seen that the optimized SSG-wavelet is also compactly supported i.e. localized in space, are smooth i.e. they decay towards high frequencies,

and have vanishing moments i.e. decay towards low frequencies. In order to have a comparison with these wavelets, a classification was performed using coif1, db1 and sym2 wavelets using the same database. The scales corresponding to the different ECG classes were selected in each case and classification performed. The results are given in Table 5.2 - 5.4. On comparing the results, it is seen that the optimized SSG-wavelet gave a better result.

Table 5.2: Classification using the Coiflet wavelet (coif1)

	Class I		Class II		Class III		Average	
Record	**% Sensitivity**	**% Positive Predictivity**	**% Sensitivity**	**% Positive Predictivity**	**% Sensitivity**	**% Positive Predictivity**	**% Sensitivity**	**% Positive Predictivity**
100	100	98	6	18	100	25	69	47
103	100	100	50	25	-	-	75	62
105	94	100	-	-	61	30	78	65
111	100	100	-	-	0	0	50	50
113	100	100	100	75	-	-	100	87
117	83	99	100	2	-	-	91	50
121	100	100	100	6	100	11	100	39
123	100	97	-	-	33	100	67	99
200	90	67	20	40	80	100	63	69
202	95	96	35	73	90	47	73	72
210	93	89	45	77	26	89	55	85
212	100	100	-	-	-	-	100	100
213	63	90	75	88	83	80	74	86
214	98	92	-	-	77	92	88	92
219	99	89	100	70	89	97	96	85
221	77	97	-	-	98	100	88	99
222	100	91	57	94	-	-	78	92
228	95	78	100	60	95	99	97	79
231	91	100	100	1	100	100	97	67
232	64	16	83	98	-	-	74	57
233	78	75	86	67	93	99	86	80
234	83	98	22	100	100	100	68	99
Average	91.01	89.54	67.40	55.82	76.71	72.99	80.24	75.52

** Scales selected: 37 for Class I, 12 for Class II and 81 for class III (sampling rate 360 Hz)*

Table 5.3: Classification using the Daubechies wavelets (db1)

	Class I		Class II		Class III		Average	
Record	**% Sensitivity**	**% Positive Predictivity**	**% Sensitivity**	**% Positive Predictivity**	**% Sensitivity**	**% Positive Predictivity**	**% Sensitivity**	**% Positive Predictivity**
100	99	98	91	37	100	100	97	78
103	98	100	100	2	-	-	99	51
105	97	99	-	-	90	45	94	72
111	100	100	-	-	0	0	50	50
113	100	100	100	100	-	-	100	100
117	100	100	100	100	-	-	100	100
121	100	100	100	0	100	50	100	50
123	100	100	-	-	100	100	100	100
200	82	62	37	12	96	100	72	58
202	97	97	29	6	90	56	72	53
210	95	91	68	7	75	89	79	62
212	100	100	-	-	-	-	100	100
213	71	76	68	95	83	59	74	77
214	89	90	-	-	77	93	83	92
219	99	97	100	2	31	91	77	63
221	99	96	-	-	98	100	99	98
222	98	92	27	20	-	-	63	56
228	89	76	100	4	95	99	95	60
231	93	100	0	0	100	67	64	56
232	100	24	65	100	-	-	82	62
233	89	88	86	30	96	100	90	73
234	99	98	32	67	100	100	77	88
Average	95.19	90.18	68.91	36.32	83.23	78.00	84.82	72.62

** Scales selected: 46 for Class I, 14 for Class II and 101 for class III (sampling rate 360 Hz)*

Table 5.4: Classification using the Symlets (sym2)

	Class I		Class II		Class III		Average	
Record	**% Sensitivity**	**% Positive Predictivity**	**% Sensitivity**	**% Positive Predictivity**	**% Sensitivity**	**% Positive Predictivity**	**% Sensitivity**	**% Positive Predictivity**
100	100	98	36	63	100	100	79	87
103	98	100	100	40	-	-	99	70
105	97	99	-	-	88	38	93	69
111	100	100	-	-	0	0	50	50
113	98	100	67	67	-	-	82	83
117	97	100	100	2	-	-	99	51
121	100	100	100	6	100	50	100	52
123	100	100	-	-	100	100	100	100
200	89	70	33	59	94	100	72	76
202	95	96	35	73	90	67	73	79
210	100	89	36	73	96	88	77	84
212	99	100	-	-	-	-	99	100
213	71	91	75	88	75	78	73	85
214	98	92	-	-	93	94	96	93
219	94	97	100	70	97	97	97	88
221	99	98	-	-	96	100	98	99
222	100	89	50	96	-	-	75	93
228	83	79	100	60	98	99	94	79
231	100	100	100	3	100	100	100	68
232	100	21	86	98	-	-	93	60
233	90	91	86	67	100	100	92	86
234	99	98	22	100	100	100	74	99
Average	95.74	91.33	70.39	60.25	89.10	81.92	86.97	79.57

** Scales selected: 31 for Class I, 10 for Class II and 68 for class III (sampling rate 360 Hz)*

5.5 Chapter summary

The new optimized SSG-wavelet has shown to be effective in classifying ECG signals. The optimized wavelet satisfied the properties of CWT including the admissibility conditions. There was much improvement in sensitivity and positive predictivity especially in the case of class II and class III as seen in the results. Further improvement in classification accuracy can be obtained by identifying finer scales corresponding to the different classes of ECG. This is carried out in the next chapter.

Chapter 6

IMPROVED CLASSIFICATION AT FINER WAVELET SCALES

Contents

This chapter proposes an approach for improved classification of ECG at finer wavelet scales. The need for identification of finer scales has been explained. Finer wavelet scales were selected and the scale at which maximum classification obtained for each class was identified. The results were compared with that obtained by Mariano Llamedo (2011). It is seen that the good time-frequency resolution of the new wavelet transform could differentiate the different types of ECG beats. Apart from these results, the detection of isolated abnormalities in the database and identification of the time/frequency interval of the QRS wave, corresponding to the three classes of ECG is also discussed.

6.1 Scale/frequency refinement

In the previous chapter it was seen that the maximum classification sensitivity had improved by optimizing the wavelet. It has to be noted that the wavelet scales considered for classification were integer values. With the fact that even a very small improvement to the reliability of the algorithm may be helpful to patients, further investigations were made into the scales used for classification.

From chapter 4, it is known that the classification accuracy varies for different classes when classified under different scales of the wavelet. To completely exploit this property of wavelet, classification were performed at more refined scales. The scales were varied in smaller step sizes and the corresponding classification accuracies were observed. The optimum step size was obtained as 0.125 based on improvement in classification accuracy. Further reducing the step size had no effect on the results. The frequency corresponding to a particular scale can be calculated using Equation 6.1.

$$F_a = \frac{F_C}{a.\nabla} \quad \text{.....(6.1)}$$

where F_a is the pseudo-frequency in Hz corresponding to any scale a, F_c is the center frequency of the wavelet in Hz and ∇ is the sampling period.

6.2 Results and Discussions

Performing classification using the optimized SSG-Wavelet gave a sensitivity of 96.88% for class I, 74.56% for class II and 92.92% for class III as mentioned in chapter 5. The scales at which maximum

classification was attained were 20, 6, 45 for class I, class II and class III respectively. To examine the variation of sensitivity at finer levels, the absolute WTC were obtained for scales with step size of 0.125 between 19 and 21 for class I, between 5 and 7 for class II and between 44 and 46 for class III. Classification was performed at all these scales and the corresponding sensitivities were tabulated for three classes.

Class I

Table 6.1 shows the variation of classification sensitivity to finer scales for class I.

Table 6.1: Scale vs sensitivity (Class I)

Class I		
Scale	**Frequency (Hz)**	**% Sensitivity**
19.000	8.29	96.85937
19.125	8.24	96.85474
19.250	8.18	96.85482
19.375	8.13	96.85482
19.500	8.08	96.85937
19.625	8.03	96.90028
19.750	7.97	96.86846
19.875	7.92	96.87982
20.000	7.88	96.88357
20.125	7.83	96.87755
20.250	**7.78**	**97.01811**
20.375	7.73	96.91541
20.500	7.68	96.85255
20.625	7.64	96.85937
20.750	7.59	96.86164
20.875	7.54	96.86164
21.000	7.50	96.86392

Figure 6.1 shows the plot of scale vs sensitivity obtained by varying the scale in the range of 18 to 20 in steps of 0.125.

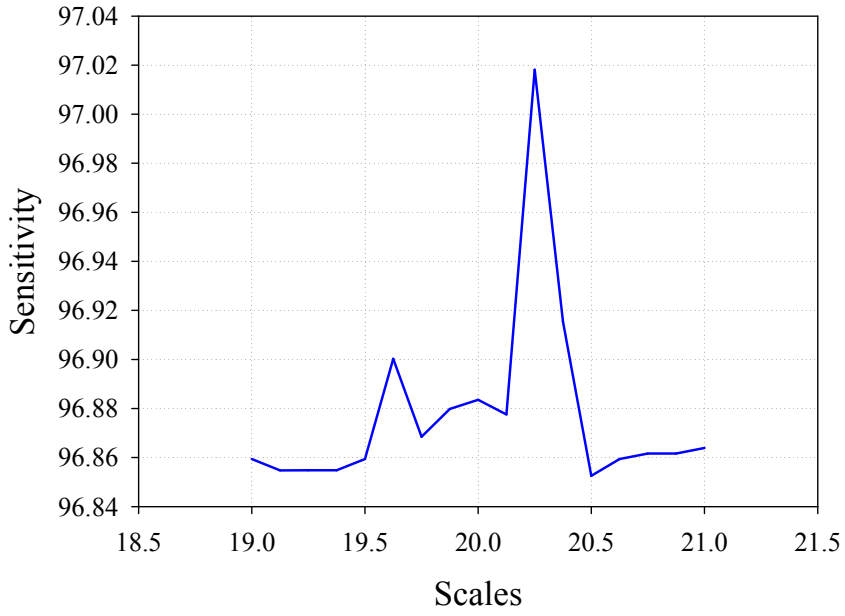

Figure 6.1: Scale vs sensitivity (class I)

From the table and the figure it can be seen that the sensitivity almost increased gradually and reached a maximum value of 97.02% at a scale of 20.250 and thereafter it falls rapidly to gain a classification accuracy of 96.87%. Hence it can be seen that even though a better classification is possible in and around scale 20, the best classification occurs at 20.25. This scale corresponds to frequency of 7.78 Hz.

Class II

Table 6.2 shows the variation of classification sensitivity to finer scales for class II and Figure 6.2 shows the plot of scale vs sensitivity, obtained by varying the scale in the range of 5 to 7 in steps of 0.125.

Table 6.2: Scale vs sensitivity (Class II)

Class II		
Scale	**Frequency (Hz)**	**% Sensitivity**
5.000	31.50	74.15294
5.125	30.73	74.15897
5.250	30.00	74.15897
5.375	29.30	74.15897
5.500	28.64	74.15124
5.625	28.00	74.16719
5.750	27.39	74.16504
5.875	26.81	74.16481
6.000	26.25	74.55976
6.125	**25.71**	**75.20750**
6.250	25.20	75.20012
6.375	24.71	74.12672
6.500	24.23	73.93596
6.625	23.77	73.80034
6.750	23.33	73.89751
6.875	22.91	73.81451
7.000	22.50	73.87118

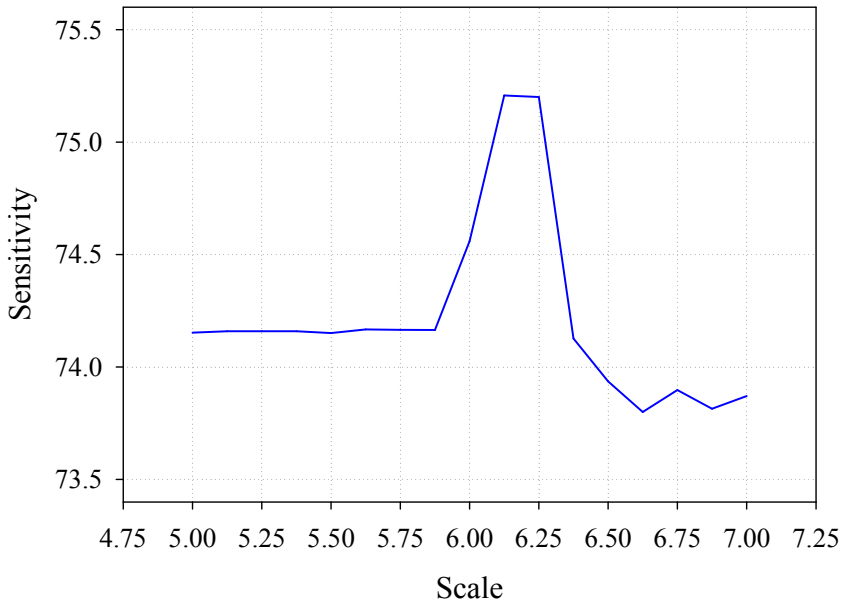

Figure 6.2: Scale vs sensitivity (class II)

From the table and the figure it can be seen that the sensitivity seems to be same at the initial scales and it increased to maximum value of 75.2075% at a scale 6.125. Again increasing the scale value the percentage sensitivity falls rapidly to lower values. Hence it can be seen that better classification is possible at a scale 6.125 which corresponds to frequency of 25.71 Hz.

Class III

Table 6.3 shows the variation of classification sensitivity to finer scales for class III. Figure 6.3 shows the plot of scale vs sensitivity obtained by varying the scale in the range of 44 to 46 in steps of 0.125.

Table 6.3: Scale vs sensitivity (Class III)

Class III		
Scale	**Frequency**	**% Sensitivity**
44.000	3.58	90.82571
44.125	3.57	91.68468
44.250	3.56	92.18343
44.375	3.55	92.79302
44.500	3.54	92.68218
44.625	3.53	92.79302
44.750	3.52	92.84843
44.825	3.51	92.89652
45.000	**3.50**	**93.06857**
45.125	3.49	92.69897
45.250	3.48	92.18952
45.375	3.47	92.18298
45.500	3.46	92.41774
45.625	3.45	92.95822
45.750	3.44	92.69913
45.875	3.43	92.66068
46.000	3.42	92.88131

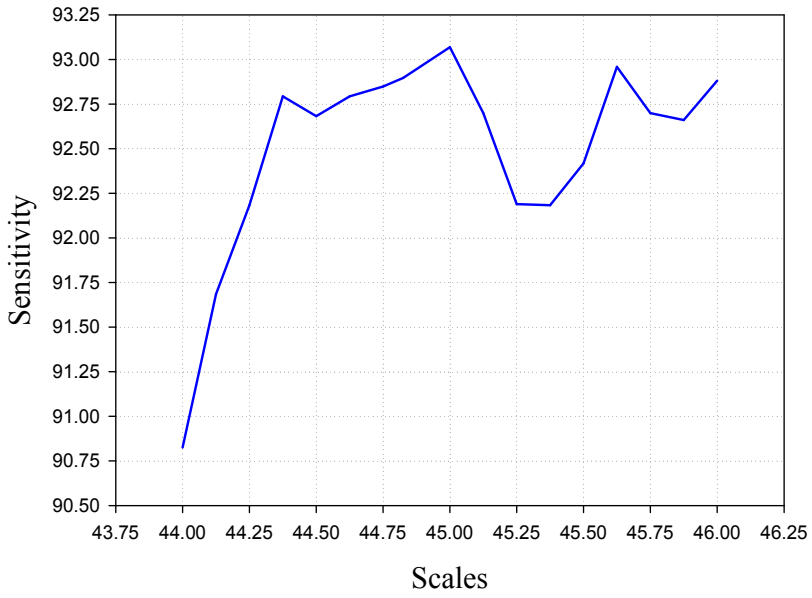

Figure 6.3: Scale vs sensitivity (class III)

From the table and the figure it can be observed that the sensitivity remains almost constant for the selected finer scales. The peak sensitivity of 93.06% was observed at a scale of 45. This scale corresponds to frequency of 3.50 Hz.

6.2.1 Results using optimized SSG wavelet at optimum scales

The classification of ECG into one of the three classes for each of the record in set II of MIT-BIH Arrhythmia database was performed using the newly identified scales (i.e. Class I – scale 20.250, Class II – scale 6.125 and Class III – Scale 45). The block diagram of the classifier is shown in the Figure 6.4. After extracting each cycle, absolute WTC were obtained with the new scales for the different ECG cycles using the SSG-Wavelet. Classification was performed using

PNN Classifier. The results were validated by using the annotations. Sensitivity and positive predictivity for each record as well for each class were calculated.

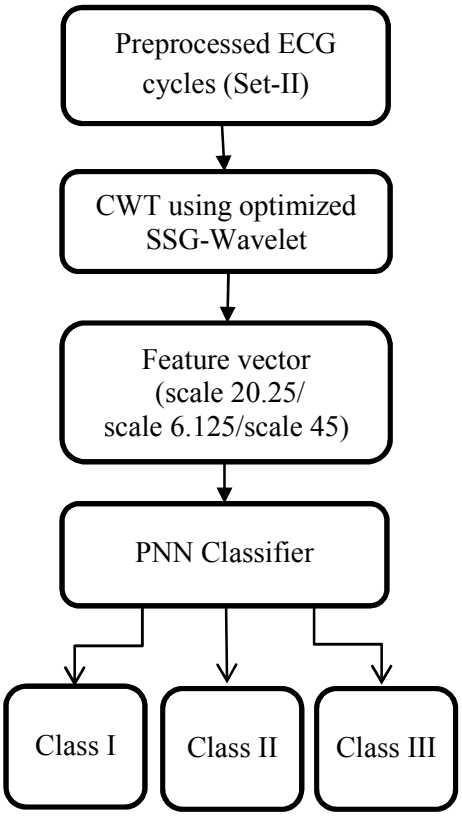

Figure 6.4: ECG classifier at finer scales

Percentage sensitivity obtained before and after refinement is given in Table 6.4. It is seen that there is an improvement in sensitivity by 0.13% for class I, 0.64% for class II and 0.14% for class III.

Table 6.4: Classification at finer scales

	Class I		Class II		Class III		Average	
	Percentage sensitivity obtained							
Record	**Before refinement**	**After refinement**	**Before refinement**	**After refinement**	**Before refinement**	**After refinement**	**Before refinement**	**After refinement**
100	100	100	18	18	100	100	73	73
103	100	100	100	100	-	-	100	100
105	99	99	-	-	90	90	95	95
111	100	100	-	-	100	100	100	100
113	100	100	100	100	-	-	100	100
117	98	100	100	100	-	-	99	100
121	100	100	100	100	100	100	100	100
123	100	100	-	-	100	100	100	100
200	90	91	47	47	93	93	76	77
202	95	97	35	35	90	90	73	74
210	100	100	64	64	77	77	80	80
212	100	100	-	-		-	100	100
213	71	71	75	75	83	83	76	76
214	98	98	-	-	77	79	88	88
219	99	99	100	100	89	89	96	96
221	99	100	-	-	98	98	99	99
222	100	100	57	57	-	-	78	78
228	95	95	100	100	95	95	97	97
231	100	100	100	100	100	100	100	100
232	100	100	90	92	-	-	95	96
233	91	91	86	86	93	95	90	90
234	99	100	22	22	100	100	74	74
Average	**96.88**	**97.01**	**74.56**	**75.20**	**92.92**	**93.06**	**90.37**	**90.54**

From the table, improvements are seen in records 117, 200, 202, 221 and 234 for class I. For class II classification of record 232 has

improved and for class III records 214 and 233 show improvements. The plots of WTC samples of ECG cycles belonging to different classes for a few records of ECG (231, 234, 100) are shown in Figures 6.5-6.7. These records were chosen since they had all the three different classes (I, II & III) of beats in them. Their nature at three different scales can be observed from the figures.

Figure 6.5 shows the WTC obtained from normal ECG cycles at scale 20.25. Figure 6.6 depicts the WTC obtained for Class II. The cycles selected from record 231 and 100 were atrial premature beats, whereas that selected from record 234 was a nodal premature beat, all belonging to the same class. The scale selected was 6.125. Class III cycles shown in Figure 6.7 contains WTC of ventricular premature beats from different patient records. The scale selected was 45.

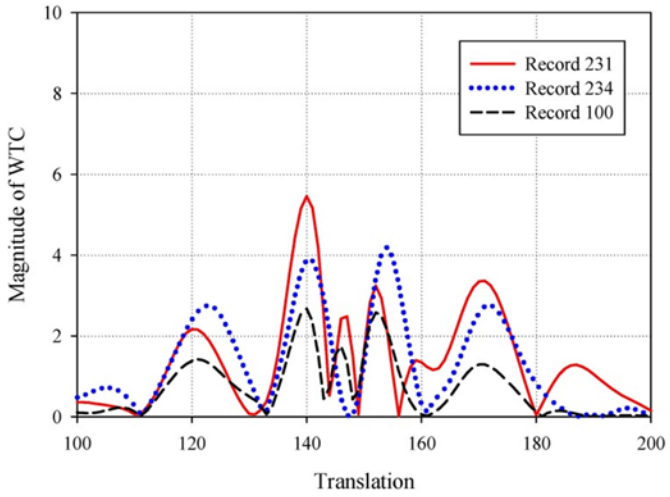

Figure 6.5: WTC for one cycle centered around the QRS complex (Class I) at scale 20.25

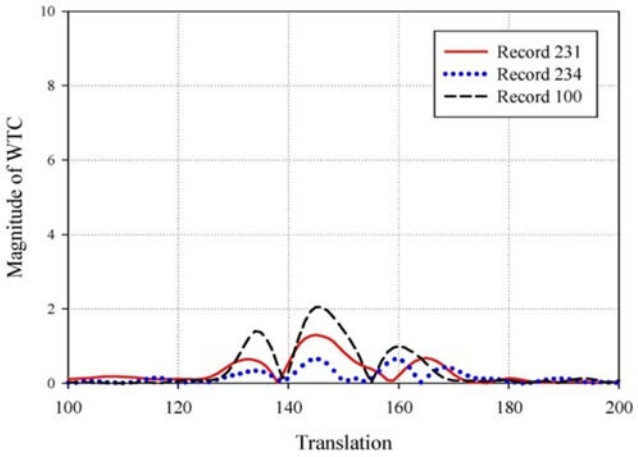

Figure 6.6: WTC for one cycle centered around the QRS complex (Class II) at scale 6.125

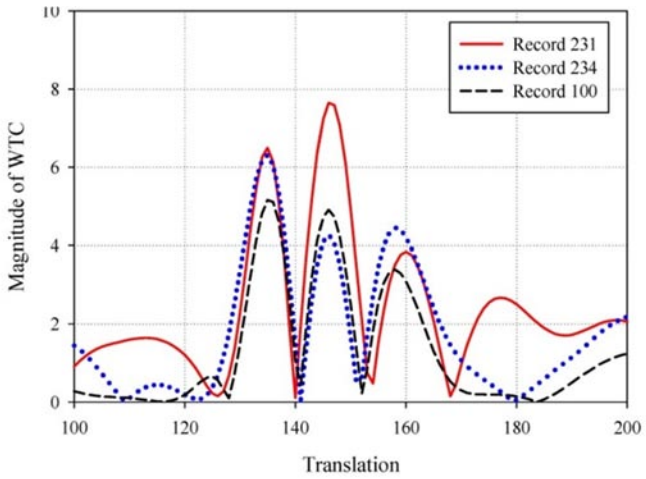

Figure 6.7: WTC for one cycle centered around the QRS complex (Class III) at scale 45

Interestingly as seen in the figures, the plots in the same class do overlap and show similar characteristics.

6.3 Performance comparison of the optimized wavelet

Table 6.5 shown below gives the overall consolidated performance comparison of the optimized SSG-Wavelet in terms of Sensitivity and Positive Predictivity for both the proposed method and by Mariano Llamedo (2011). The proposed method used CWT based features while Mariano Llamedo (2011) have used features from the RR series, as well as features computed from the ECG samples and different scales of the wavelet transform. They used a floating feature selection algorithm to obtain the best performing and generalizing models in the training and validation sets for different search configurations. In both methods, a total of 49629 beats from MIT-BIH Arrhythmia was used during the testing phase. It is seen that sensitivity of a few records have improved further. The overall sensitivity obtained was 97.01% for class I, 75.20% for class II and 93.06% for class III. The positive predictivity attained was 92.16% for class I, 73.93% for class II and 83.05% for class III.

The positive predictivity is low in some cases which mean that there are a few false detections, However the overall response is good since none of the actual diseased cycles are missed.

Table 6.5: Comparison of classification accuracies obtained on 22 records for Normal, Supraventricular and Ventricular beats of the proposed method and (Mariano Llamedo, March 2011)*

Record	No. of beats in each Class			Class I (% classification)				Class II (% classification)				Class III (% classification)				Total (% classification)			
				Proposed		*Ref.* *		Proposed		*Ref.* *		Proposed		*Ref.* *		Proposed		*Ref.* *	
	I	II	III	S	P+	*S*	*P+*	S	P+	*S*	*P+*	S	P+	*S*	*P+*	S	P+	*S*	*P+*
100	2235	33	**1**	100	98	*100*	*77*	18	46	*70*	*100*	100	100	*100*	*100*	73	82	*90*	*92*
103	2079	**2**	0	100	100	*99*	*50*	100	50	*0*	*0*	-	-	-	-	100	75	*50*	*25*
105	2524	0	41	99	99	*97*	*100*	-	-	-	-	90	49	*51*	*94*	95	74	*74*	*97*
111	2120	0	**1**	100	100	*99*	*100*	-	-	-	-	100	1	*100*	*99*	100	51	*100*	*100*
113	1785	**6**	0	100	100	*99*	*100*	100	75	*100*	*99*	-	-	-	-	100	88	*100*	*100*
117	1531	**1**	0	100	100	*100*	*100*	100	40	*100*	*100*	-	-	-	-	100	70	*100*	*100*
121	1858	**1**	**1**	100	100	*99*	*100*	100	50	*100*	*99*	100	70	*100*	*100*	100	73	*100*	*100*
123	1512	0	**3**	100	100	*100*	*100*	-	-	-	-	100	100	*0*	*0*	100	100	*50*	*50*
200	1733	30	826	91	75	*96*	*58*	47	70	*27*	*81*	93	100	*92*	*91*	77	82	*72*	*77*
202	2059	55	20	97	97	*67*	*87*	35	83	*93*	*56*	90	66	*50*	*87*	74	82	*70*	*77*
210	[24]19	22	205	100	94	*94*	*86*	64	82	*91*	*81*	77	90	*69*	*87*	80	89	*85*	*85*
212	2745	0	0	100	100	*100*	*100*	-	-	-	-	-	-	-	-	100	100	*100*	*100*
213	2637	28	582	71	91	*100*	*63*	75	88	*46*	*100*	83	64	*44*	*47*	76	81	*63*	*70*
214	2000	0	257	98	93	*97*	*100*	-	-	-	-	77	93	*94*	*98*	88	93	*96*	*99*
219	2080	**7**	65	99	97	*86*	*46*	100	70	*0*	*0*	89	97	*82*	*100*	96	88	*56*	*49*
221	2029	0	396	100	98	*93*	*99*	-	-	-	-	98	100	*99*	*100*	99	99	*96*	*100*
222	2271	208	0	100	91	*72*	*92*	57	94	*89*	*76*	-	-	-	-	78	93	*81*	*84*
228	1685	**3**	362	95	82	*100*	*60*	100	70	*33*	*84*	95	99	*93*	*100*	97	84	*75*	*81*
231	1565	**1**	**2**	100	100	*98*	*49*	100	100	*0*	*0*	100	100	*50*	*100*	100	100	*49*	*50*
232	397	1381	0	100	22	*100*	*90*	92	99	*78*	*100*	-	-	-	-	96	61	*89*	*95*
233	2227	**7**	841	91	94	*100*	*92*	86	67	*71*	*90*	93	99	*83*	*74*	90	87	*85*	*85*
234	2697	50	**3**	100	99	*100*	*78*	22	100	*72*	*100*	100	100	*100*	*100*	74	100	*91*	*93*
Total	**44188**	**1835**	**3606**	**97.01**	**92.16**	***95***	***83***	**75.20**	**73.93**	***61***	***73***	**93.06**	**83.05**	***75***	***86***	**90.54**	**83.94**	***80***	***82***

6.4 Isolated abnormalities

As seen in the literature survey isolated PVC, isolated supraventricular beats, sudden prolongation of P-P interval, isolated APB, isolated LVNC are some of the isolated abnormalities commonly seen. Table 6.6 shows the records which had isolated abnormalities in the MIT-BIH Arrhythmia database (Set 2) and their corresponding abnormality. PVC and APB are the prominent isolated abnormalities, while abberated atrial premature beat is also present in record 113.

Table 6.7 shows the record number and their details corresponding to isolated abnormalities alone. It can be seen that all isolated abnormalities except from record 233 were identified successfully. Hence this new wavelet can be used as an efficient tool to successfully detect all abnormalities including isolated ones which were the major drawback till date.

Table 6.6: Types of isolated abnormalities in Set - 2

Record name	Type of abnormality	No. of cycles
100	Premature Ventricular beats	1
103	Atrial Premature beats	2
111	Premature Ventricular beats	1
113	Abberated Atrial premature beats	6
117	Atrial premature beats	1
121	Atrial Premature beats	1
121	Premature Ventricular beats	1
123	Premature Ventricular beats	3
228	Atrial Premature beats	3
231	Atrial Premature beats	1
231	Premature Ventricular beats	2
234	Premature Ventricular beats	3

Table 6.7: Detection of isolated abnormalities in the proposed method as compared to (Mariano Llamedo, March 2011)*

Record	No. of beats in each class			Class I % sensitivity		Class II % sensitivity		Class III % sensitivity		Total	
	I	II	III	Proposed	Ref*	Proposed	Ref*	Proposed	Ref*	Proposed	Ref*
100	2235	33	**1**	100	*100*	18	*70*	100	*100*	73	*90*
103	2079	**2**	0	100	*99*	100	*0*	-	-	100	*50*
111	2120	0	**1**	100	*99*	-	-	100	*100*	100	*100*
113	1785	**6**	0	100	*99*	100	*100*	-	-	100	*100*
117	1531	**1**	0	100	*100*	100	*100*	-	-	100	*100*
121	1858	**1**	**1**	100	*99*	100	*100*	100	*100*	100	*100*
123	1512	0	**3**	100	*100*	-	-	100	*0*	100	*50*
219	2080	**7**	65	99	*86*	100	*0*	89	*82*	96	*56*
228	1685	**3**	362	95	*100*	100	*33*	95	*93*	97	*75*
231	1565	**1**	**2**	100	*98*	100	*0*	100	*50*	100	*49*
233	2227	**7**	841	91	*100*	86	*71*	93	*83*	90	*85*
234	2697	50	**3**	100	*100*	22	*72*	100	*100*	74	*91*

6.5 Chapter summary

The classification results show that the proposed method can be used to distinguish different arrhythmias in the ECG records. The classification results achieved is comparable to the published results on the classification of cardiac arrhythmias.

Abdelhamid Daamouchea (2011) has proposed a DWT optimization approach for ECG classification and obtained the overall classification accuracy of 89.74%. Karpagachelvi (2014) using an ELM classifier attained an overall accuracy of 89.74%. Mariano

Llamedo (2011) has described a simple classifier based on ECG feature models that used both interval and morphological features for classification. They have reported a sensitivity of 95% for normal beats, 61% for Supraventricular beats and 75% for ventricular beats. Some of the authors in their study use only less number of ECG cycles for classification, while others have used reconstructed databases (Roshan Joy Martis (2013b,2013c)).

Maximum sensitivity observed were 97.01% for class I, 73.20% for class II and 97.06% for class III. As shown in Table 6.1 the maximum percentage of sensitivity for class I was obtained at a scale of 20.250 which corresponds to a frequency of 7.78 Hz. This frequency corresponds to the duration of normal QRS wave (Chugh, 2012), (David Gray, 2000), (K. George Mathew, 2008). The maximum sensitivity in class II was observed at a scale of 6.125 which corresponds to a frequency of 25.71 Hz as seen in Table 6.2. A Supraventricular ectopic beat usually has a narrow QRS complex with duration less than 0.12 seconds (Chugh, 2012), (David Gray, 2000), (K. George Mathew, 2008). The optimized wavelet could group these beats with a frequency greater than that of normal beats into class II. A ventricular ectopic beat (class III) occurs as a result of the impulse generating other than in the SA node, such as atrium or AV junction. This may be characterized by a QRS complex having duration more than 0.12 seconds (Chugh, 2012) (David Gray, 2000) (K. George Mathew, 2008). The maximum sensitivity for class III occurred at a scale of 45 which corresponds to a frequency of 3.50 Hz as given in

Table 6.3. Thus these beats with time durations greater than that of normal beats (> 0.12 seconds) were correctly identified.

It is seen that sensitivity as well as positive predictivity has further improved at the finer scales. The proposed method uses CWT coeffcient based features and PNN clssifier for Arrhytmia detection. It is seen that sensitivity as well as positive predictivity has further improved at the finer scales. Tabulated results show that there is an improvement in percentage sensitivity and percentage positive predictive values than that was obtained in the previous chapter. Comparing results, it is seen that there is an improvement in all the classes, except positive predictive valve of class III as compared with that of Mariano Llamedo (2011). The proposed wavelet efficiently detected all the abnormalities which were difficult to be detected. The overall sensitivity obtained was 97.01% for class I, 75.20% for class II and 93.06% for class III.

Automatic detection and classification of arrhythmias in ECG plays an important role in diagnosis and treatment of critically ill patients. In fact even the very small improvement obtained while selecting the finer scales will add to the dependability of this algorithm.

Chapter 7

CONCLUSION

The main conclusion and contribution of this research work as well as scope for further work is presented in this chapter.

Wavelet transform techniques are extensively used in ECG signal processing. The ECG records are first denoised by using the proposed GA tuned SD-LMS algorithm. An optimized wavelet transform (SSG-Wavelet) along with a PNN classifier, which effectively detects the different classes of ECG signal including isolated abnormalities is proposed. The classification at finer scales ensured the identification of precise frequency bands corresponding to each class.

A thorough review of the most frequent methods used in wavelet design, noise removal and ECG classification was performed. The following limitations were noted.

i) An efficient filtering technique for ECG noise removal that could be used for ambulatory monitoring proposed by different authors had limitations.

ii) Even though the classification results obtained were acceptable, a better ECG sorting methodology does not exist in the literature.

iii) No attempt has been given in the literature in identifying the isolated abnormalities, which pose a silent threat to patients.

iv) Standard classification scheme of arrhythmia such as ANSI/AAMI EC57:1998 standard were not followed by many researchers.

a) ECG noise removal

Based on the findings, a new algorithm for denoising ECG was implemented which is capable to deal with strong noise in ECG data.

An adaptive filtering technique for denoising the ECG which is based on GA tuned Sign-Data Least Mean Square (SD-LMS) algorithm was implemented. The proposed algorithm gave an average signal to noise ratio improvement of 10.75 dB for baseline wander and 24.26 dB for power line interference. It is seen that the step size 'μ' optimized with GA helps in obtaining better SNR value. The results showed that the useful information in the ECG was not altered by the application of the algorithm.

b) ECG classification

A new continuous wavelet transform was proposed for efficient ECG classification. It was then optimized using genetic algorithm. It is seen that the optimized wavelet does not have the shape of the initial wavelet constructed using Gaussians. The optimized wavelet has only two peaks. Even though optimizing has encountered in a change in the shape of the wavelet, it was checked and seen that it satisfied all the properties of a traditional wavelet. In chapter 5 (Fig 5.3) it is seen that $|\Psi(\omega)|$ goes to zero as $\omega \to 0$ and has unit energy. The features extracted by this wavelet were used to classify ECG signals. The newly designed and optimized wavelet gave better classification results too. While comparing with the results reported in the literature, there is good improvement in percentage sensitivity and percentage positive predictivity. Most of the isolated abnormalities were detected by the new wavelet. The ANSI/AAMI EC57:1998 standard was followed. On performing classification using MIT-BIH arrhythmia database a sensitivity of 97.01% was obtained for class I, 75.20% for class II and

93.06% for class III. The positive predictivity obtained is 92.16% for class I, 73.93% for class II and 83.03% for class III. Comparing to the work done by Mariano Ilamedo (2011) it is seen that there is an improvement of sensitivity by 2% for class I, 14% for class II and 18% for class III. The percentage improvement in positive predictivity for class I is 9% and class II is 1%. For class III there is a slight decrease in the positive predictive value.

The classification methodology could sort out almost all the isolated abnormalities in the ECG records. Classification was performed on the complete ECG record rather than partial or reconstructed data. Many referred papers have used reconstructed databases which have given them good results while this method has taken into account the ECG records without any modification.

The major contribution of this research include

- Design and development of a new continuous wavelet transform for effective ECG arrhythmia detection. The wavelet is formed as a sum of shifted Gaussian functions.
- Optimization of the new wavelet using Genetic algorithm for better classification accuracy.
- Enhancing the accuracy by performing classification using features obtained at finer wavelet scales.
- Detection of the isolated abnormalities like PVC, AP and *a*AP beats in class II and class III patient records.

- Development of an adaptive filter using SD-LMS technique to be used with a continuous ECG monitoring machines such as Holter monitors.

This classification scheme could be used effectively in ambulatory monitoring and mass ECG screening. While this thesis has demonstrated how the optimized wavelet can be used for ECG classification, many opportunities for extending the scope of this thesis remain.

It is shown that wavelets could be optimized for ECG classification. The optimized wavelet could identify the three classes of ECG. But in actual case each class contains different subclasses of ECG. For e.g. Class I contains ECG cycles with LBBB, RBBB, AE, NE in addition to the normal beats. Similar is the case with class II and class III. Identification of diseases in each of the sub-classes could be achieved by further optimizing the wavelets considering these classes.

Since the pulse width of different waves in ECG, changes with different diseases, standard deviation of the Gaussians was first considered for optimization. As a future direction, it may be thought of optimizing the mean as well as standard deviation using multi-objective optimization techniques in order to obtain a more perfect wavelet for classification.

Currently during optimization and in calculating the fitness function, all three classes of ECG were considered together. It would be more beneficial if all the three classes were considered separately,

and wavelets corresponding to each of the scales were optimized seperately.

The optimized wavelet works well with MIT-BIH Arrhythmia database as explained. But it need to be validated on a real-time database. Implementing a real-time analyzer with a 'self-adaptive wavelet' that optimizes itself whenever a new isolated abnormality is detected would aid in future studies.

Bibliography

A. S. AI-Fahoum, I. Howitt. (1999). "Combined wavelet transformation and radial basis neural networks for classifying life-threatening cardiac arrhythmias." *Medical & Biological Engineering & Computing* Vol. 37, pp. 566-573.

AAMI. (2008). Testing and reporting performance results of cardiac rhythm and ST-segment measurement algorithms. *American National standard*, ANSI/AAMI/ISO EC57.

Abdelhamid Daamouchea, Latifa Hamamib, Naif Alajlanc and Farid Melgania. (2011). "A wavelet optimization approach for ECG signal classification." *Biomedical Signal Processing and Control,*. Volume 7, Issue 4, pp. 342-349.

Acharya U. Rajendra (2007). Advances in Cardiac Signal Processing. *Springer.*

Adam Gacek, Witold Pedrycz. (2011). ECG Signal Processing, Classification and Interpretation: A Comprehensive Framework of Computational Intelligence. *Springer Science & Business Media*.

Andina D, Pham D.T. (2009) Computational Intelligence for Engineering and Manufacturing. *Springer. 2nd edition* .

Carlo J. De Luca, L. Donald Gilmore, Mikhail Kuznetsov, Serge H. Roy. (2010). "Filtering the surface EMG signal: Movement artifact and baseline noise contamination." *Journal of Biomechanics (Elsevier)* pp. 1573–1579.

Catalano, Joseph T. (2002). Guide to ECG analysis. *Lippincott Williams and Wilkins*.

Chen, S., C.F.N. Cowan, P. M. Grant. (1991). "Orthogonal Least Squares Learning Algorithm for Radial Basis Function Networks." *IEEE Transactions on Neural Networks* vol. 2, pp. 302-309.

Chugh, SN. (2012). Textbook of Clinical Electrocardiography for Postgraduates, residents and Practising Physicians. *Jaypee brothers Medical Publishers* (P) Ltd.

David Gray, Andrew R Houghton. (2000). Making sense of the ECG: Cases for self-assessment. CRC *Press*.

Dickinson, David F (2005). The normal ECG in childhoodand adolescence. *Heart-BMJ Journal*, Vol. 91, Issue. 12, pp.1626–1630.

Dingfei Ge, Narayanan Srinivasan, Shankar M Krishnan. (2002). "Cardiac arrhythmia classification using autoregressive modeling." *BioMedical Engineering online* pp. 1-12.

Eskola MJ, Kosonen P, Sclarovsky S, Vikman S, Nikus KC. (2007). The ECG pattern of isolated right ventricular infarction during percutaneous coronary intervention. *PubMed*, Vol. 12, Issue. 1, pp. 83-90.

Fakroul Ridzuan Hashim, Lykourgos Petropoulakis, John Soraghan, Sairul Izwan Safie. 2012. "Wavelet Based Motion Artifact Removal for ECG Signals." IEEE EMBS International Conference on *Biomedical Engineering and Sciences. Langkawi*. pp. 339-342.

Filtering & Processing Tools. Retrieved from *ecg.sharif. ir/Download/ Packages/Filtering & ProcessingTools/KLP*.

George Mathew K, Praveen Aggarwal. (2008). Medicine: Prep Manual for undergraduates. *Elsevier.*

George Mathew K, Praveen Aggarwal. (2008). Medicine: Prep Manual for undergraduates. *Elsevier.*

Goldberg, David E. (1989). Genetic Algorithms in Search, Optimization and Machine Learning. *Addison Wesley*.

Goldberger A.L., L.A.N Amaral, L. Glass, J.M. Hausdorff, P.Ch. Ivanov, R.G. Mark, J.E. Mietus, G.B. Moody, C.-K. Peng, H.E. Stanley. (2000). "PhysioBank, PhysioToolkit, and PhysioNet: components of a new research resource for complex physiologic signals." *Circulation - American Heart Association*. Vol. 101, pp. e215-e220.

Hassan, Ashraf Mohamed Ali. (2014). "Power Line Interference (PLI) Reduction in Electrocardiogram (ECG) Using Multiple Sub-Adaptive Filters Approach." *International Journal of Scientific Engineering and Technology* Vol. 3, Issue.5, pp. 694-697.

Haykin, Simon. (2009). Adaptive Filter Theory. India: *Pearson Education, Inc and Dorling Kindersley Publishing.*

Henry Marriott JL, Neil ScSchwartz L, Harlod H. (1962) "Ventricular fusion beats." *Circulation published by Americal Heart Association. Vol. 26, pp. 880-884*

Hu Y.H., Palreddy S., and Tompkins W.J. (1997). "A patient-adaptable ECG beat classifier using a mixture of experts approach." *IEEE Trans.Biomed. Eng.* Vol. 44, pp. 891–900.

Hu Y.H., Tompkins W.J., Urrusti J. L., and Afonso V. X.. (1993). "Applications of artificial neural networks for ECG signal detection and classification*." Journal in Electro cardiology*. Vol. 26, pp. 66–73.

Inaki Romero, Torfinn Berset, Dilpreet Buxi, Lindsay Brown, Julien Penders, Sunyoung Kim. Nick Van Helleputte, Hyejung Kim, Chris Van Hoof, Firat Yazicioglu. (2011). "Motion Artifact Reduction in Ambulatory ECG Monitoring: An Integrated System Approach." *WH '11 Proceedings of the 2nd Conference on Wireless Health*. pp. 1-8.

Jacobsen JR, Garson A Jr, Gillette PC, McNamara DG. (1978). Premature ventricular contractions in normal children. *The Journal of Pediatrics*. Vol. 92, Issue. , pp. 36-42.

Johnson, L.Shen. P. (2010). "A review of Electrocardiogram Filtering." *Journal of Electrocardiology* vo1.43, no.6, pp. 486-496.

Kannathal N, Rajendra Acharya U , Choo Min Lim, PK Sadasivan, and SM Krishnan. (2007). Classification of Cardiac Patient States using Artificial Neural Networks. In J. S. U. Rajendra Acharya, Advances in Cardiac Signal Processing. *Springer-Verlag Berlin Heidelberg*. pp. 204,205

Karpagachelvi, S. (2014). "Classification of ECG signals using hybrid particle swarm optimization in extreme learning machine." *Int. Journal of Applied Sciences and Engineering Research* Vol. 3, Issue 5, pp. 1086-1095.

Lewis, Kathryn M. (2000). Sensible Analysis of 12-Lead ECG. Canada: *Thomson Delmar Learning*.

Lewis, Kathryn. (2010). Multiple Lead ECGs: A practical Analysis of Arrhythmias. *Delmar, Cengage Learning.*

Lifshits, M.A. (1995). Functions, Gaussian Random. Springer Science.

Malmivuo J., Plonsey R. (1995). Bio electromagnetism: Principles and Applications of Bioelectric and Biomagnetic Fields. *USA: Oxford University Press*.

Mariano Llamedo, Juan Pablo Martinez. (2011 March). "Heartbeat Classification using feature selection driven by database generalization criteria." *IEEE transactions on biomedical engineering* Vol.58, No.3, pp. 616 - 625.

Mertins, A. (1999). Signal Analysis: Wavelets, Filter Banks, Time-Frequency transforms and applications. *John Wiley & sons Ltd.*

Mitchell, Melanie. (1998). An introduction to Genetic algorithm. *MIT press paperback edition*.

Mithun P., Prem C. Pandey, Toney Sebastian, Prashant Mishra, and Vinod K. Pandey. 2011. "A Wavelet Based Technique for Suppression of EMG Noise and Motion Artifact in Ambulatory ECG." *33rd Annual International Conference of the IEEE EMBS* pp. 7087-7090.

Mneimneh M.A., E.E. Yaz, M.T. Johnson, R.J. Povinelli. (2006). "An adaptive Kalman Filter for removing Baseline Wandering in ECG signals." *Computers in Cardiology*. Vol. 33, pp. 253-256.

Mohamed I. Owis, Ahmed H. Abou-Zied, Abou-Bakr M. Youssef, Yasser M. Kadah. 2002. "Features Based on Nonlinear Dynamical Modeling in ECG Arrhythmia Detection and Classification." *IEEE Transactions on Biomedical Engineering* Vol. 49, pp. 733-736.

Mohammad Zia Ur Rahman, Rafi Ahamed Shaik, DV Rama Koti Reddy. (2009). "Noise cancellation in ECG signals using computationally simplified Adaptive filtering techniques: Application to biotelemetry." *Signal Processing: An International Journal(SPlJ).* Volume (3), Issue (5), pp. 120-131

Mohammad Zia Ur Rahman, Rafi Ahamed Shaik, DV Rama Koti Reddy. (2010). "Noise Cancellation in ECG signals using normalised sign-sign LMS algorithm." *IEEE International Symposium on Signal Processing and Information Technology (ISSPIT),. Narasaraopet, India,:* Print ISSN: 2162-7843, DOI: 10.1109/ISSPIT.2009.5407510

Moody George B. (1997) "An Introduction to Cygwin,[Online]." *http://physionet.org/physiotools/cygwin.*

Moody, George B. (2014). WFDB Programmer‟s Guide. *http://www.physionet.org/physiotools/wpg/wpg.pdf.*

Moody, R. Mark and G. (1997). MIT-BIH Arrhythmia Database. *http://ecg.mit.edu/dbinfo.*

Morita Seiji (2015). Isolated T Wave Inversion in Lead aVL: An ECG Survey and a Case Report. *Hindawi*, Volume 2015, Article ID 250614, 7 pages.

Nitish V. Thakor, Vi-Sheng Zhu. (1991). "Applications of Adaptive Filtering to ECG Analysis: Noise Cancellation and Arrhythmia Detection." *IEEE Transactions on Biomedical Engineering*. Vol. 38, No. 8, pp. 785-794.

Omer T. Inan, Laurent Giovangrandi, Gregory T. A. Kovacs. (2006). "Robust Neural-Network-Based Classification of Premature Ventricular Contractions Using Wavelet Transform and Timing Interval Features." *IEEE Transactions on Biomedical Engineering* Vol. 53, pp. 2507-2515.

Paul S, Addison. (2002). The Illustrated Wavelet Transform Handbook. *IOP Publishing.*

Philip de Chazal, Maria O'Dwyer and Richard B. Reilly. (2004). "Automatic classification of heart beats using ECG morphology and heart beat interval features." *IEEE trasactions on Biomedical Engineering* Vol. 51, Issue. 7, pp. 1196 - 1206.

PhysioNet. http://www.physionet.org/.

Rajashekaran S., Vijayalakshmi Pai G.A.. (2013). Neural Networks, Fuzzy Logic And Genetic Algorithms: Synthesis and Applications. *PHI Learning Private Limited*.

Rangayyan, Rangaraj M. (2004). Biomedical Signal Analysis-A case study approach. *John Wiley & Sons(Asia)* Pte Ltd.

Roshan Joy Martis, U Rajendra Acharya, Hojjat Adeli. (2014 May). "Current methods in electrocardiogram characterization." *Elsevier, Computers in biology and medicine* Vol. 48, pp. 133-149.

Roshan Joy Martis, U. Rajendra Acharya, Choo Min Lim, Jasjit S. Suri. (2012 June). "Characterisation of ECG beats from cardiac arrhythmia using discrete cosine transform in PCA framework." Knowledge-Based Systems, *Elsevier* Vol. 45,pp. 76-82.

Roshan Joy Martis, U. Rajendra Acharya, Hari Prasad, Chua Kuang Chua,. Choo Min Lim, Jasjit S. Suri. (2013 November). "Application of higher order statistics for atrial arrhythmia classification." Biomedical Signal Processing and Control Vol. 8, Issue 6, pp.888-900.

Roshan Joy Martis, U. Rajendra Acharya, K.M. Mandana, A.K. Ray, Chandan Chakraborty. (2012 October). "Application of Principal Component Analysis to ECG signals for automated diagnosis of cardiac health*." Expert Systems with Applications, Elsevier.* Vol. 39, Issue. 14, pp. 11792-11800.

Roshan Joy Martis, U. Rajendra Acharya, K.M. Mandana, A.K. Ray, Chandan Chakraborty. (2013 March). "Cardiac decision making using higher order spectra." *Elsevier, Biomedical signal processing and control* Vol. 8 Issue. 2, pp. 193-203.

Roshan Joy Martis, U. Rajendra Acharya, Lim Choo Min. (2013 August). "Application of higher order cumulant features for cardiac health diagnosis using ECG signals." International Journal of Neural Systems, *World Scientific Publishing Company* Vol. 23, No. 4, pp. 1350014-23

Roshan Joy Martis, U. Rajendra Acharya, Lim Choo Min. (2013 September). "ECG beat classification using PCA, LDA, ICA and Discrete Wavelet Transform." *Elsevier, Biomedical Signal Processing and Control*. pp. 437– 448.

Ross T. Murphy, Rajesh Thaman, Juan Gimeno Blanes, Deirdre Ward, Elias Sevdalis, Efi Papra, Anatoli Kiotsekolglou, Maria T. Tome, Denis Pellerin, William J. McKenna, Perry M. Elliott. (2005). Natural history and familial characteristics of isolated left ventricular non-compaction. *European Heart Journal*, Volume 26, Issue 2, 187-192.

Sandra Atwood, Cheryl Stanton, Jenny Storey-Davenport. (2011). Basic Cardiac Dysrhythmia. *Jones and Bartlett Learning, LLC, an Ascend Learning Company.*

Saul G. Myerson, Robin P. Choudhury, Andrew R.J. Mitchell. (2009). *Emergencies in Cardiology*. OUP Oxford.

Sayadi O, Mohammad Bagher Shamsollahi (2008). ECG Denoising and Compression Using a Modified Extended Kalman Filter Structure. Biomedical Engineering, *IEEE Transactions on Signal Processing* (Volume:55 , Issue: 9), 2240 - 2248.

Seema Rani, Amanpreet Kaur, J.S. Ubhi. (2011). "Comparitive Study of FIR and fIR filters for the removal of Baseline noises from ECG signal." *International Journal of Computer Science and Information Technologies* Vol. 2(3), pp. 1105-1108.

Senhadji L., G. Carrault, J. J. Bellanger, and G. Passariello. (1995). "Comparing wavelet transforms for recognizing cardiac patterns." *IEEE Eng. MedBiol*. Vol. 14, pp. 167–173.

Silipo R., Marchesi C. (1998). Artificial Neural Network for Automatic ECG Analysis. *IEEE Transactions in Signal Processing*, 46(5), pp 1417-1425.

Simon Haykin, Widrow B. (2003). Least Mean Square Adaptive Filters. *United States of America: John Wiley & Sons*.

Sivanandam S.N., Deepa S.N. (2006). Introduction to Neural Networks using Matlab 6.0. *Tata McGraw-Hill Education.*

Soman K.P., Ramachandran K.I.. (2005). Insight Into Wavelets From Theory To Practice. *Prentice-Hall Of India Pvt. Limited.*

Taylor G.J. (2002). 150 Practice ECGs: Interpretation and review. *Oxford U.K.: Blackwell.*

Vijay S. Chourasia, Anil Kumar Tiwari. (2013). "Design Methodology of a New Wavelet Basis Function for Fetal Phonocardiographic Signals." *The Scientific World Journal*. Vol. 2013, Article ID 505840, 12 pages.

Viljoen M.J. (1989). General Nursing, Medical and Surgical Text Book- Part 2. L.R. Uys(EDS), *Copyright-Kagiso Tertiary.*

Von R.F., J.H. Pierluiss, H. Nazeran. (2005). "Wavelet Transform based ECG Baseline Drift Removal for body surface potential mapping." Proc. 27'" *International conference of the IEEE Engineering in Medicine and Biology Society*. pp. 3891-3894.

Wasserman P.D. (1993). Advanced Methods in Neural Computing. *New York: Van Nostrand Reinhold.*

Weituo Hao, Yu Chen, Yi Xin. (2011). "ECG Baseline Wander Correction by Mean-Median Filter and Discrete wavelet Transform." in Proc. *33rd Annual International conference of the IEEE EMBS Boston*. DOI: 10.1109/IEMBS.2011.6090744

Wolter, Kirk M. (2007). Introduction to variance estimation. *Springer.*

Y. Sun, K.L. Chan, S.M. Krishnan. (2002). "ECG signal conditioning by morphological filtering." *Computers in Biology and Medicine* Vol 32, no.6, pp. 465-479.

Yeap T.H., F. Johnson, and M. Rachniowski. (1990). "ECG beat classification by a neural network,." in Proc. Annual International Conference *IEEE Engineering Medicine and Biology Soc*. Vol. 12, Issue. 3, pp. 1457–1458.

Ziad F Issa, John M Miller, Douglas P. Zipes. M. (2012). Clinical Arrhythmology and Electrophysiology: A Companion to Braunwald's Heart Disease. *Elsevier Saunders*.

List of Publication

[1] Baby Paul, Mythili P. (2012). ECG noise removal using GA tuned sign-data least mean square algorithm,. *Proc. Annual International IEEE Conference on Advanced Communication Control and Computing Technologies (ICACCCT)* (pp. 978-1-4673-2045-0, pp.100-103.). IEEE explore.

[2] Baby Paul, Shanavaz K.T., Mythili P. (August 2012), *Towards the development of a new wavelet for ECG classification, Pro. Annual International IEEE Conference on Power, Signals, Controls and Computation* (pp. 978-1-4673-0446-7,pp.1-5), IEEE explore.

[3] Baby Paul, Shanavaz K.T., Mythili P. (October 2015). "A New Optimized Wavelet Transform for Heart Beat Classification." *International Journal of Mechanics in Medicine and Biology, World Scientific Publishing Company.* Vol.15, Issue.05, pp.1550081 (1-19). doi:10.1142/S0219519415500815.